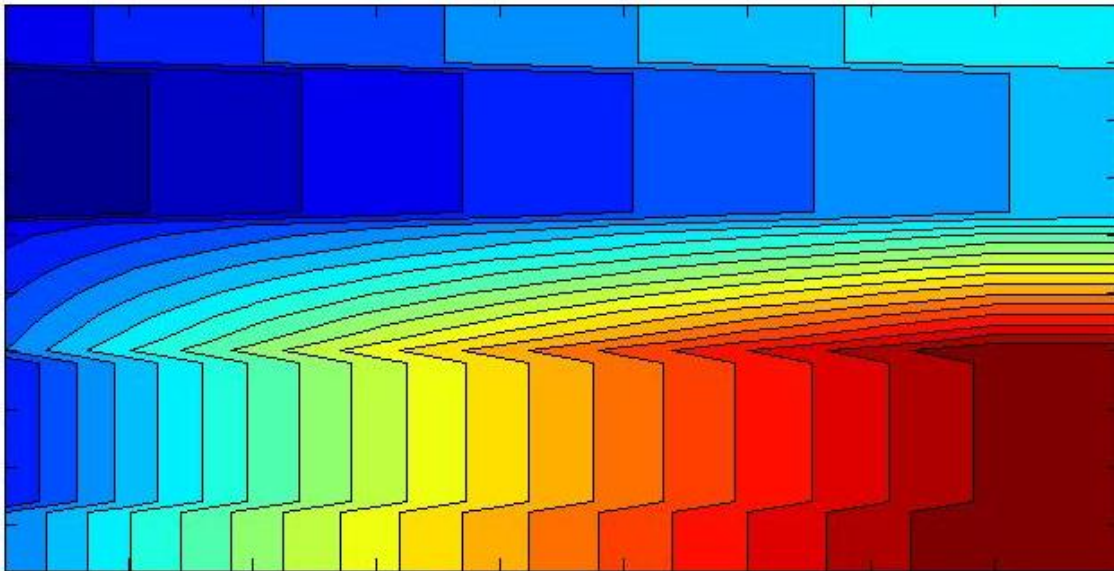


CHALMERS



Investigating the possibility of developing a 3-D
DOC model using Matlab 7.8.0 (R2009a)

Transient simulations of temperature

Master of Science Thesis [Innovative and sustainable chemical engineering]

ROBIN SVENSSON

Department of Chemistry and Bioscience
Division of chemical reaction engineering
CHALMERS UNIVERSITY OF TECHNOLOGY
Göteborg, Sweden, 2011

Investigating the possibility of developing a 3-D DOC model using Matlab 7.8.0 (R2009a)

Transient simulations of temperature

Master's thesis

Robin Svensson

© Robin Svensson, 2011

Department of Chemistry and Bioscience

Chalmers University of Technology

SE-412 96 Göteborg

Sweden

Telephone + 46 (0)31-772 1000

Göteborg, Sweden 2011

Front picture:

Temperature distribution between channels 1 and 3 along the channels, bottom part is channel 1 and top part is channel 3. The flow is higher in the top channel compared to the bottom channel. Note the difference in the top channel to the bottom one, a higher flow in the top channel results in lower temperature increase.

Acknowledgement

I would like to express my thankfulness to my supervisor Fredrik Jareman at epsilon UC Väst AB for his support in this master thesis, and for believing in me and assigning me this task. All of my coworkers at Epsilon also deserve thanks.

I would also like to express my gratitude to PhD student Björn Lundberg at the division of chemical reaction engineering at Chalmers University of Technology for his great support and for answering my never ending swarm of questions. Also my examiner Prof. Bengt Andersson at Chalmers University of Technology at the division of chemical reaction engineering has my gratitude in this work.

I would also like to thank my girlfriend for her support and her belief in me.

Abstract

A model has been created in Matlab 7.8.0 (R2009a) to simulate a diesel oxidation catalyst, a DOC. The reason for developing the model in Matlab and not using commercial CFD-tools is the need to simulate complete driving cycles for the DOC. Doing this in a CFD-software would result in a short time step since the time scales for the reactions is much shorter than the time scales for the temperature development. This would in a CFD-software make the number of time steps too many to practically perform. The model can now handle cycles of hours.

Initially an attempt was made to discretize code in a similar manner to CFD-code. However this turned out to be much too time consuming and the idea was abandoned. Instead a tanks in series procedure was performed, where derivatives in space was handled as differences. This allows for the solution of ordinary differential equations using an ode-solver instead of partial differential equations. This procedure leads to large time steps when the equations turns towards and reaches steady state.

The model can describe systems of 1, 4, 9, 16 and 25 channels in a quadratic configuration. The model also includes the possibility of describing 24 channels in a near circular configuration. The components included in the model are carbon monoxide, hydrocarbons described by the properties of propylene, nitric oxide, nitrogen dioxide and oxygen. The reactions included in the model are oxidation of carbon monoxide, oxidation of hydrocarbons, oxidation of nitric oxide and self dissociation of nitrogen dioxide. All the reactions are exothermic except the self dissociation of nitrous oxide. This leads to a temperature increase in the system. The increase of temperature is highly related to the initial temperature in the system and the increase is higher with higher initial temperature.

The model is ready to validate to experimental data. Since no experimental data has been obtained a parameter study has been performed on the behavior of the model varying a number of system properties. Conversion of all the components increases with temperature, for carbon monoxide up to a certain point to level out and then to slowly decrease. Increasing the flow to the system leads to lower conversion of the included components and this is related to a shorter residence time in the system. The effects from varying the system pressure is limited on the conversion of the components, however somewhat increasing for carbon monoxide.

Keywords: Diesel Oxidation Catalyst, DOC, Matlab model, flue gas after treatment, transient simulation, tanks in series model

Nomenclature*

Roman

| | |
|----------------------|---|
| F_{tot} | Total molar flow [mole/s] |
| $y_{i,k,n}$ | Mole fraction of component i in segment k in layer n [-] |
| $C_{i,k,n}$ | Concentration of component i in segment k in layer n [mole/m ³] |
| C_{tot} | Total concentration [mole/m ³] |
| $V_{k,n}$ | Volume in segment k and layer n [m ³] |
| $r_{j,k,n}$ | Reaction rate of reaction j in segment k in layer n [mol/m ² /s] |
| S_{Pt} | Specific platinum surface area [m ² /gPt] |
| m_{Pt} | Mass of Pt in a cell [gPt] |
| $c_{p,g}$ | Heat capacity of the gas phase [J/kg/K] |
| $c_{p,s}$ | Heat capacity of the solid phase [J/kg/K] |
| $T_{g,k}$ | Temperature in the gas phase in segment k [K] |
| $T_{s,k}$ | Temperature in the solid phase in segment k [K] |
| A_k | Mass and heat transfer area between two layers [m ²] |
| A_s | Cross sectional area of a channel [m ²] |
| V_g | Gas volume in a channel segment, for $n=1$ [m ³] |
| q_k | Heat flux between two segments [J/m ² /s] |
| $-\Delta H_j$ | Heat of reaction for reaction j [J/mole] |
| $m_{s,k,n}$ | Mass in the solid phase in segment k and layer n [kg] |
| $m_{\text{Pt},k,n}$ | Mass platinum in segment k and layer n [g] |
| Δx_k | Distance between nodes in two neighboring segments [m] |
| Δz_k | Distance between nodes in two neighboring layers [m] |
| $k_{c,i,k}$ | Mass transfer coefficient for component i in segment k [m/s] |
| $D_{i,k}$ | Binary diffusivity between component i and air in segment k [m ² /s] |
| $D_{K,i,k}$ | Knudsen diffusivity of component i in segment k [m ² /s] |
| $D_{\text{eff},i,k}$ | Effective diffusivity for component i in segment k [m ² /s] |
| D_h | Hydraulic diameter [m] |
| D_{AB} | General binary diffusion coefficient between component A and B [m ² /s] |
| f_D | Porosity and tortuosity factor [-] |
| d_p | Mean pore diameter [m] |
| R_u | Universal gas constant, 8.3143 [J/mole/K] |
| M_i | Molar mass of component i [g/mole] |
| $X_{S,i}$ | Solid fraction of component i [-] |
| G | Inhibition factor [K] |
| K | Adsorption pre-exponential factor [-] |
| E_a | Adsorption heat/R [K] |
| Sh | Sherwood number [-] |
| Nu | Nusselt number [-] |

Greek

| | |
|------------------|--|
| $\Gamma_{i,k,n}$ | Mass transfer coefficient for component i in segment k and layer n [m ³ /s] |
| $\nu_{i,j}$ | Stoichiometric coefficient for component i in reaction j [-] |
| ρ_g | Density in the gas phase [kg/m ³] |
| ρ_s | Density in the solid phase [kg/m ³] |
| λ | Thermal conductivity [W/m/K] |
| α | Heat transfer coefficient [W/m ² /K] |

Indexes

| | |
|------|---|
| i | Component $i=1,2\dots5$ |
| j | Reaction $j=1,2\dots4$ |
| k | Segment $k=1,2\dots10$ |
| n | Wash coat and gas layer $n=1,2\dots5$ |
| s | Solid phase |
| g | Gas phase |
| d | Direction in the channels $d=1,2\dots4$ |
| l | Wall layer $l=1,2\dots5$ |
| surr | Surrounding |

* Note that nomenclature regarding discretised code can be found under relevant sections in appendix 3. The above nomenclature only handles the tanks in series procedure.

Content

| | |
|--|----|
| 1. Introduction | 3 |
| 1.1 General..... | 3 |
| 1.2 Background..... | 3 |
| 1.1.1 The difference between a diesel engine and a gasoline engine | 3 |
| 1.1.2 Regulations for emissions from diesel engines | 3 |
| 1.1.3 Particulate matter effects on public health | 4 |
| 1.3 Limitations..... | 4 |
| 1.4 Purpose | 5 |
| 2. Theory | 5 |
| 2.1 Catalyst setups | 5 |
| 2.1.1 Diesel oxidation catalyst (DOC) | 5 |
| 2.1.2 Diesel particulate filter (DPF) | 6 |
| 2.2 Langmuir-Hinshelwood kinetics | 6 |
| 2.2.1 Implementation of Langmuir-Hinshelwood kinetics | 7 |
| 2.3 Heat of reaction | 9 |
| 2.3.1 Heat of formation | 9 |
| 2.3.2 Implementing heat of reaction..... | 10 |
| 2.4 Physical and thermal properties of gas and solid phase | 11 |
| 2.4.1 Density | 11 |
| 2.4.2 Viscosity | 12 |
| 2.4.3 Mass transfer coefficients..... | 13 |
| 2.4.4 The binary diffusion coefficient..... | 13 |
| 2.4.5 Implementing the mass transfer coefficient | 14 |
| 2.4.6 Heat transfer coefficient | 14 |
| 2.4.7 Thermal conductivity | 14 |
| 2.4.8 Implementation of heat transfer coefficient | 15 |
| 2.4.9 Heat capacity | 15 |
| 2.5 One channel DOC the CFD-way | 16 |
| 2.6 Tanks in series approach..... | 16 |
| 2.6.1 Mass balances..... | 17 |
| 2.6.2 Lumped mass transfer coefficients..... | 17 |
| 2.6.3 Heat balances..... | 18 |
| 2.6.4 Effective diffusivity..... | 19 |
| 2.7 Description of the wall | 19 |
| 2.7.1 The wall between two channels..... | 19 |
| 2.7.2 The wall connected to the surrounding | 20 |
| 3. Methodology | 21 |
| 3.1 Configurational setup | 21 |
| 3.2 Matlab configuration | 22 |
| 4. Results | 24 |
| 4.1 Discretised code results | 24 |
| 4.2 Investigation of kinetic data used | 25 |
| 4.3 One channel results..... | 27 |
| 4.3.1 Basic values used in simulation | 27 |
| 4.3.2 Varying temperature..... | 36 |

| | | |
|--------|---|----|
| 4.3.3 | Varying pressure | 37 |
| 4.3.4 | Varying flow | 39 |
| 4.3.5 | Varying DOC dimensions | 39 |
| 4.3.6 | Varying composition (Fraction of O ₂ and HC) | 40 |
| 4.3.7 | Varying catalyst load..... | 42 |
| 4.3.8 | Varying cell density | 43 |
| 4.3.9 | Temperature increase in the system | 43 |
| 4.3.10 | Summary of one channel results | 44 |
| 4.4 | Multiple channel results..... | 45 |
| 4.4.1 | Four (4) channel configuration..... | 45 |
| 4.4.2 | Nine (9) channel configuration..... | 48 |
| 4.4.3 | Circular configuration | 50 |
| 5. | Discussion | 51 |
| 5.1 | Discretized code discussion | 51 |
| 5.2 | Tanks in series discussion..... | 52 |
| 5.2.1 | Program discussion | 52 |
| 5.2.2 | Program limitations | 52 |
| 5.2.3 | One channel results | 53 |
| 5.2.4 | Multiple channel results | 56 |
| 5.2.5 | Future work | 57 |
| 6. | Conclusions | 57 |
| | References | 59 |
| | Appendix 1 – Program user manual | |
| | Appendix 2 – Calculation of system properties | |
| | Appendix 3 – One channel DOC the CFD-way | |

1. Introduction

1.1 General

This master thesis is performed as part of a Master of Science degree in *Innovative and sustainable chemical engineering* at Chalmers technical University in Gothenburg, Sweden. It is also a part of obtaining the Swedish “civilingenjör” degree in chemical engineering with physics at Chalmers technical University.

1.2 Background

1.1.1 The difference between a diesel engine and a gasoline engine

In the regular gasoline engine, also referred to as the Otto cycle, a vaporized mixture of gasoline and air is delivered to the combustion chamber. There the mixture is compressed by the cylinder piston and ignited using a sparkplug. In the diesel engine the air is instead compressed in the cylinder and the fuel is then sent in to the cylinder and is self ignited when meeting the hot air. This means that no spark plug is used in the diesel engine. (Siuru, B., 2007)

Furthermore, looking at the fuels diesel contains more long carbon chains compared to the gasoline, the diesel is heavier, oilier and have a higher energy density than the gasoline.

In Europe there is a stride towards more use of the diesel engine hence much of the oil refining focuses on producing diesel before ordinary gasoline. The reason for using a diesel engine instead is that higher mileage can be obtained per unit of volume than for gasoline. The reason for this is that the compression of the air/fuel mixture is more efficient and more effective work is obtained in the process. (Siuru, B., 2007)

The disadvantage resulting from the higher compression ratio in the diesel engine is that the engine must be more robust in its mechanical composition and will therefore become heavier than the gasoline engine. This results in a higher price for the diesel engine but this fact is counteracted by a longer lifetime. (Siuru, B., 2007)

One advantage with using a diesel engine in a car compared to a gasoline engine is that it has lower emissions of green house gases. This is because the emissions of green house gases are directly proportional to the amount of fuel used. This is one major reason why the retail of diesel cars is increasing rapidly, especially in Europe. Beside all the emissions that are the same as in the gasoline engine such as carbon monoxide, unburned hydrocarbons and nitrogen oxides, the diesel engine is known to also emit large amounts of particulate matter. (Siuru, B., 2007)

1.1.2 Regulations for emissions from diesel engines

Since the use of diesel engines has increased over the last years and is still increasing, the emissions of particulate matter into the atmosphere are increasing. The particulate matter in difference from the emissions of the green house gases give rise to local problems. Urban areas are highly affected by particulate matter. This has forced regulations regarding the amount of emissions that can be released by diesel driven vehicles, both private and commercial. Not only is the particulate matter emissions regulated but also the emissions of

carbon monoxide, hydrocarbons and the nitrogen oxides, also known as the NO_x-gases. Below is a diagram of the emission standards in the European Union from 1992 until 2014. This diagram is included to give a feel about the strict regulations that are put on emissions from diesel engines. It also gives an idea about the work that needs to be put in, to develop and produce diesel oxidation catalysts (DOC) and diesel particulate filters (DPF) and other flue gas after treatment systems that can meet these requirements. (DieselNet, 2010)

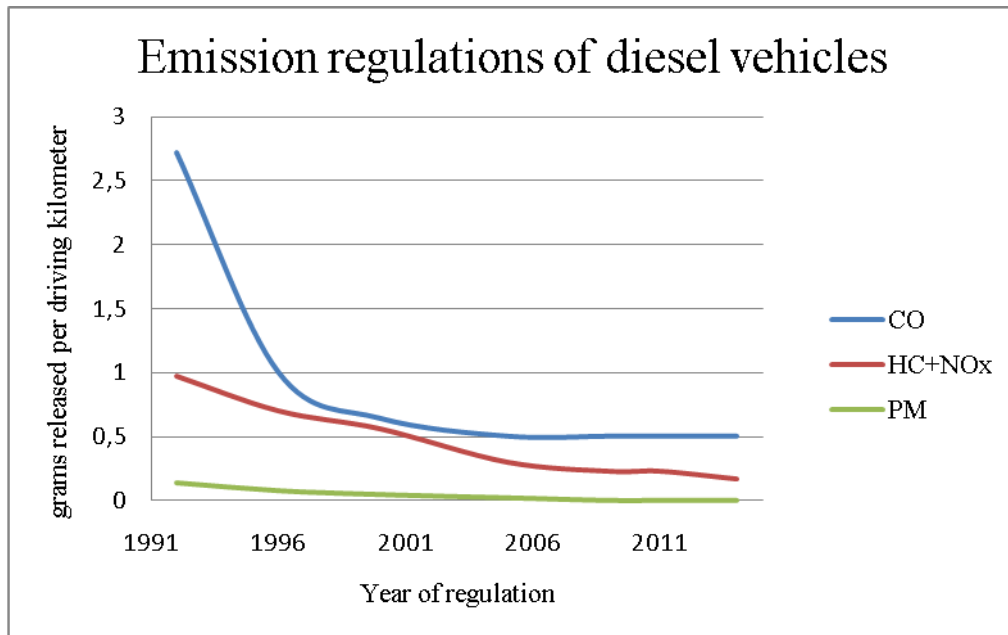


Figure 1. Emission standards for passenger cars in the European Union in the years between 1992 and 2014. The values are roughly yearly based even if the regulations entered in different months of the different years (DieselNet, 2010)

The values in Figure 1 are for passenger cars that use a diesel engine as propulsion system and there are different regulations for other types of vehicles. The common denominator being that all types of emission are to be lowered in all types of vehicles. (DieselNet, 2010)

1.1.3 Particulate matter effects on public health

There are a number of reasons why the regulations regarding diesel vehicles and regular engines are set so strict. One of them being the effects on human health is unknown. There are reasons to believe that particulates from diesel exhaust gases effects the human respiratory system, the vascular functions and brain activity in the short term. Data that has been extracted from clinical studies are inconclusive regarding the type of particles that effect the human body, if it is the particulates from diesel exhaust or other nanoparticles. Because of this, it is not yet decided that increased emissions of nanoparticles from diesel exhausts give rise to toxicity. In general however it has been concluded that particulate matter has an effect on the public health and it is therefore necessary to keep such emissions as low as possible. (Hesterberg, 2010) (Patel, 2011) (EPA, 2003)

1.3 Limitations

There are a number of limitations to this project. First of all the coding is limited to the software Matlab 7.8.0 (R2009a). The report is written in Microsoft Office Word 2007 with

included figures and graphs from Microsoft Office Power Point 2007 and from Microsoft Office Excel 2007.

Only a DOC is investigated in this project, initially a DPF was an interesting component to include in the simulations. This was excluded during the project due to high workload from the DOC programs. In the DOC model it is only possible to simulate carbon monoxide, hydrocarbons in the form of propylene, nitric oxide, nitrous oxide and oxygen.

This project is performed without any kind of experimental data; instead literature is the supporting pillar. Literary values are combined to find a suitable model. This makes the model ready to use after calibration towards experimental data. For future versions of the program, if experimental data is obtained this might be included. It is highly recommended to let experimental data validate the model to reach its fullest capacity.

1.4 Purpose

This thesis is performed together with Epsilon high tech in Gothenburg and in collaboration with Volvo Powertrain. The objective is to develop a model treating flue gas treatment for diesel engines using Matlab. The model will be able to treat 3-dimensional analyses in diesel oxidation catalyst of heat and mass transfer. The purpose is to be able to calculate the temperature development in the catalyst during complete cycles.

In the end the model is supposed to be used in the design process to increase the lifetime of the DOC:s in the flue gas system.

2. Theory

2.1 Catalyst setups

In this section a number of different catalytic devices will be presented further. Main focus is put on the DOC but some other options and additions to the DOC are presented.

2.1.1 Diesel oxidation catalyst (DOC)

A diesel oxidation catalyst (DOC) is a structure placed after a diesel engine before a diesel particulate filter (DPF) and or a selective catalytic reduction (SCR) device. It has a number of channels in parallel with a square or sometimes honeycomb structure. The inside of these channels is coated with some type of catalyst, e.g. palladium or platinum and this catalyst helps reducing the emissions of particulate matter, hydrocarbons, nitrogen oxides and carbon monoxide by oxidation. Figures regarding the efficiency of the DOC vary in literature but it is suggested that soluble organic fractions (SOF) can be removed up to 90 percent and the reduction of particulate matter is suggested to between 20 and 50 percent. However the figures regarding the reductions of the different compound vary with diesel sulfur level, engine type, age, size etc. (EPA, 2003) (WSUEEP, 2003) In Figure 2 a description of DOC is displayed.

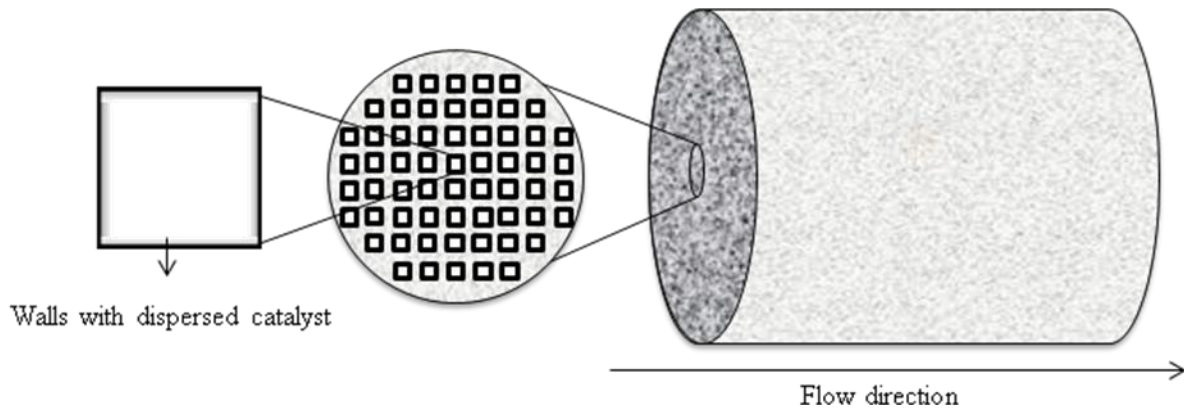


Figure 2. Description of a diesel oxidation catalyst from macro scale down to size of channel opening. .

2.1.2 Diesel particulate filter (DPF)

In a diesel particulate filter the channels are not open in the same way as in the DOC, instead every channel has a neighboring channel to which it has a porous wall. This is mainly to reduce the particulate matter in the exhaust gas entering the DPF. There is also the option of using a DPF that has been impregnated with catalytic material such as platinum. This is called a catalyzed diesel particulate filter (CDPF). (Schejbal, 2010) A schematic figure of the diesel particulate filter can be found below. Particulate matter is filtered in the DPF and is accumulated on the wall that the gas mixture is flowing through. This increases the pressure drop over the DPF. (Zheng, 2009)

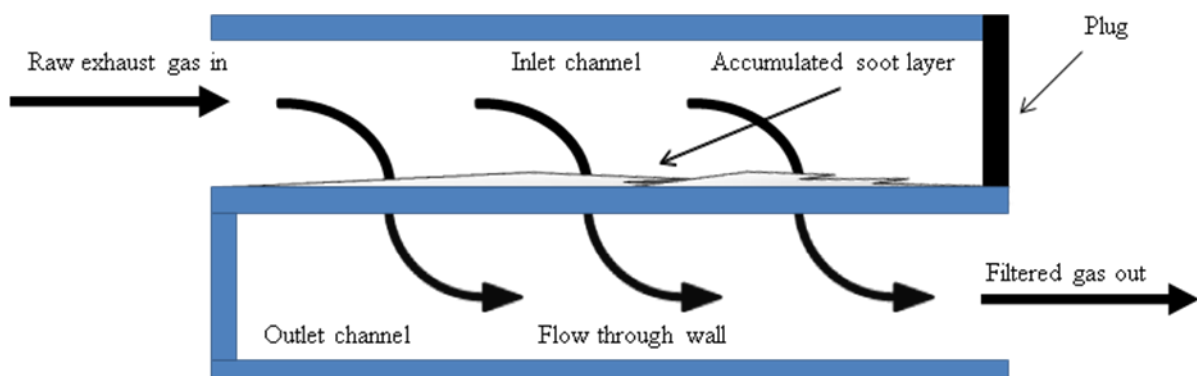


Figure 3. Schematic description of a diesel particulate filter. Two channels with a porous wall between them where the flow is forced through.

2.2 Langmuir-Hinshelwood kinetics

Langmuir-Hinshelwood kinetics is the most applied model for describing the kinetics of heterogeneous catalytic processes. The expression describes the surface reaction taking place on a catalyst, for instance a dual site reaction between carbon monoxide and an oxygen atom. In Figure 4 an example is presented on how the Langmuir-Hinshelwood kinetics is used. (Vasanth Kumar, 2008) (Fogler, 2006)



Figure 4. A schematic figure of the reaction of adsorbed carbon monoxide and oxygen forming carbon dioxide over a platinum catalyst.

For the reaction in Figure 4, between CO and O forming CO₂ the generic expression is written as:



And the reaction rate law is written as:

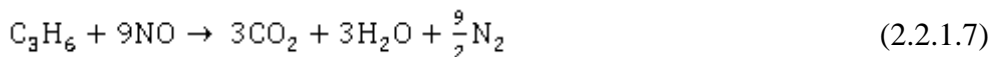
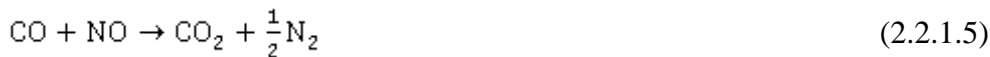
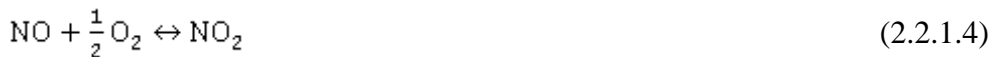
$$r_s = k_s \left(C_{A \cdot s} C_{B \cdot s} - \frac{C_{C \cdot s} C_{D \cdot s}}{K_s} \right) \quad (2.2.0.2)$$

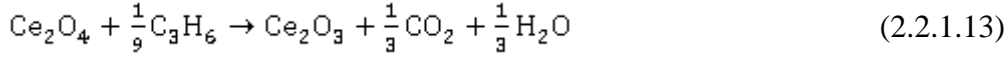
where $r_s = \left(\frac{\text{mol}}{\text{gcat} \cdot \text{s}} \right)$, $k_s = \left(\frac{\text{gcat}}{\text{mol} \cdot \text{s}} \right)$ and the surface rate K_s is the reaction rate equilibrium constant $K_s = \frac{k_{+s}}{k_{-s}}$ hence being dimensionless.

The Langmuir-Hinshelwood kinetics will be utilized in the formulation of the model describing the reactions inside the DOC. (Fogler, 2006)

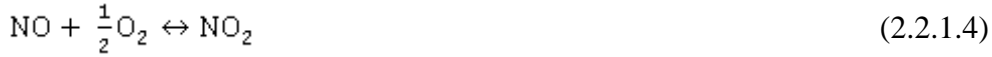
2.2.1 Implementation of Langmuir-Hinshelwood kinetics

There are a number of reactions taking place on a DOC in reality. Schejbal et al. lists the reactions to the following thirteen reactions: (Schejbal, 2010)





The reactions taking place in the DOC in the model are reduced for calculation reasons down to the three most important and common reactions, oxidation of carbon monoxide, nitric oxide and propene also known as propylene;



Propylene is the only hydro carbon simulated to reduce the calculation load of the simulations and the reason for this simplification is that it has been found that hydrocarbons from exhaust gases can be divided into to groups; easily oxidized hydro carbons and hydro carbons that are hard to oxidize. The easily oxidized hydrocarbons constitute 80 % of the total load of hydro carbons and are well represented by propylene. (Wang, 2008), (Zheng, 2009) The rate law expressions used are written on the form first suggested by Voltz et al. and later modified by Oh and Cavendish. For carbon monoxide and propylene; (Wang, 2008)

$$R_{\text{CO}} = \frac{k_1 X_{s,\text{CO}} X_{s,\text{O}_2}}{G(X_{s,j}, T_s)} \quad (2.2.1.15)$$

$$R_{\text{C}_3\text{H}_6} = \frac{k_2 X_{s,\text{C}_3\text{H}_6} X_{s,\text{O}_2}}{G(X_{s,j}, T_s)} \quad (2.2.1.16)$$

The term $G [K]$ is the inhibition factor and is dependant on the temperature and on mole fraction of the components and is expressed as: (Wang, 2008)

$$G(X_{s,j}, T_s) = T_s \left(1 + K_1 X_{s,\text{CO}} + K_2 X_{s,\text{C}_3\text{H}_6} \right)^2 \dots \left(1 + K_3 X_{s,\text{CO}}^2 X_{s,\text{C}_3\text{H}_6}^2 \right) \left(1 + K_4 X_{s,\text{NO}}^{0.7} \right) \quad (2.2.1.17)$$

The constant $K_i [-]$ where i varies between 1 and 4 is the adsorption equilibrium constants and it is calculated from the Arrhenius equation: (Wang, 2008)

$$K_i = K_i^0 \exp\left(-\frac{E_{a,i}}{R_u T_g}\right) \quad (2.2.1.18)$$

The constants in equation 2.2.1.18 are the adsorption heat, E_a [J/mol], the universal gas constant, R_u [J/mol/K] and the pre-exponential factor K_i^0 [-]. (Wang, 2008).

The rate law expression for nitric oxide differs slightly from the others, this is because at higher temperatures the self dissociation of nitric dioxide is favored before the oxidation of nitric oxide. If the rate law expression for nitric oxide is supposed to work over a wide range of temperature an extra term has been added to the expression: (Wang, 2008)

$$R_{NO} = \frac{k_g x_{g,NO} x_{g,O_2}}{G(x_{g,i}, T_g)} \left(1 - \frac{K'}{K_p}\right) \quad (2.2.1.19)$$

The term K' describes the deviation from equilibrium K_p , and is described as:

$$K' = \frac{x_{NO_2}}{x_{NO} x_{O_2}^{1/2}} \quad (2.2.1.20)$$

The equilibrium constant K_p is calculated from basic thermodynamics and is given by: (Pandaya, 2009)

$$\ln(K_p) = 5.0462 + \frac{6343.4}{T} - 2.2973 \ln(T) + 3.0315e^{-3}T - 8.2812e^{-7}T^2 + 1.1412e^{-10}T^3 \quad (2.2.1.21)$$

The expression for nitrogen dioxide is based in the expression for nitric oxide and is calculated:

$$R_{NO_2} = \frac{k_g x_{g,NO} x_{g,O_2}}{G(x_{g,i}, T_g)} \left(\frac{K'}{K_p}\right) \quad (2.2.1.22)$$

The rate law expression for oxygen is calculated assuming that all of the reactions take place in stoichiometric conditions and no accumulation take place: (Wang, 2008)

$$R_{O_2} = \frac{1}{2} R_{CO} + \frac{9}{2} R_{C_8H_8} + \frac{1}{2} R_{NO} \quad (2.2.1.23)$$

Reaction rates are calculated as described above and is estimated for every different temperature and compositions of the included components.

2.3 Heat of reaction

2.3.1 Heat of formation

In order to obtain the temperature dependence of the heat of formation the 91st edition of the *Handbook of chemistry and physics* was used. In there, the heat of formation was extracted for each component over a temperature range from about 300 K up to 1500 K.

2.3.2 Implementing heat of reaction

The heat of formation data extracted from the 91st edition of the *Handbook of chemistry and physics* was used in order to calculate the heat of reaction for the reactions that is assumed to take place in the DOC. For the generic reaction:



the heat of reaction can be expressed as:

$$\Delta H_R = [c\Delta H_{C,f} + d\Delta H_{D,f}] - [a\Delta H_{A,f} + b\Delta H_{B,f}] \quad (2.3.2.2)$$

where the lower-case letters denote stoichiometric coefficients and upper-case letters denote compounds or molecules involved in the reaction.

The extracted data for heat of formation was then used in order obtain the heat of formation for the reaction in equations (2.2.1.1), (2.2.1.14) and (2.2.1.4) described earlier in this paper. Below is an example of how this was done, the example is for the reaction described in equation (2.2.1.1), oxidation of carbon monoxide to carbon dioxide. The procedure is described in equation (2.3.2.1) and (2.3.2.2) and the result from the plot and the basic fitting can be seen in Figure 5.

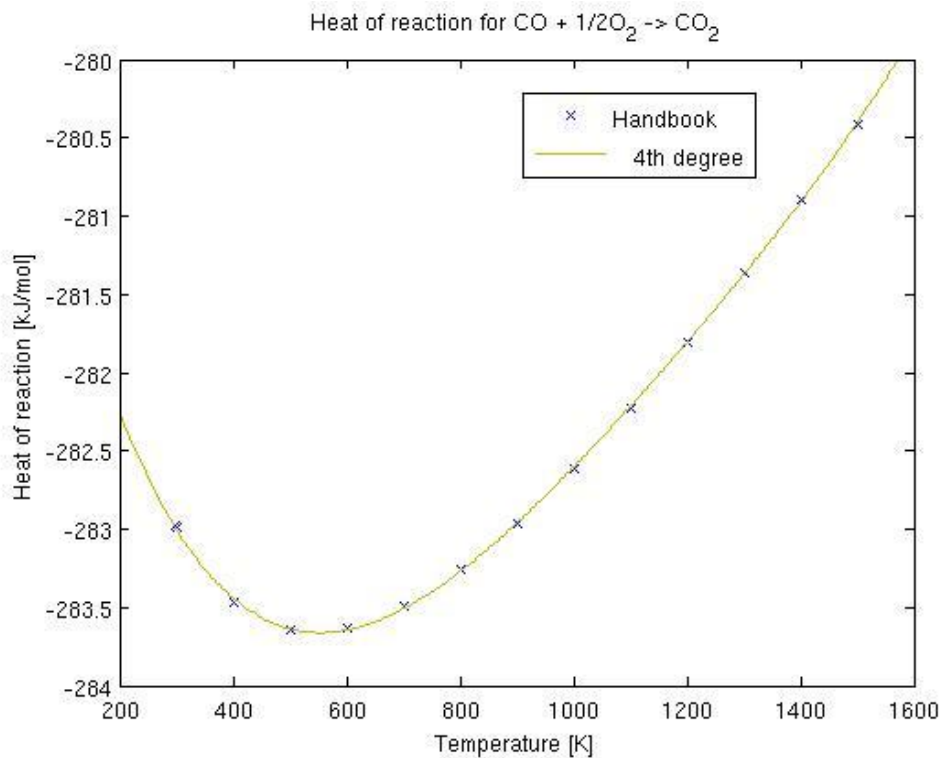


Figure 5. The data for heat of reaction (blue x) and the fitting to the data (yellow line) describing the heat of reaction for the oxidization of carbon monoxide.

With the result from the basic fitting the heat of reaction is expressed as a fourth degree polynomial:

$$\Delta H_R = p_1 T^4 + p_2 T^3 + p_3 T^2 + p_4 T + p_5 \quad (2.3.2.3)$$

T is the temperature in Kelvin and p_1 to p_5 is a number of constants summarized in

Table 1.

Table 1. Summary of the constants in the basic fitting equation describing the heat of reaction for the oxidation reaction of carbon monoxide.

| p_1 | p_2 | p_3 | p_4 | p_5 |
|------------|------------|-----------|-----------|---------|
| 3.2351e-12 | -1.4985e-8 | 2.7078e-5 | -0.018392 | -279.54 |

In Figure 5 it can be seen from the y-axis of the graph that the absolute value of the heat of reaction varies only slightly over the given temperature range, it is therefore concluded that this method is safe to use and the total error obtained from the estimation of heat of reaction is small when used in the algorithm compared to other errors that might occur in the numerical solution. The same procedure has been used also to the oxidation of hydrocarbons and the oxidation of nitric oxide, and the absolute errors for these calculations are in the same order of magnitude. It can also be seen from the y-axis that the heat of reaction is smaller than zero which means that the reaction is exothermic, releasing heat up on reaction, resulting in a temperature increase to its surrounding.

2.4 Physical and thermal properties of gas and solid phase

2.4.1 Density

Density of a fluid varies with temperature and pressure in general. This applies in theory both to gases, liquids and solids. However the effects of density of solids as well as liquids are small. This investigation do not handle liquids at all, but there is a solid part and a gaseous part included in the DOC. The density of the solid is set constant which is assumed to be valid simplification. The density of the gas however is not set constant because it is highly affected by the temperature in the system. It is assumed that the gas inside the DOC is air at all times and all locations, this is since the composition of the gas is close to that of air. The interesting components in the gas, the ones that are to be oxidized are only occupying small fractions of the total composition. An advantage of using air is that it is fairly easy to find data for it.

This renders a subroutine to calculate the density for different pressures and temperatures. This is done using the built in function in Matlab known as `interp2`, a function handling two dimensional interpolations. Data is extracted from the 91st edition of *Handbook of chemistry and physics*. The temperature and pressure range that is covered by the data is between 120-1000 K and 0.1-2 MPa respectively. This should well cover the range of operation for the DOC. The data is built up into a matrix containing four rows representing four different pressure data points in the above mentioned range and 21 columns representing 21 different temperature points in the temperature range.

These data are treated in a separate m-file and called upon requirement. The interpolation is linear and the m-file requires the input of both current pressure and temperature. Figure 6 shows the importance of employing both a temperature and pressure dependence of the density within a wide possible range.

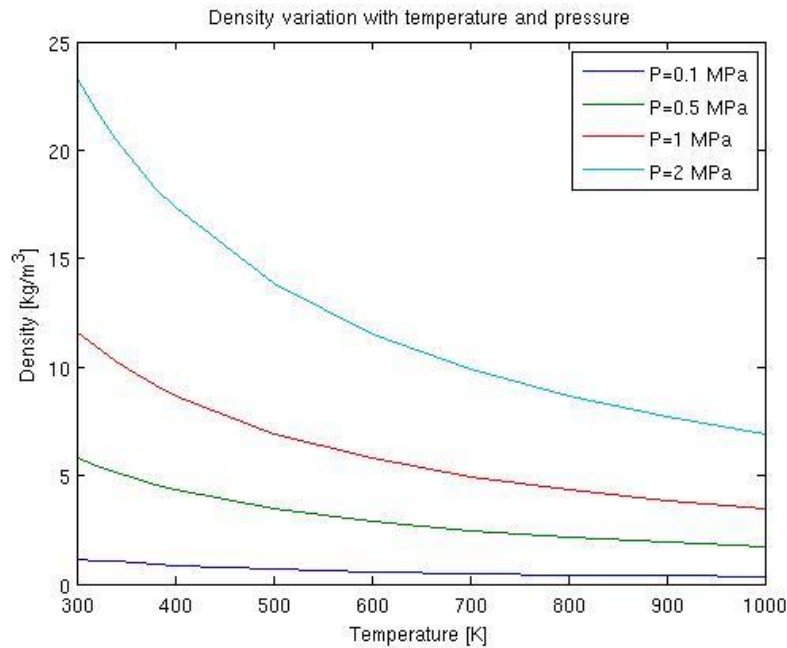


Figure 6. The variation in density of the gas phase with temperature and pressure over the temperature interval 300 to 1000 K and the pressure interval 0.1 to 2 MPa.

Note that the m-file contains a failsafe if the allowed range of both pressure and temperature is exceeded. If the pressure is too high or too low a basic fitting has been made to the nearest pressure point of data accessible and there is in theory a possible temperature range of 0 to infinity to calculate the density. However this procedure should be used with caution because density dependence on pressure is fairly high. If instead the temperature exceeds its range which is the most probable case a basic fitting has been made to the closest pressure. This should also be used with caution because the polynomial is only of fourth degree, and far outside the temperature range there is no physical explanation to the polynomial behavior.

2.4.2 Viscosity

Viscosity is a measure of the resistance rate of deformation in a fluid. A fluid with high viscosity is not easily deformed e.g. tar. A fluid with low viscosity on the other hand is easily deformed, such as most gases. (Welty, 2001)

The viscosity is used when solving the Navier-Stokes equation and it needs to be calculated at the correct properties. The viscosity dependence of absolute pressure is negligible and will not be taken into account. Instead temperature dependence is employed. Data is extracted from the 91st edition of *Handbook of chemistry and physics*. The data is plotted and a basic fitting to the data is made and used in the m-file that calculates the viscosity at the current temperature. The basic fitting is a second order polynomial. The correspondence between the polynomial and the experimental data in the temperature range of 120-1000 K is displayed in Figure 7 below. It should be noted that the viscosity is not a part of the tanks in series model.

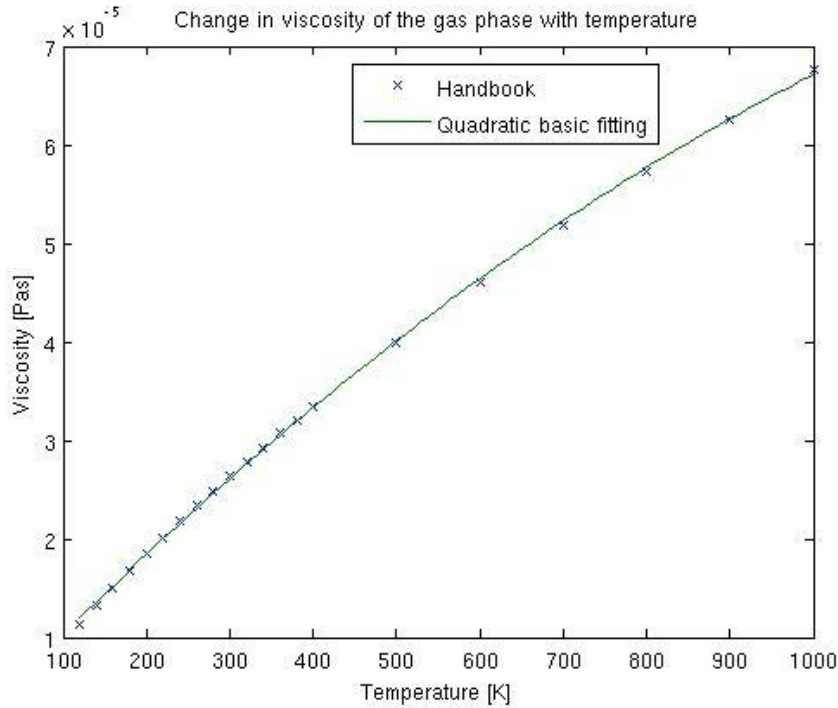


Figure 7. The variation of viscosity with temperature. Data is taken at $P=0.1$ MPa. The temperature interval is between 100 and 1000 K.

2.4.3 Mass transfer coefficients

The mass transfer coefficient k_m [m/s] is used in both the mass balance for the solid phase and the mass balance for the gas phase. It describes the rate at which mass transfers between phases, in this case between the gas phase of the bulk and the solid phase on the surface on the catalyst material. The actual transfer between phases is obtained by multiplying the mass transfer coefficient with a gradient corresponding to concentration or fraction between phases. The mass transfer coefficient between phases is for each component here calculated as: (Wang, 2008)

$$k_{m,j} = \frac{Sh_{\infty} D_i}{D_h} \quad (2.4.3.1)$$

where the asymptotic Sherwood number, Sh_{∞} is set to 2.89 which corresponds to fully developed laminar flow with a constant wall temperature. D_h is the hydraulic diameter of a channel and D_i is the binary diffusion coefficient of component i with the mixture. The calculation of the binary diffusion coefficient is further explained in the following subsection. (Wang, 2008)

2.4.4 The binary diffusion coefficient

A general diffusion coefficient D_{AB} [m²/s] describes the rate at which component A diffuses in to component B. In general gas diffuses faster than liquids which in turn diffuse faster than solids. Here for simplification all the binary diffusion coefficients are between component i and air, which is a fairly good approximation of the bulk gas in the system. In order to calculate the diffusion coefficients for all components the Fuller correlation is used: (Welty, 2001)

$$D_{AB} = \frac{10^{-3} T^{1.75} \left(\frac{1}{M_A} + \frac{1}{M_B} \right)^{1/2}}{P \left[(\sum v)_A^{1/3} + (\sum v)_B^{1/3} \right]^2} \quad (2.4.4.1)$$

The different parameters included in the equation are the temperature, T [K], the molar weight of the components, M_i [g/mol], the pressure, P [atm] and the diffusion volumes, v [\AA^3]. All of the binary diffusion coefficients are calculated for 1 atm and 300 K as reference temperature. Assuming that the pressure variations in the system are small only a correction term for the temperature is necessary. The temperature dependence for the diffusivities is calculated as:

$$D_{AB}(T) = D_{AB}(T_0 = 300 \text{ K}) \left(\frac{T}{T_0} \right)^{1.75} \quad (2.4.4.2)$$

2.4.5 Implementing the mass transfer coefficient

In the algorithm the m-file calculating the mass transfer coefficient calls the function file calculating the diffusion coefficients which in turn sends back the diffusion coefficients at a specified temperature. These data are extractable calling the mass transfer coefficient files with a specific temperature.

2.4.6 Heat transfer coefficient

The heat transfer coefficient, $[\text{W}/\text{m}^2\text{K}]$ is a part of both the solid phase and the gas phase heat balances. It is used to measure the heat transfer between the two phases in the presence of a temperature gradient. The heat transferred between the phases is obtained by multiplying the heat transfer coefficient with the temperature difference. It is calculated as: (Zheng, 2009)

$$\alpha = \frac{Nu_{\infty} \lambda_g}{D_h} \quad (2.4.6.1)$$

The Nu_{∞} [-] is the Nusselt number at fully developed laminar flow of exhaust gas with constant wall temperature and is set to 2.89. λ_g [W/mK] is the thermal conductivity and D_h is the hydraulic diameter of the channel. (Zheng, 2009) The correlation is known as the Dittus-Boelter correlation.

2.4.7 Thermal conductivity

Thermal conductivity is a measure on the ability for a material to conduct heat. (Welty, 2001) Data is taken from the 91st edition of the *Handbook of chemistry and physics* for air which is assumed to be a valid assumption. The data is taken at 1 MPa and at the temperature range 120 to 1000 K. Note that the data differs very little if the pressure is changed, hence the error to this estimation will be kept to a minimum. Basic fitting has been used in order to obtain an equation describing the thermal conductivity change with temperature. The equation obtained is a quadratic equation, the correspondence between the handbook data and the basic fitting can be seen in Figure 8.

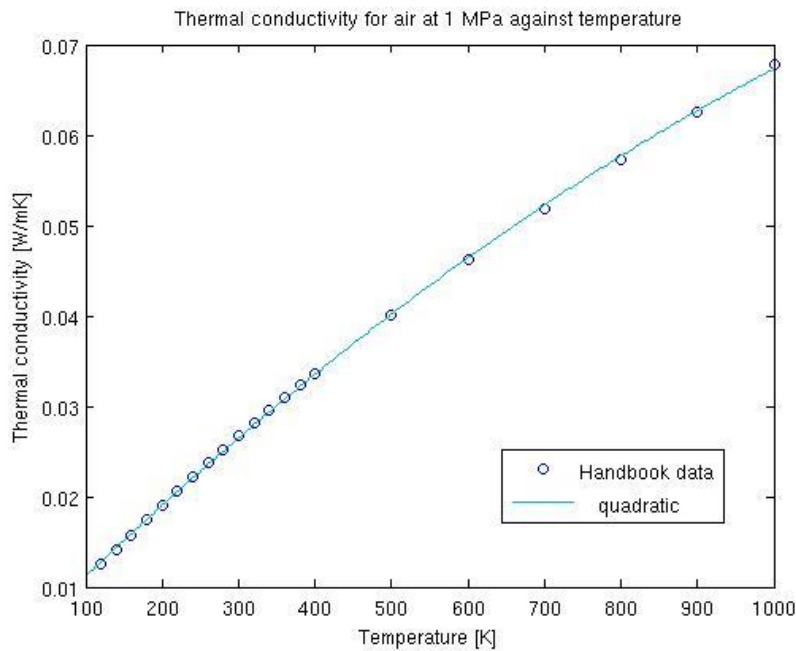


Figure 8. The data describing the correspondence between scientific data and basic fitting for thermal conductivity. The temperature interval is 100 to 1000 K.

2.4.8 Implementation of heat transfer coefficient

Similar to the mass transfer coefficient the temperature needs to be specified in calculation of the thermal conductivity and returning this value. In turn the heat transfer coefficient is calculated.

2.4.9 Heat capacity

The heat capacity is calculated for air for the gas phase using interpolation between database figures. Data is taken from the 91st edition of the *Handbook of chemistry and physics* in the temperature range 120 K to 1000 K and the pressure range is 0.1 MPa to 2 Mpa. The interpolation is 2-dimensional using the built in Matlab function `interp2`. The m-file calculating the heat capacity for the gas phase requires the inputs of pressure and temperature and returns the heat capacity in SI-units (J/kg/K). Figure 9 shows the impact that temperature and pressure has on the heat capacity for air.

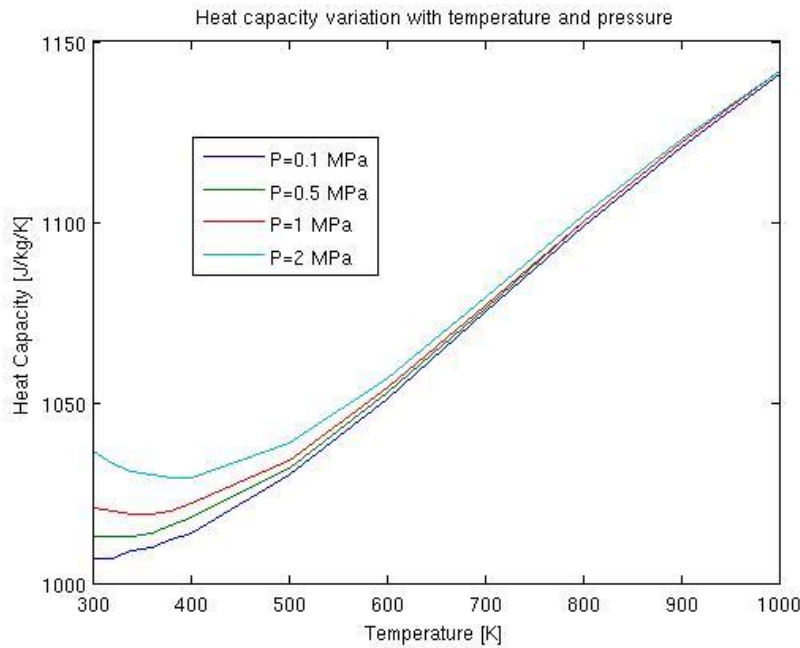


Figure 9. The variation in heat capacity of the gas phase with temperature and pressure. The temperature interval is 300 to 1000 K and the pressure interval is 0.1 to 2 MPa.

2.5 One channel DOC the CFD-way

In order to describe the diesel oxidation catalyst a one channel model is used at first. The channel is seen as one dimensional with a gas phase and a solid phase. In the gas phase the mixture of exhaust gases flows while the solid phase is none moving and the phase where the reactions take place inside the DOC. The one dimensional procedure for describing a DOC is often used and well validated. (Wang, 2008) (Hauff, 2010). It should be noted while reading this section that only three reactions are handled instead of four like described under section 2.2. The reason for this is that the self dissociation of nitrogen dioxide was not included in this part.

The reader is referred to appendix 3 to read about the theory regarding CFD discretization. This is a massive theory section and is put in appendix 3 in order to not hold up the interested reader.

2.6 Tanks in series approach

As an option to using discretization of all the included balances there is the possibility of employing the tanks in series approach. This formulation removes the derivative in space expressing the derivative as a difference instead allowing a partial differential equation to be expressed as an ordinary differential equation. The approach still divides the DOC into discrete points that are each treated as a tank reactor. A visualization of tank in series can be seen in Figure 10.

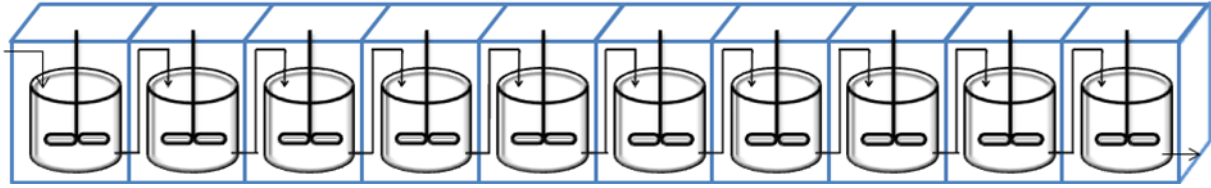


Figure 10. The DOC displayed as ten discrete nodes with a tank in each node. The behavior in one segment is represented by a CSTR.

In order to obtain a more accurate description of the system the washcoat is simulated assuming it contains layers. These layers are also treated as tanks only having interaction with the layer above and below. There is no diffusion in the layers next to each other, only perpendicular to the flow direction. Figure 11 below describes the situation.

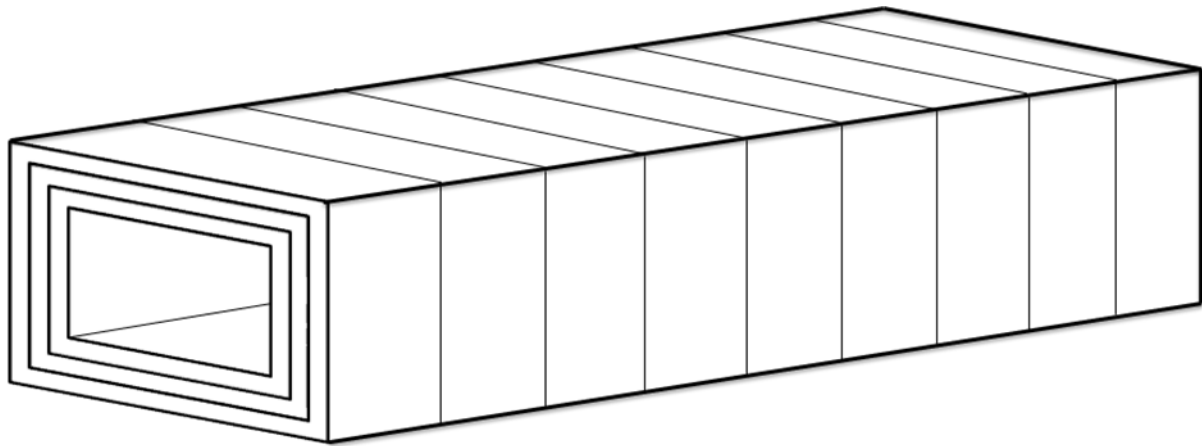


Figure 11. One channel with the segments both in flow direction and in the washcoat perpendicular to the flow direction.

2.6.1 Mass balances

Included in the mass balance are axial flow and radial diffusion and a transient term. This generates a number of ordinary differential equations using the tank in series approach. There are five components included in the mass balance, these five components are CO, HC, NO, NO₂ and O₂ and they constitute the minimum number of components to fully describe the system. The components are indexed i . The channel length is divided into segments as described above and have index k . The layers in the washcoat are denoted n . For the gas phase the mass balance can be written as: (Wang, 2008)

$$\frac{dy_{i,k,1}}{dt} C_{\text{tot}} V_{k,n} = F_{\text{tot}} (y_{i,k-1,1} - y_{i,k,1}) - \Gamma_{i,k,1} (C_{i,k,1} - C_{i,k,2}) \quad (2.6.1.1)$$

The solid phase mass balance is written as:

$$\begin{aligned} \frac{dy_{i,k,n}}{dt} C_{\text{tot}} V_{k,n} &= \Gamma_{i,k,n-1} (C_{i,k,n-1} - C_{i,k,n}) - \Gamma_{i,k,n} (C_{i,k,n} - C_{i,k,n+1}) \\ &+ \sum_j v_{j,i} r_{j,k,n} S_{\text{Pt}} m_{\text{Pt},k,n} \end{aligned} \quad (2.6.1.2)$$

2.6.2 Lumped mass transfer coefficients

The term $\Gamma_{i,k,n}$ is the lumped mass transfer coefficient and is given by: (Tronconi, 1992)

$$\Gamma_{i,k,1} = \frac{A_k}{\frac{1}{k_{c,i,k}} + \frac{0.5\Delta z_1}{D_{eff,i,k}}} \quad (2.6.2.1)$$

$$\Gamma_{i,k,n} = \frac{D_{eff,i,k}A_k}{0.5\Delta z_n + 0.5\Delta z_{n+1}} \quad (2.6.2.2)$$

for $n=2 \dots N-1$

$$\Gamma_{i,k,N} = 0$$

The lumped mass transfer coefficients originate from the equation of diffusive mass transfer at constant temperature and pressure and the equation of convective mass transfer. (Welty, 2001)

$$N_{i,z} = -D_{eff,i} \frac{dc_i}{dz} + y_i \sum_j N_{j,z} \quad (2.6.2.3)$$

$$N_{i,z} = k_{c,j} \Delta C_j \quad (2.6.2.4)$$

Assuming equimolar counter diffusion and a linear concentration profile in the washcoat the molar flux can be simplified to: (Welty, 2001)

$$N_{i,x} = -D_{eff,j} \frac{C_{i,k,2} - C_{i,k,surface}}{0.5\Delta z_2} \quad (2.6.2.5)$$

At the surface the transport by diffusion is equal to the transport of convection giving:

$$\begin{aligned} N_{i,x} &= -D_{eff,j} \frac{C_{i,k,2} - C_{i,k,surface}}{0.5\Delta z_2} = k_{c,j,1} (C_{i,k,1} - C_{i,k,surface}) \\ \Rightarrow N_{i,x} &= \frac{C_{i,k,1} - C_{i,k,2}}{\frac{1}{k_{c,i,k}} + \frac{0.5\Delta z_2}{D_{eff,i,k}}} \end{aligned} \quad (2.6.2.6)$$

Multiplication with the mass and heat transfer area gives total flow rate:

$$N_{i,x}A_k = \frac{A_k}{\frac{1}{k_{c,i,k}} + \frac{0.5\Delta z_2}{D_{eff,i,k}}} (C_{i,k,1} - C_{i,k,2}) = \Gamma_{i,k,1} (C_{i,k,1} - C_{i,k,2}) \quad (2.6.2.7)$$

Using the same assumptions for two solid layers gives:

$$\begin{aligned} N_{i,x}A_k &= \frac{A_k}{\frac{0.5\Delta z_n}{D_{eff,i,k}} + \frac{0.5\Delta z_{n+1}}{D_{eff,i,k}}} (C_{i,k,n} - C_{i,k,n+1}) = \\ &\Gamma_{i,k,n} (C_{i,k,n} - C_{i,k,n+1}) \end{aligned} \quad (2.6.2.8)$$

2.6.3 Heat balances

The number of heat balances is limited to only two. One for the gas phase and one for the solid phase where the solid phase heat balance sums up the heat from the reactions taking

place in all layers in the washcoat. For the gas phase the heat balance is written as: (Wang, 2008)

$$\frac{dT_{g,k}}{dt} c_{p,g} \rho_g V_g = F_{tot} C_{p,g} (T_{g,k-1} - T_{g,k}) - h_k A_k (T_{g,k} - T_{s,k}) \quad (2.6.3.1)$$

And for the solid phase the heat balance is written as:

$$\begin{aligned} \frac{dT_{s,k}}{dt} c_{p,s} \sum_n m_{s,k,n} &= h_k A_k (T_{g,k} - T_{s,k}) - A_s (q_{k+1} - q_k) \dots \\ \dots + A_l \frac{(\alpha_w + \lambda_s)}{2} \left(\frac{T_{s,k} - T_{l,k}}{0.5\Delta x_k + 0.5\Delta l} \right) &+ \sum_n \sum_j r_{j,k,n} (-\Delta H_j) m_{s,k,n} S_{Pt} \end{aligned} \quad (2.6.3.2)$$

Where q_k is calculated as:

$$q_k = -\lambda_s \frac{T_{s,k} - T_{s,k-1}}{0.5\Delta x_k + 0.5\Delta x_{k-1}} \quad (2.6.3.3)$$

for $k=2 \dots K-1, K$

$$q_k = 0$$

for $k=1$ and $k=K+1$

2.6.4 Effective diffusivity

The effective diffusivity for pore diffusion is given by: (Welty, 2001)

$$D_{eff,j,k} = \frac{f_D}{\frac{1}{D_{i,k}} + \frac{1}{D_{K,i,k}}} \quad (2.6.4.1)$$

Where $D_{i,k}$ is the binary diffusivity between component i and air as described under section 2.4.4 and the $D_{K,i,k}$ is the Knudsen diffusivity calculated by:

$$D_{K,j,k} = \frac{d_p}{3} \sqrt{\frac{8RT_{s,k}}{\pi M_i}} \quad (2.6.4.2)$$

2.7 Description of the wall

There are two kinds of walls in the system, the first kind being one that is connected to a neighboring channel and the second one is one that is connected to the surrounding.

2.7.1 The wall between two channels

In the wall between two channels only heat transfer taking place is conduction. The wall is described with by dividing it into five segments from each channel side. It is assumed that no mass is transferred between the walls. This gives only one heat equation to solve in the walls. A wall segment is denoted by l , short for layer and the heat balance is written like:

$$\frac{dT_1}{dt} c_{p,l} m_l = -A_s (q_{l+1} - q_l) \quad (2.7.1.1)$$

Where the heat flux is calculated as:

$$q_l = -\lambda_l \frac{T_l - T_{l-1}}{0.5\Delta l + 0.5\Delta l} \quad (2.7.1.2)$$

for $l=2 \dots L$

$$q_l = -\lambda_l \frac{T_l - T_s}{0.5\Delta l + 0.5\Delta l} \quad (2.7.1.3)$$

for $l=1$ (Where T_s is the temperature of the washcoat next to the first wall layer)

$$q_{l+1} = -\lambda_{l+1} \frac{T_{l+1} - T_l}{0.5\Delta l + 0.5\Delta l} \quad (2.7.1.4)$$

for $l=1 \dots L$ (Note that T_{l+1} is the neighboring cells last wall layers temperature if $l=L$)

2.7.2 The wall connected to the surrounding

As in the wall between two channels the wall connected to the surrounding the only transport taking place is the conduction. The balance for each layer in the wall connected to the surrounding is simulated adiabatic due to the insulation outside the DOC. The heat balance for the wall layers in a wall connected to the surrounding is written like:

$$\frac{dT_1}{dt} c_{p,l} m_l = -A_s (q_{l+1} - q_l) \quad (2.7.2.1)$$

Where the heat flux is calculated as:

$$q_l = -\lambda_l \frac{T_l - T_{l-1}}{0.5\Delta l + 0.5\Delta l} \quad (2.7.2.2)$$

for $l=2 \dots L$

$$q_l = -\lambda_l \frac{T_l - T_s}{0.5\Delta l + 0.5\Delta l} \quad (2.7.2.3)$$

for $l=1$ (Where T_s is the temperature of the washcoat next to the first wall layer)

$$q_{l+1} = -\lambda_{l+1} \frac{T_{l+1} - T_l}{0.5\Delta l + 0.5\Delta l} \quad (2.7.2.4)$$

for $l=1 \dots L-1$

$$q_{l+1} = 0 \text{ (adiabatic)} \quad (2.7.2.5)$$

for $l=L$

3. Methodology

This section will describe the methods used in describing the DOC. Focus lie on the methodology of the tanks in series approach.

3.1 Configurational setup

The channels in the system is related to each other so that number one is always located in the bottom left corner of the setup. If there only is one channel in the system the number one is the only one. If the system has four channels number one is still in the bottom left corner, number two is in the bottom right corner, number three is in the top left corner and number four in the top right corner. If the system contains more than four channels e.g. nine, sixteen or twenty five they are always calculated from the bottom row to the right in a n times n structure. Figure 12 shows how nine channels are simulated.

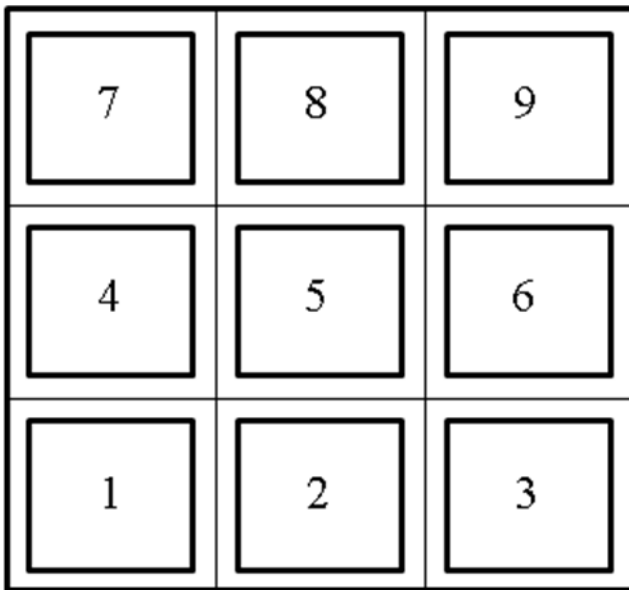


Figure 12. Description of a three times three setup of channels. Note the channel numbering from left bottom corner to the right corner then up to the second bottom row etc.

Every channel is built up by 470 nodes. These nodes represent both fractions and temperature in the system. The different nodes stem from the fractions of the included components together with the temperatures in the system. Table 2 clarifies the setup of nodes in the system.

Table 2. A description of the number of nodes in the system.

| Fractions | Index | Number |
|---------------------------------|-------|-------------------|
| Components | i | 5 |
| Segments | k | 10 |
| Washcoat layers (including gas) | n | 5 |
| | | $i * k * n = 250$ |

| | | |
|---------------------|---|-------------------------|
| Temperatures | | |
| Gas phase | k | 10 |
| Washcoat | k | 10 |
| Wall layers | l | 5 |
| Wall directions | d | 4 |
| Wall segments | k | 10 |
| | | $k+k + l * d * k = 220$ |

Figure 13 exemplifies the cross section setup of one channel. When the system is bigger than one channel these channels are connected to each other communicating between the outer wall layers.

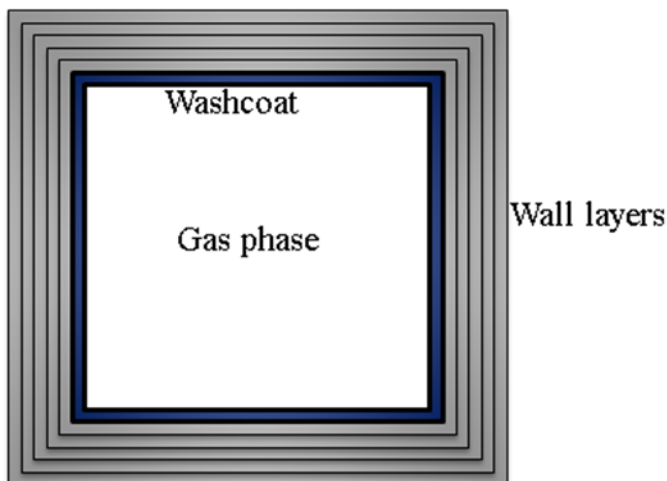


Figure 13. A cross section of one channel. Shows how the wall layers are simulated in the heat balances.

3.2 Matlab configuration

This section describes the structure of the Matlab program that has been produced and used. Figure 14 describes the connection between the different subroutines in the code. The different programs are explained more detailed later in this section. The arrows describing the communication between the programs will be explained as well.

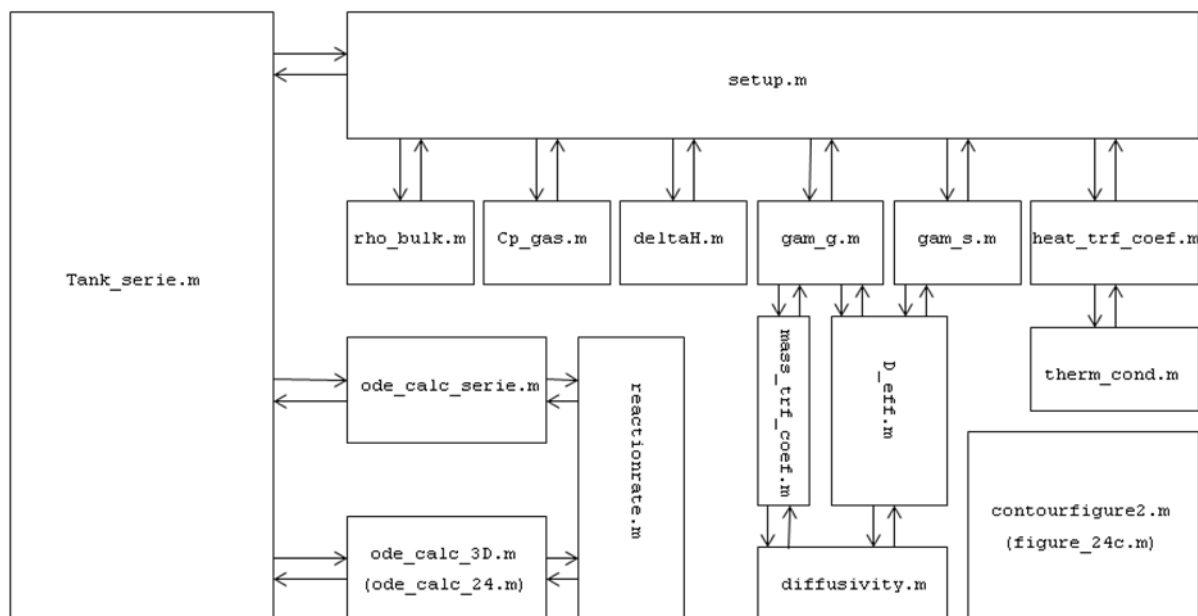


Figure 14. Explanation of the subroutines in the simulation program. The arrows represent the directions of which information is sent between programs.

The different files are described in Table 3 below. The table specifies the program name, the information it receives from connected programs and the information the file sends and/or returns to connected programs.

Table 3. Explanation of included program files. Gives the program name, received information together with information that is sent.

| Program name | Received information | Sent/Returned information |
|--------------|---|--|
| Tank_serie.m | All information regarding the simulation from setup.m, such as physical properties, dimensions, initial fractions. Receives the solutions from the ode files. | Sends the initial conditions to the ode files along with all ode settings. |
| setup.m | Receives physical properties from the subroutines | Returns physical properties that have been received along with data that the user specifies in the file, such as flow, flow profile, DOC dimensions. |
| rho_bulk.m | Temperature and pressure | Gas phase density that has been interpolated from a database. |
| Cp_gas | Temperature and pressure | Heat capacity that has been interpolated from a database. |
| deltaH.m | Temperature | Heat of formation for all compounds included in the reactions. |
| gam_g.m | Temperature, pressure and system dimensions. Calls for mass transfer coefficient and effective diffusivity | Lumped mass transfer coefficient for gas phase. |
| gam_s.m | Temperature, pressure and system | Lumped mass transfer coefficient |

| | | |
|-----------------------------------|---|--|
| | dimensions. Calls for effective diffusivity. | for the solid phase. |
| heat_trf_coef.m | Temperature, pressure and system dimensions. Calls for thermal conductivity of the gas phase. | Heat transfer coefficient for the gas phase. |
| mass_trf_coef.m | Temperature, pressure and system dimensions. Calls for diffusivity. | Mass transfer coefficient. |
| D_eff | Temperature, pressure and system dimensions. Calls for diffusivity. | Effective diffusivity. |
| diffusivity.m | Temperature and pressure. | Diffusivity for all components |
| therm_cond.m | Temperature and pressure. | Gas phase thermal conductivity that has been interpolated from database. |
| ode_calc_serie.m | All properties in the heat and mass balances. Is called using ode15s. Simulate only a short time to receive steady state values of the reactions. | Solution to the fractions (and temperatures) for a short interval of time. Calculates one channel at the time. |
| ode_calc_3D.m (ode_calc_24.m) | All properties in the heat and mass balances. Is called using ode15s. (Different configuration to solve a system of 24 channels in a circular system) | Solution to specified simulation time for the entire system. Using steady state solution for the mass balances but solves transient heat balances. |
| reactionrate.m | Fractions of all reacting components and temperature. | Reaction rates at specified fractions and temperature. |
| contourfigure.m (figure_24c.m) | Uses the results from Tank_serie.m to plot results. | A number of plots of the simulation. |

4. Results

4.1 Discretized code results

The discretized code results are not presented further than the theoretical procedure shown under the section theory. The reason for this is that an early version of the code showed this procedure to be far too time consuming when it came to calculation time. Since the desire is to simulate multiple channels in a connected configuration with temperature transport between the channels, it turned out to be too complex. Already while only one channel was simulated, excluding the temperature in the channel, simulating 2 seconds took about 30 hours. Extrapolating this result to a simulation time of an hour or more and multiplying the number of channels up to ten this gives in theory more than 50 years in simulation time. There is no doubt that this procedure could have been improved and made faster, but instead of putting time into doing this, a new procedure was investigated, the tanks in series. This turned out to be way more time efficient and was therefore used throughout the work.

4.2 Investigation of kinetic data used

Since no experimental data has been received in order to validate and calibrate the model that has been created, it is instead important to investigate the behavior if the data used. As mentioned earlier the kinetics used has been adopted from (Wang, 2008). Data in experiments by the authors has been calibrated to fit the experimental data of a 2.0 liter, 4-cylinder in-line diesel engine with a power of 126 hp at 4000 rpm. The resulting kinetics for this type of engine behaves according to the following tables. First are the parameters for determining the adsorption equilibrium constants in Table 4 and second is the kinetic parameters used in Table 5.

Table 4. Parameters for determining adsorption equilibrium constants.

| Adsorption pre-exponential factor [-] | | Adsorption heat /R, [K] | |
|---------------------------------------|--------|-------------------------|--------|
| K ₁ | 65.5 | E _{a,1} | -961 |
| K ₂ | 2.08e3 | E _{a,2} | -361 |
| K ₃ | 3.98 | E _{a,3} | -11611 |
| K ₄ | 4.79e5 | E _{a,4} | 3733 |

Table 5. Kinetic parameters used in the simulations.

| Species | Pre-exponential factor [mol·K/(m ² s)] | Activation temperature [K] |
|---------|---|----------------------------|
| CO | 1.30060e15 | 12661.39 |
| HC | 8.30871e7 | 5915.68 |
| NO | 5.9565e6 | 4733.13 |

The reason for investigating the kinetic data is to find whether or not the specific reaction rates of any of the components acts oddly compared to the others. If this is the case it could be possible to explain simulations that give unexpected results. Table 6 shows the relevant data used for the comparison of the reaction rates of the included components.

Table 6. Fractions used when kinetic data has been investigated.

| Component | Fraction [-] | Fraction [ppm] |
|-----------------|--------------|----------------|
| CO | 3.51e-4 | 351 |
| HC | 1.66e-4 | 166 |
| NO | 1.09e-4 | 109 |
| NO ₂ | 4.2e-5 | 42 |
| O ₂ | 0.085 | 85000 |

The reaction rate of the included components has been plotted against temperature in Figure 15 and Figure 16.

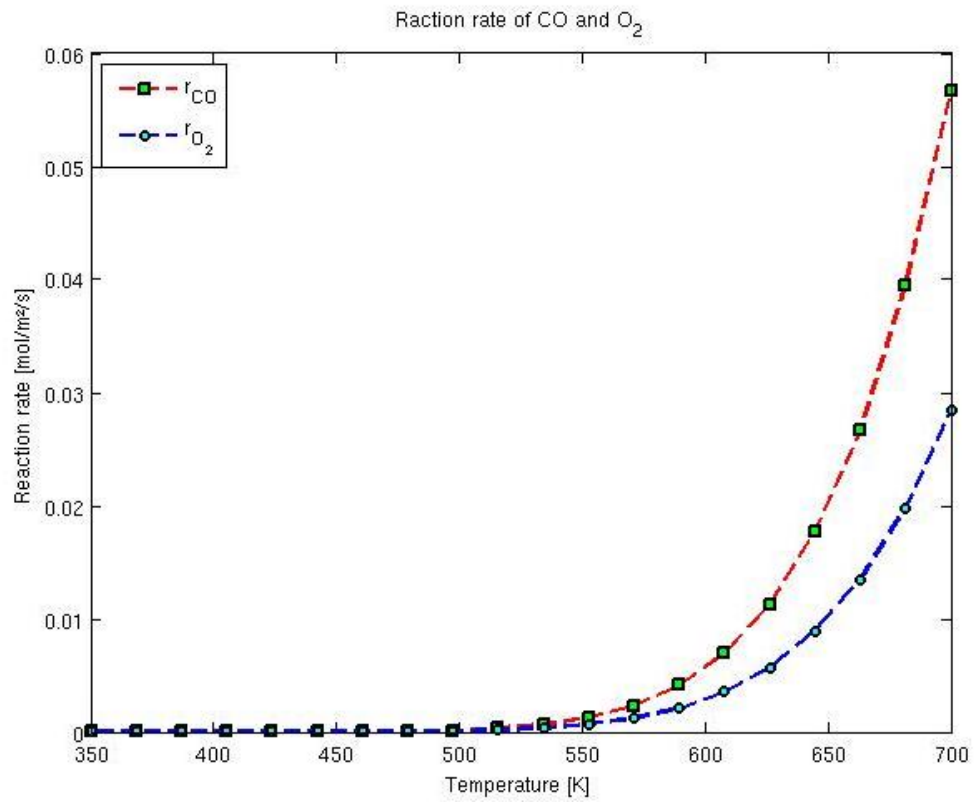


Figure 15. Reaction rates for carbon monoxide (CO) and oxygen (O₂) in the model on the temperature interval 350 to 700 K.

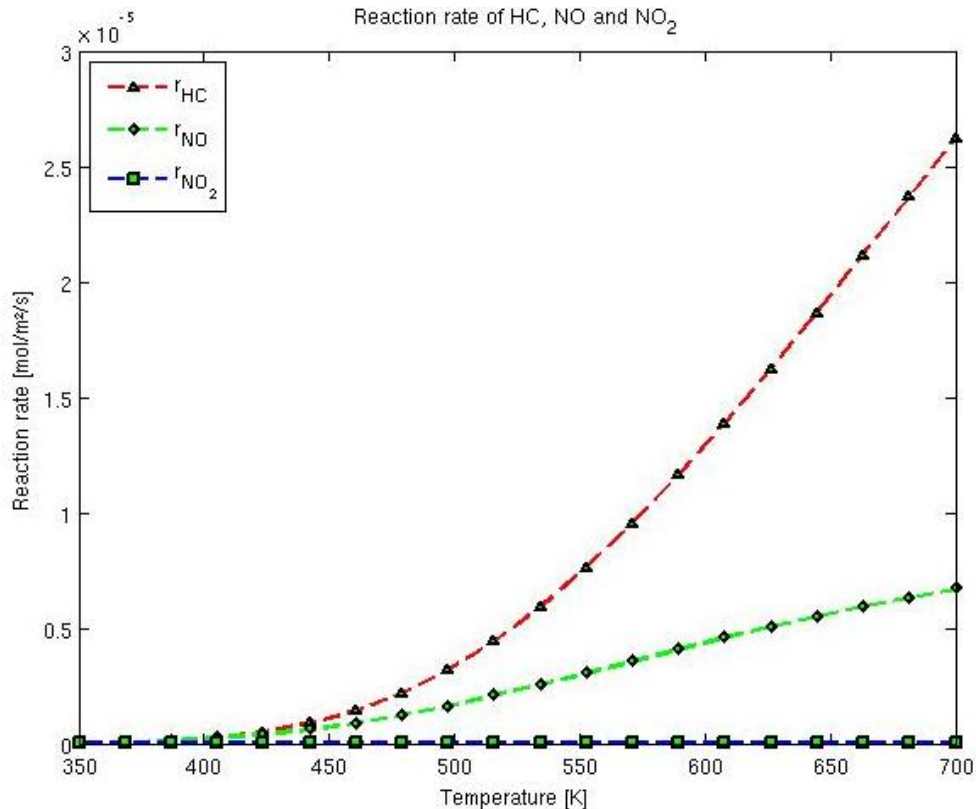


Figure 16. Reaction rates for hydrogen carbons (HC), nitric oxide (NO) and nitrogen dioxide (NO₂) in the model on the temperature interval 350 to 700 K.

In the figures it is obvious that all components increase their reaction rate with increased temperature. This might not come as a surprise due to the different reaction rate expressions. It can be seen that the highest reaction rate is that of carbon monoxide, especially after about 450 K in temperature. The self dissociation of NO₂ can not be seen at these low temperatures using these basic settings.

4.3 One channel results

The one channel results will mainly deal with the DOC behavior in terms of conversion of the included components. These results will be used to investigate the properties of the model. The reason for this is that temperature distribution and propagation is rather uninteresting when it comes to one channel, since no interaction between channels take place.

4.3.1 Basic values used in simulation

There are a number of different values in a work like this that needs to be determined and rated in order for a model to describe real experimental data. Since no data has been given in order to calibrate and validate the model these numbers and constants has been set according to the best ability. The used constants and figures do not represent a real DOC, but rather a mixture of different DOC:s found throughout literature.

It is these different numbers that has been investigated in the resulting section in order to validate the physical behavior of the DOC. Below in Table 7 is a list with the basic dimensions and physical properties and conditions presented. These values are to be seen as some kind of starting values for the model behavior.

Table 7. User specified entities to the DOC model. The initial fractions to the DOC can be found in Table 6.

| Description | Value | Unit |
|--------------------|----------|-------|
| DOC length | 0.2 | m |
| DOC diameter | 0.2667 | m |
| Temperature | 500 | K |
| Pressure | 150000 | Pa |
| Wall thickness | 1.651e-4 | m |
| Washcoat thickness | 1.1e-4 | m |
| Flow to the DOC | 0.5 | mol/s |
| Cell density | 400 | cpsi |
| Channel size | 8.849e-4 | m |
| Catalyst load | 0.7 | g/l |

Using all these values for a one channel simulation renders a series of results that is presented in Matlab. Below is a series of data and graphs that is obtained by simulating, these results are supposed to be used in order to understand the behavior of the model. The first result is a table displayed in the command window of MATLAB giving the mean values for all the channels simulated. The values in Table 8 are from a simulation of one channel.

Table 8. Data calculated automatically by the MATLAB program that is presented after one simulation in the command window.

| Component | Inlet (ppm) | Outlet (ppm) | Reduction (ppm) | Conversion (%) |
|-----------------|-------------|--------------|-----------------|----------------|
| CO | 351 | 96.88 | 254.12 | 72.40 |
| HC | 166 | 140.75 | 25.25 | 15.21 |
| NO | 109 | 95.62 | 13.38 | 12.27 |
| NO ₂ | 42 | 55.38 | -13.38 | -31.85 |
| O ₂ | 85000 | 84752.63 | 247.37 | 0.29 |

In order to obtain more detailed information about the system it is necessary to run the program `contourfig.m`. This will generate a number of figures with information regarding the conversion along the DOC and temperatures in the system. Figure 17 gives the fractions of CO in each layer in the washcoat during the first seconds. This is to investigate if the components have reached a steady state behavior. The steady state results from the first part of the simulation are then used as a starting guess for the full simulation. It is there assumed that the reactions are steady state while the temperature is simulated transient in the system.

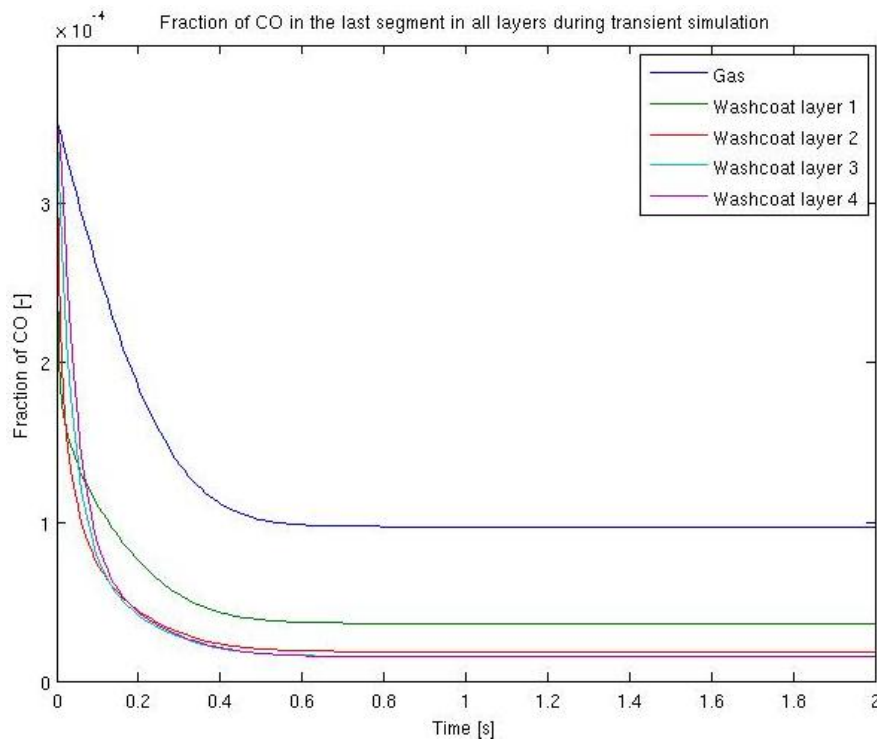


Figure 17. Result for CO from the initial transient simulation to investigate steady state behavior. The transient result is for a 2 second simulation.

Similar graphs are presented not only for CO, but also for HC, NO and NO₂. These figures will not be presented here due to similarity to Figure 17 and space limitations. Instead the reader is referred to the actual program in Matlab to investigate remaining components. The next figure gives the steady state conversions of CO, HC and NO along the DOC.

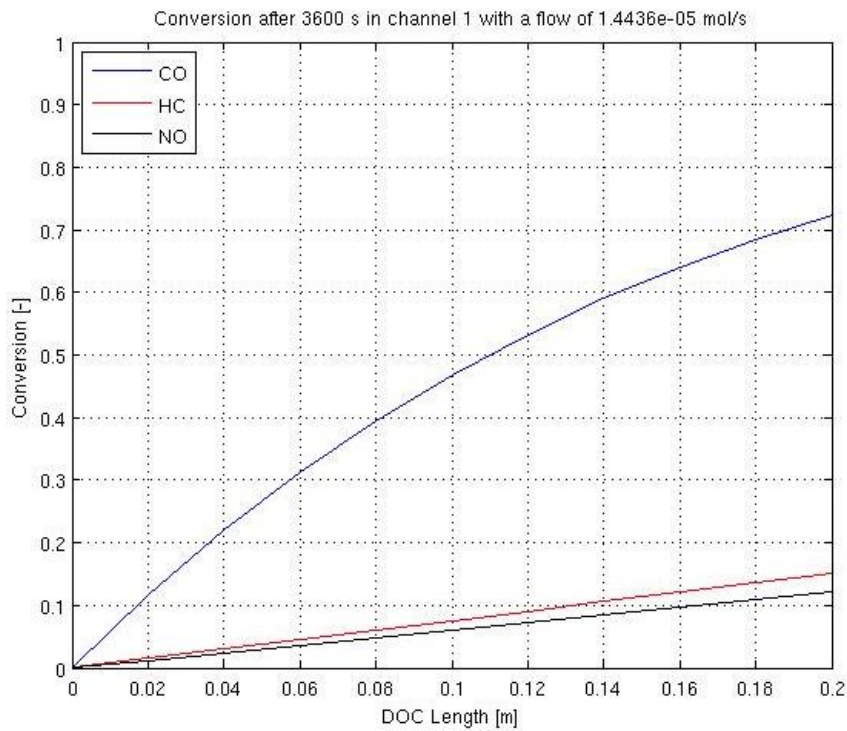


Figure 18. Steady state conversions in the simulated channel of components CO, HC and NO. The result is the calculated result along the channel of the DOC.

As a complement to the plot of the conversion a figure with the actual fractions are plotted as well. The fractions of CO, HC, NO and NO₂ along the DOC is shown. This can be seen in Figure 19.

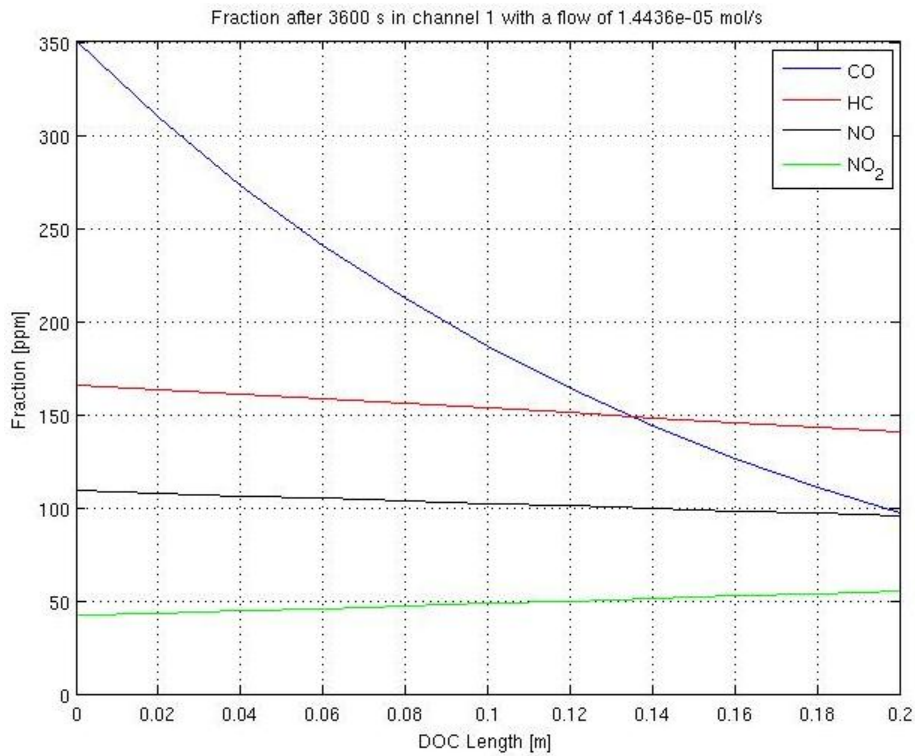


Figure 19. Steady state fractions along the DOC of carbon monoxide, hydro carbons, nitrous oxide and nitric dioxide.

The following figures are plotting temperature in different ways. Figure 20 shows the temperature across one channel. The values in the figure are the five wall layers on each side of a channel together with the washcoat temperature and the gas phase temperature in the center.

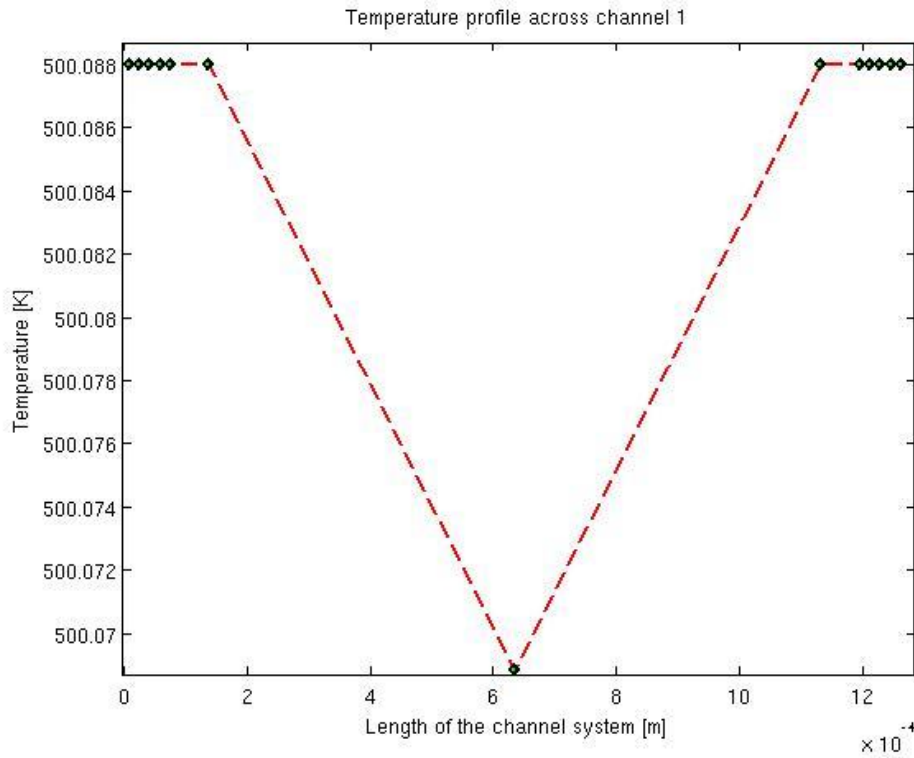


Figure 20. *Temperature profile across the channel simulated in segment 5 on the length of DOC, which means just next to but after the center. The center value represents the gas phase the two values next to the center represents the washcoat and the other values are the wall temperatures.*

Figure 21 shows the steady state temperature along the DOC, in the washcoat and in the gas phase of the channel simulated. Since the washcoat is simulated as one section, this figure will represent the temperature in the washcoat all around the DOC.

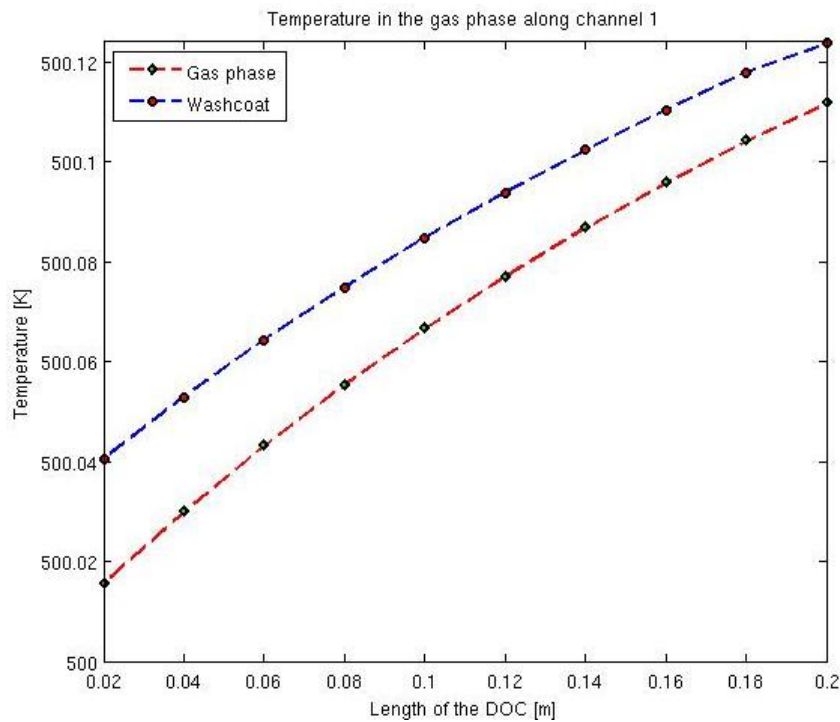


Figure 21. Temperature along the DOC in both gas phase and in the washcoat. The figure represents the steady state temperature in the channel.

In Figure 22 the temperature change with time is presented for the same domain as in the previous figure. Here segment five is investigated during the first 80 seconds of the simulation. This figure gives a good hint on how long it takes with the current system settings before the temperature reaches steady state in the system.

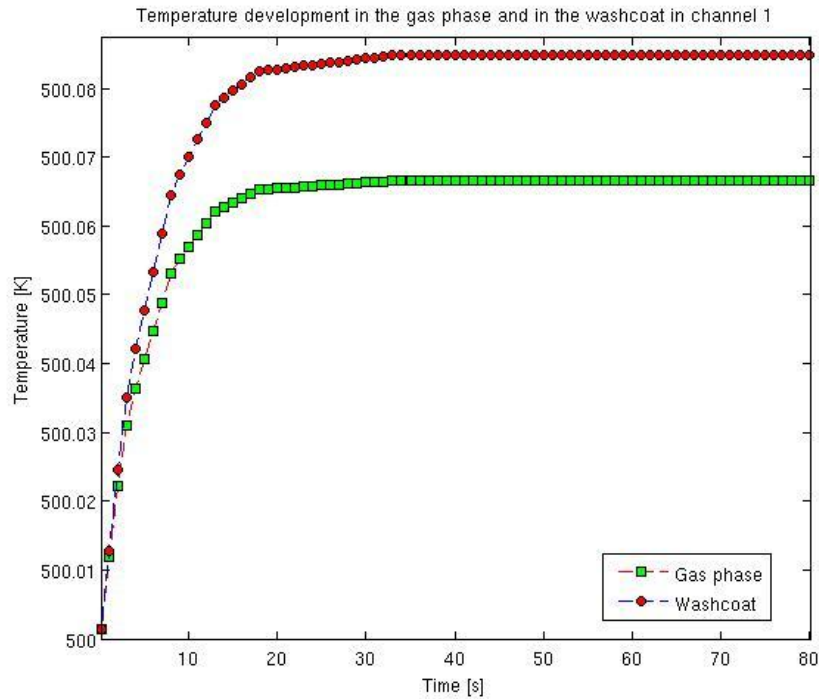


Figure 22. Temperature development in gas phase and in washcoat with time in segment 5 of the DOC. The result is from a transient simulation of temperature in one channel.

The following figure gives contour temperature profile along the channel that is simulated. The result is displayed in a short movie, but here it is presented as contour plots at different times. Since only one channel has been simulated the channels has been cut in half due to symmetry and space reasons.

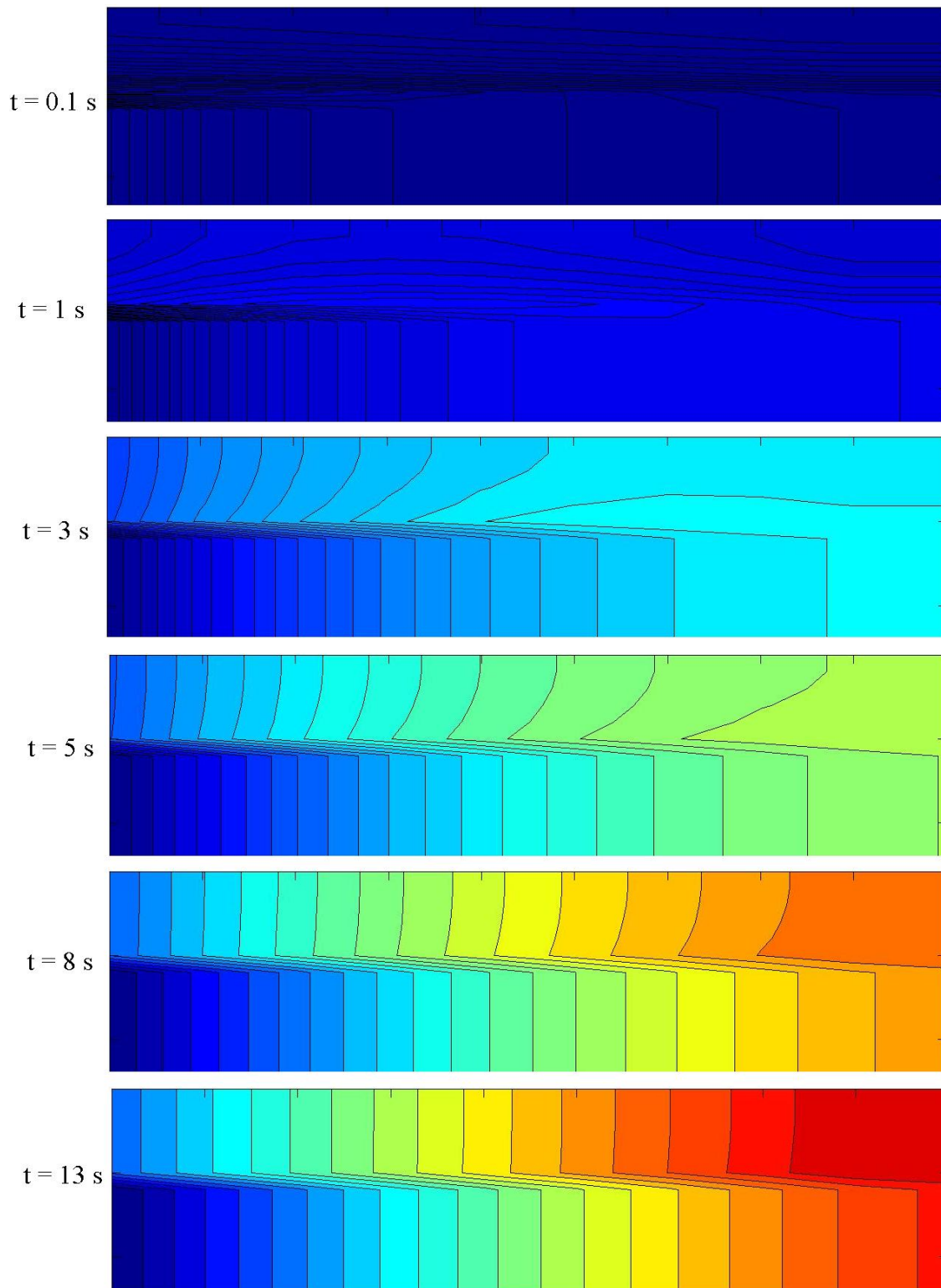


Figure 23. Contour plot of temperature along the DOC channel (half) for 6 different times. The different pictures represents different times and makes it possible to evaluate the temperature development in time.

The other possible contour plot is shown in Figure 24 and is the temperature in a cross section of the channel. This way of displaying the temperature profile in the cross section of the channels are more interesting when the flow profile varies for a number of channels simulated

together. The included pictures in Figure 24 has been cut in quarters, once again from only simulating one channel giving total symmetry in the quadratic channels and its surrounding.

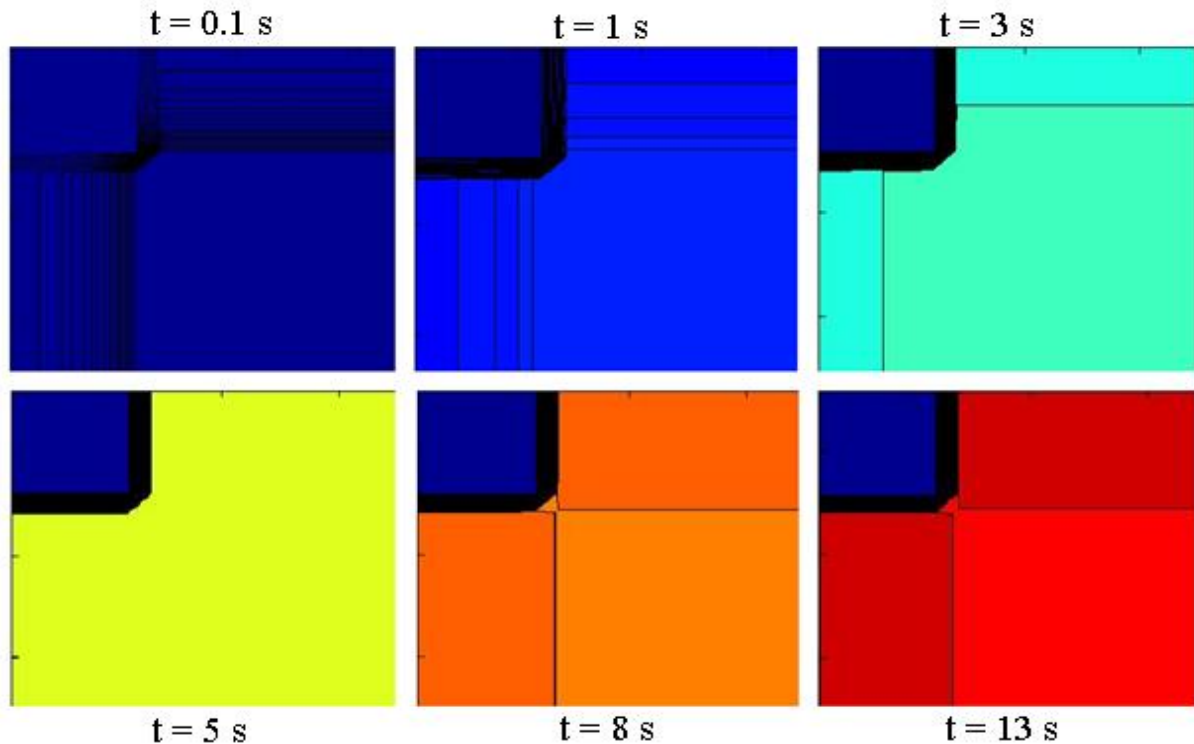


Figure 24. Contour plot of temperature in a quarter of the cross section of a DOC channel. The different pictures represents different times and makes it possible to evaluate the temperature development in time.

All the data presented in this subsection is the result of using the settings presented in Table 7. The following sections will mainly focus on conversions of the included components and investigate the effect of changing physical properties.

4.3.2 Varying temperature

Temperature is a large factor when it comes to chemical reactions, probably the biggest contributor to changes in reaction rate. It is therefore of largest interest to find out how changes in temperature affect the conversion in the DOC. In this test temperature has been changed between 300 and 680 K. In Figure 25 the conversions at steady state has been plotted against temperature for a number of simulations. Once again only one channel has been simulated, with the setting that is specified in Table 7. The conversion of oxygen has been multiplied with a factor hundred in order for the change to be noticed in the figure.

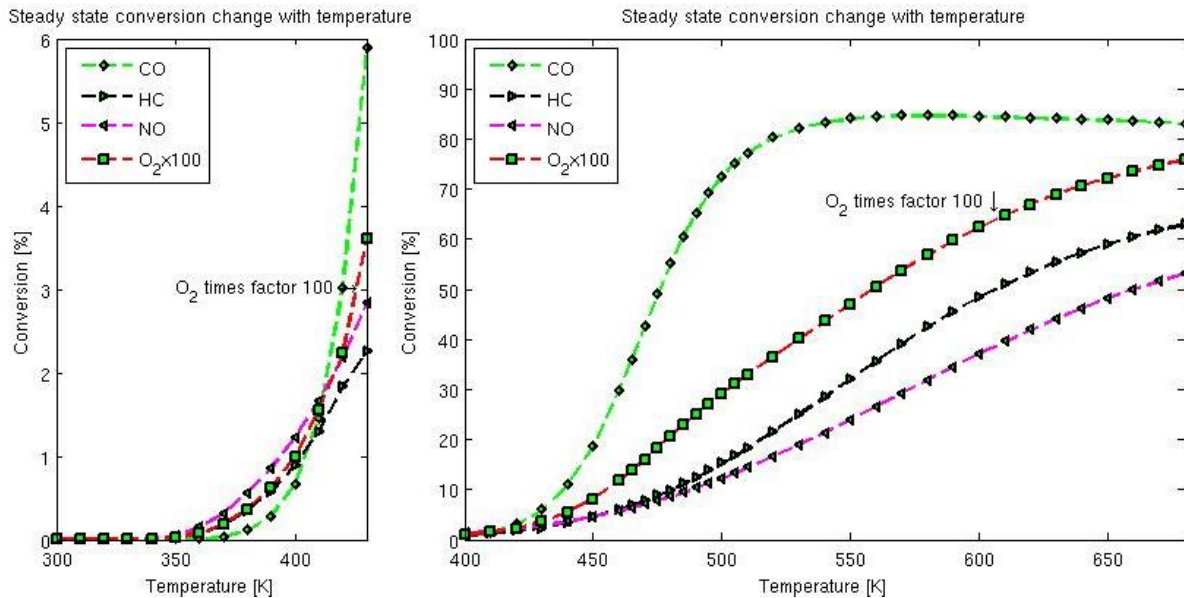


Figure 25. (Left) Change in steady state conversion with temperature on the interval 300 to 430 K. (Right) Change in steady state conversion with temperature on the interval 400 to 680 K. In general the steady state conversion increases with increasing temperature.

From Figure 25 it is possible to see that the conversion of carbon monoxide is most heavily affected by a change in temperature. At the lower temperatures around 400 up to 500 K the rate of change in conversion is strongly positive while it is reduced after 500 K and even becomes somewhat negative at temperatures above 550 K. The conversion of the other components, hydrocarbons, nitrous oxide and oxygen are steadily increasing as temperature increases. It seems that there is a theoretical maximum conversion for carbon monoxide using earlier specified settings and varying temperature. However it is impossible to say that is the case, because the behavior at even higher temperatures is not investigated due to simulation limitations. It is however possible to say that according to the model there is a local maximum present.

Increasing the temperature further will result in a high temperature increase in the system; this temperature increase will result in a higher system temperature and will push the steady state conversions higher. When these data are used in the part of the simulation where fractions are simulated as steady state the change in temperature results in difficulties to find the steady state fractions. This is partially counteracted by increasing the initial simulation time for the transient simulations with temperature. However after a certain point this difference becomes too large for the ode-solver to handle.

4.3.3 Varying pressure

In general it is the difference in pressure between inlet and outlet that keeps the gas flowing in the system. However in this simulation the pressure is assumed to be constant. The theoretical lowest pressure interesting is that of normal atmospheric pressure. That will be the lower limit of the pressure variation. Figure 26 displays the result of the pressure variation.

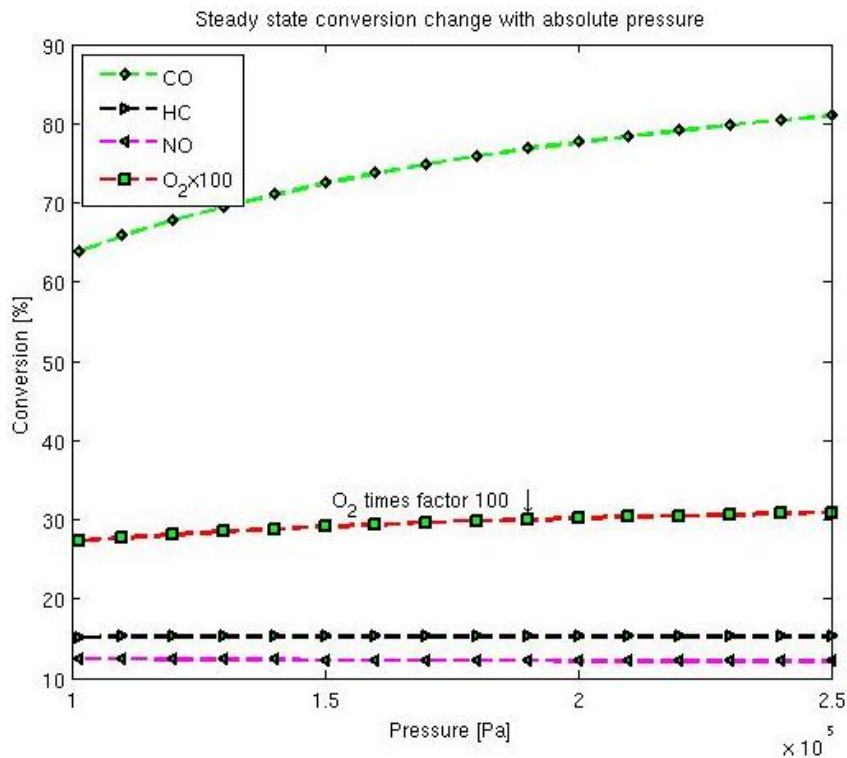


Figure 26. Change in steady state conversion with system pressure. The effect of pressure on steady state conversion is small and is from this figure only affecting the conversion of CO and O₂.

From Figure 26 it is possible to see that the highest absolute impact to conversion from pressure is on carbon monoxide. There is also a change for oxygen in the system. This is however directly related to the amount of carbon monoxide catalyzed. Note that in the figure none of the graphs are actually linear. Oxygen is slightly increasing, nitric oxide is actually decreasing with increasing absolute pressure and hydrocarbons display some kind of local maximum over the specified interval, initially increasing.

4.3.4 Varying flow

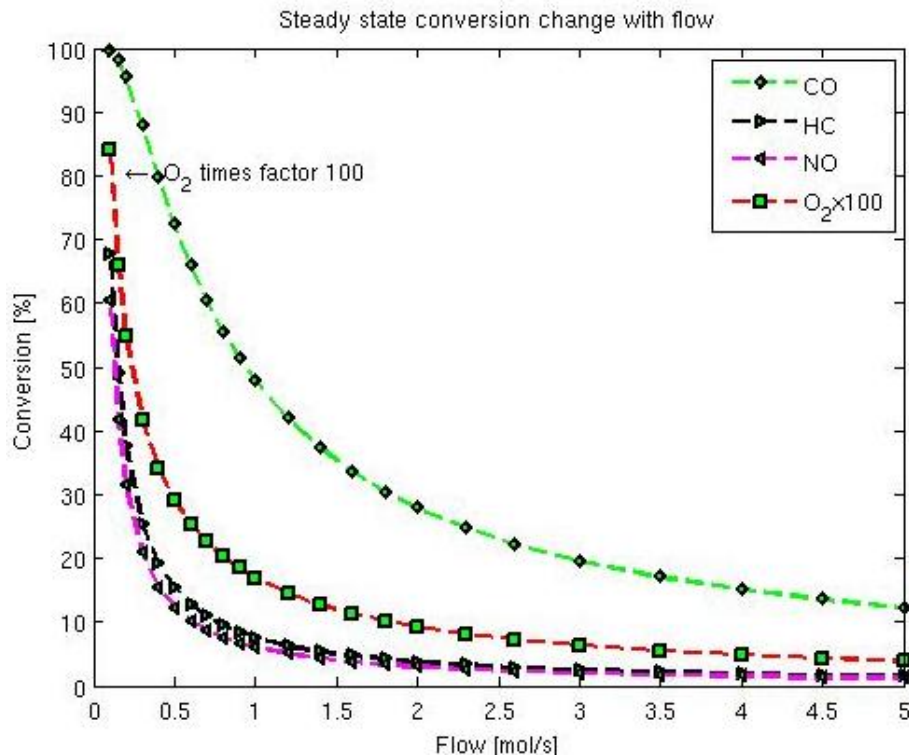


Figure 27. Change in steady state conversion with flow to the DOC. Increasing the flow in the system will reduce the steady state conversion of all included components.

Increasing flow will result in a lower conversion of all the components categorical. This can be seen in Figure 27. Increasing flow will result in a shorter residence time in each node and in the entire channel. This is because the velocity is increased when the flow is increased. The velocity increases linearly with the flow.

4.3.5 Varying DOC dimensions

In testing the behavior of the model when the DOC dimensions are changed, it is possible to change the diameter of the DOC together with the DOC length. It should be noted that changing the diameter of the DOC does not give any real changes to the dimensions in a specific channel. Instead it is the flow to the individual channels that is varied e.g. if the area is doubled the velocity is reduced by a factor 2. This makes the investigation closely related to when flow is varied. However the length is a rather interesting parameter to vary in the DOC. Intuitively one could imagine that the conversion in the DOC would double if the length of the DOC was doubled. Figure 28 shows that this is not the case at all.

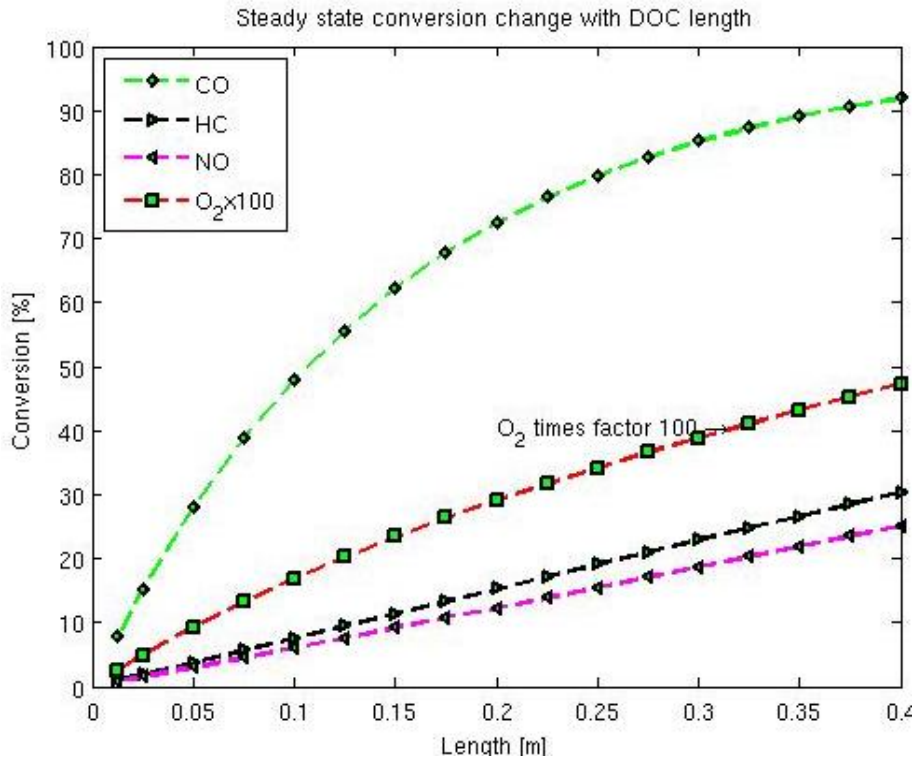


Figure 28. Change in steady state conversions with DOC dimensions, more specifically the length of the DOC is investigated. Increasing the length of a channel will result in higher conversion for all components.

Using the base case as a reference where the diameter is 10.5 inches (0.2667 m) and the length of the DOC is 0.2 meters the conversion of carbon monoxide and hydrocarbons are 72.4 % and 15.21 % respectively. Doubling the length of the DOC gives a conversion of 91.89 and 30.31 respectively.

4.3.6 Varying composition (Fraction of O₂ and HC)

There is always the possibility of varying fractions from the engine. This is rather the usual pattern in an engine. Initially a change in the level of oxygen will be tested and then also a change in the hydrocarbon level. The reason for testing hydrocarbon level is that propylene has the highest heat of reaction, hence a increase in hydrocarbons is expected to result in a higher temperature. For this reason the highest temperature in the system will be investigated as well. In Figure 29 the inlet level of oxygen is varied. Note that the conversion of oxygen has been excluded from the figure. This is because this is the varied entity in the investigation. A lower level of oxygen will increase the conversion and vice versa.

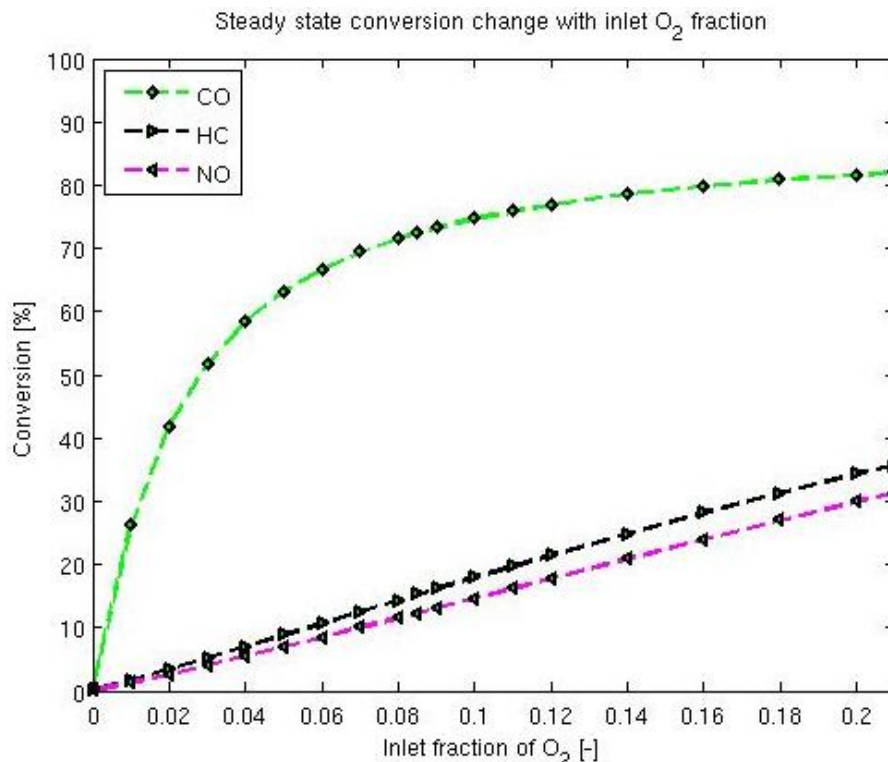


Figure 29. Change in steady state conversion with inlet fraction of oxygen. When the fraction of oxygen is increased the steady state conversion of all the components is increased.

An increased inlet fraction of oxygen gas increases the conversion of each component. The investigation is limited between 0 and 21 %, this is because 21 % is the amount of oxygen present in air. It would be therefore be unrealistic to simulate a higher fraction of oxygen than 21 %.

It is assumed that the change in temperature is mostly affected by the fraction of hydrocarbons in the system. This is because the hydrocarbons have the highest reaction heat of all the components included. Simulating at the base case of 500 K will not result in a temperature increase big enough to highly increase the general level of conversion but it is possible to investigate the increase of the temperature in the outlet of the DOC still.

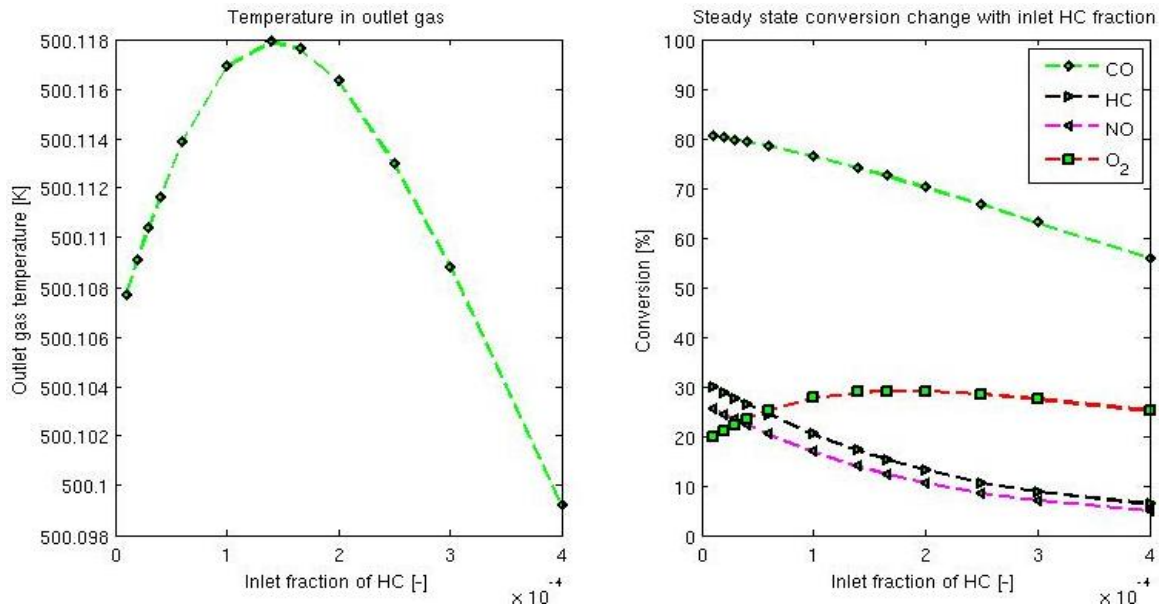


Figure 30. (Left) Change in steady state outlet gas temperature with inlet fraction of hydro carbons. (Right) Change in steady state conversions with inlet fraction of hydrocarbons.

The result from Figure 30 leads to somewhat of a predicament. Initially the temperature increases with increased inlet fraction of hydro carbons, but after a certain point (a simulated value of hydro carbon inlet fracture of 1.4×10^{-4}) the outlet gas temperature instead decreases. From the result in the right section of Figure 30 it can also be seen that the inlet fraction of HC affects the total steady state conversion of all the components. When the inlet fraction of hydro carbons is increased the reaction steady state conversion of all the included components are reduced.

4.3.7 Varying catalyst load

The effect of varying the catalyst load can be seen in Figure 31. The base case catalyst load is 0.7 g/l, and the load is changed between 0 and 1.4 g/l. It is expected that a higher catalyst load will result in higher conversion of all the included components. This can be seen in the solid phase mass balance where the reaction rate is expressed in terms of mol/s/m^2 and the mass of catalyst load will affect the total catalyst area, hence increasing the amounts of mol per second reacting.

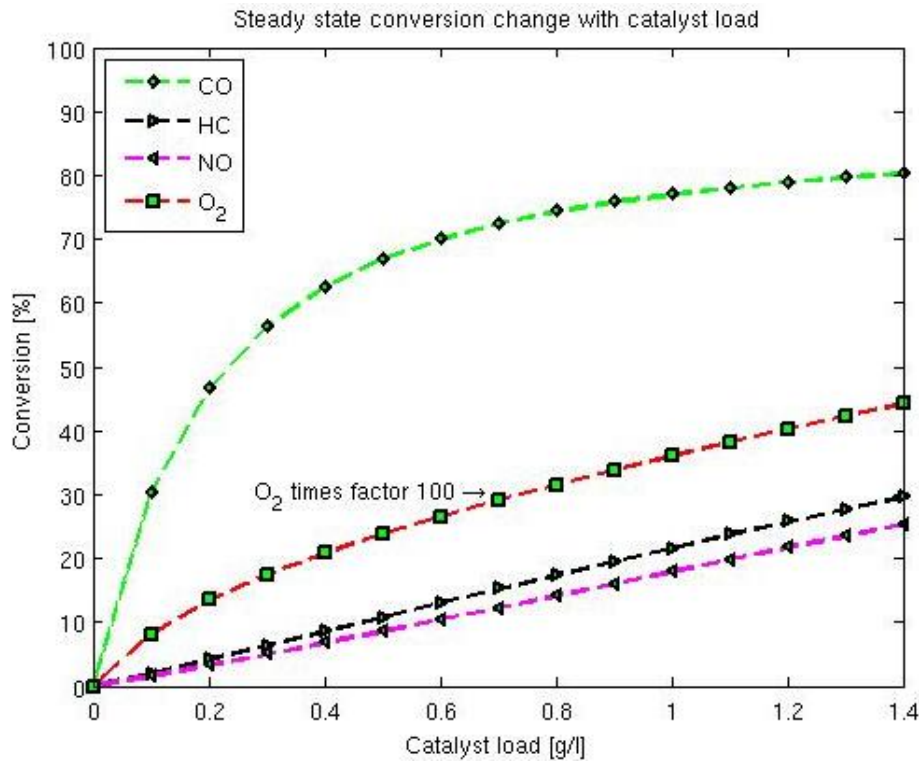


Figure 31. Change in steady state conversion with amount catalyst load. Increasing the amount of catalyst load in the system will increase the conversion of all the components.

4.3.8 Varying cell density

Commercial diesel oxidation catalyst are most often produced with a cell density of either 400 cpsi or 600 cpsi. Therefore only these two will be tested. The base case consists of 400 cpsi. The conversion of the interesting component can be seen in Table 9. Note that in this investigation the washcoat thickness and the wall thickness is kept constant. What is actually changed between the two different cell densities are the cell opening, and of course the flow to each channel. It is found that the conversion becomes slightly higher of all the components when the cell density is increased; this is even though the velocity of the system is increased and then the residence time decreased.

Table 9. Steady state conversion at two different cell densities.

| | 400 cpsi | 600 cpsi |
|----------------------------------|----------|----------|
| Conversion of CO [%] | 72.40 | 76.93 |
| Conversion of HC [%] | 15.21 | 17.37 |
| Conversion of NO [%] | 12.37 | 14.06 |
| Conversion of O ₂ [%] | 0.29 | 0.32 |
| Velocity [m/s] | 0.51093 | 0.58847 |

4.3.9 Temperature increase in the system

Investigating the temperature increase in the system is very wide. Changing any of the earlier varied entities gives changes to the temperature development and distribution. However most differences can be seen when the system start temperature is increased. The actual distribution

is often similar to what can be found in Figure 23 and in Figure 24 even if the absolute values are changed. The reason for this is that only simulating one channel with a constant temperature at the outer walls does not give big changes. In Figure 32 the system starting temperature is plotted against the difference between the system starting temperature and the system maximum temperature. This will give an idea about what running temperature that is required to get a relatively high temperature increase in the one channel DOC model.

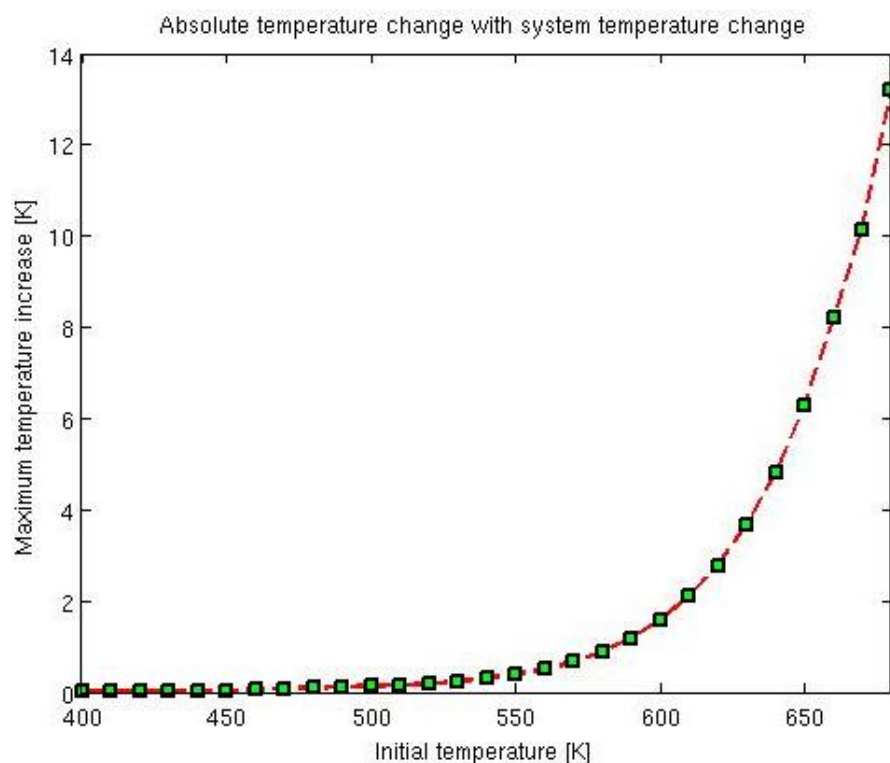


Figure 32. Change in system maximum temperature with system starting temperature over the interval 400-680 K. Increasing the inlet temperature will increase the temperature increase in the system.

4.3.10 Summary of one channel results

The results presented under section 4.3.1 are based on the basic values used. All the following sections do not include the graphs that are produced by the file contourfig2.m. The reason for this is that doing so would require enormous amounts of space, making this report only filled with similar figures. The reader would then be lost in all the figures and the report would be too promiscuous. Instead if there is an interest in a specific setting the reader is referred to the actual code and running the specific system individually.

The focus under section 4.3 is instead on varying settings that normally would change during a realistic use of the DOC, and to see how this would affect the steady state conversions of the included components.

It is extremely important to remember when looking at the temperature contour plots in the following section that the colors are scaled individually for every figure. Looking at the segments between the channels are always experienced as deep blue, this is because these section has automatically been awarded the system initial temperature. The temperature development in the channels, walls and wash coats is then scaled with each individual systems

maximum temperature. This will make the minimum and maximum temperature colors the same even if the absolute temperatures between simulations are different.

4.4 Multiple channel results

In this section a number of different flows will be investigated mainly in a system with 4 channels in a 2x2 configuration. The flow to each channel will be different and the interaction between the channels will be investigated, especially the steady state temperature profile in the system. Note again that if nothing else is specified the base settings are used and they can be found in Table 7. Section 4.4.2 handles a setup of 9 channels and section 4.4.3 handles a setup of 24 channels in a near circular configuration. Note that it is possible to run the program using 16 and 25 channels as well. These are not included in the result section due to the smaller individual channels in the figures.

4.4.1 Four (4) channel configuration

Different four channel flow setups will be tested in this section and the result will be evaluated.

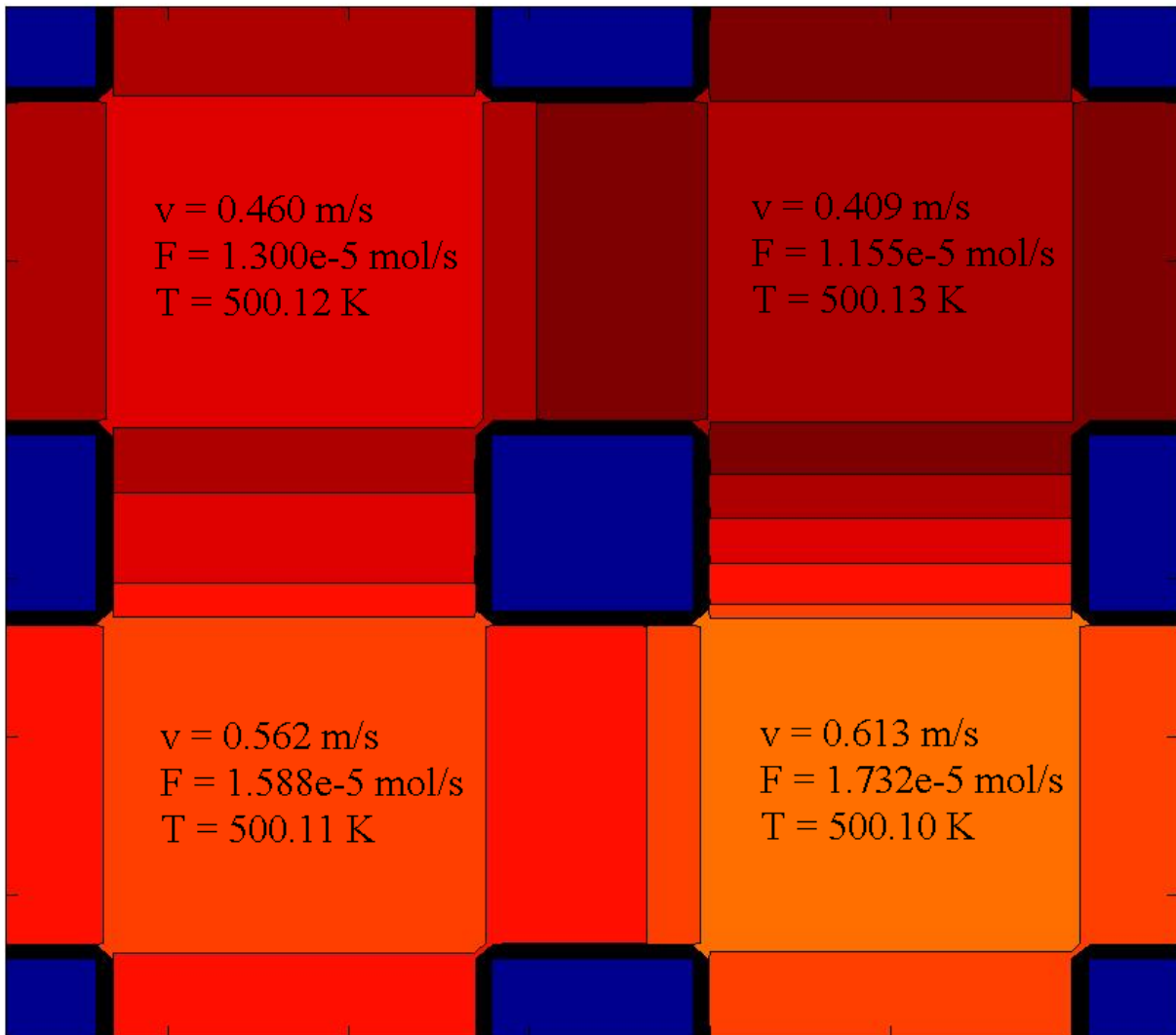


Figure 33. Four channel model with different flows to each channel. Bottom left is channel 1, bottom right is channel 2, top left is channel 3 and top right is channel 4. Note that the cross section is in segment 10.

In Figure 33 the steady state temperature distribution in the last part of the DOC, segment 10, is displayed. It is shown that the temperature is affected by the individual flow of each channel. Where the flow is higher and the temperature is lower and vice versa. The flow to a channel is directly proportional to the velocity of that channel. Note also that the total flow to the system is still the same. The different flows result in different conversion in each channel. These conversions of carbon monoxide, hydro carbons, nitric oxide and oxygen can be seen in Table 10 below, the values are for each individual channel and the total value of the system.

Table 10. Comparison between conversion in individual channels and the entire system in a 4 channel configuration. The inlet temperature is 500K.

| Channel | Flow (mole/s) | CO | HC | NO | O ₂ |
|---------|---------------|-------|-------|-------|----------------|
| 1 | 1.588e-5 | 69.05 | 13.82 | 11.13 | 0.27 |
| 2 | 1.732e-5 | 65.93 | 12.65 | 10.17 | 0.25 |
| 3 | 1.300e-5 | 75.99 | 16.91 | 13.68 | 0.31 |
| 4 | 1.155e-5 | 79.81 | 19.04 | 15.45 | 0.34 |
| System | 0.5 | 71.83 | 15.21 | 12.28 | 0.29 |

In Figure 34 the temperature distribution along the DOC is displayed, here in the channels and in the walls of channels 1 and 3. It is possible to see that the temperature increases along the DOC and the highest temperature is in the end of the DOC.

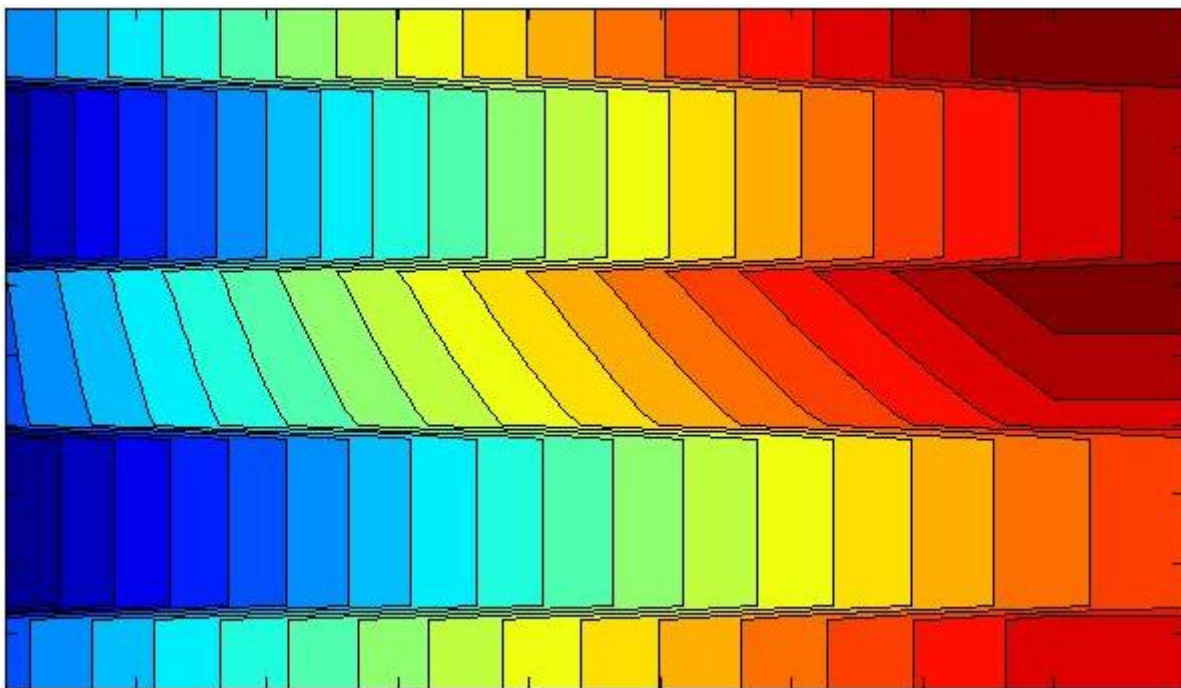


Figure 34. Temperature distribution between channels 1 and 3 along the channels, bottom part is channel 1 and top part is channel 3. The inlet is to the left and the temperature is increasing while the coloring turns redder.

In the next 4 channel experiment the flow configurations have bigger difference between the channels. Channels 1 and 2 have very low flow while channels 3 and 4 have a much higher flow. The steady state result from this simulation is found in Figure 35.

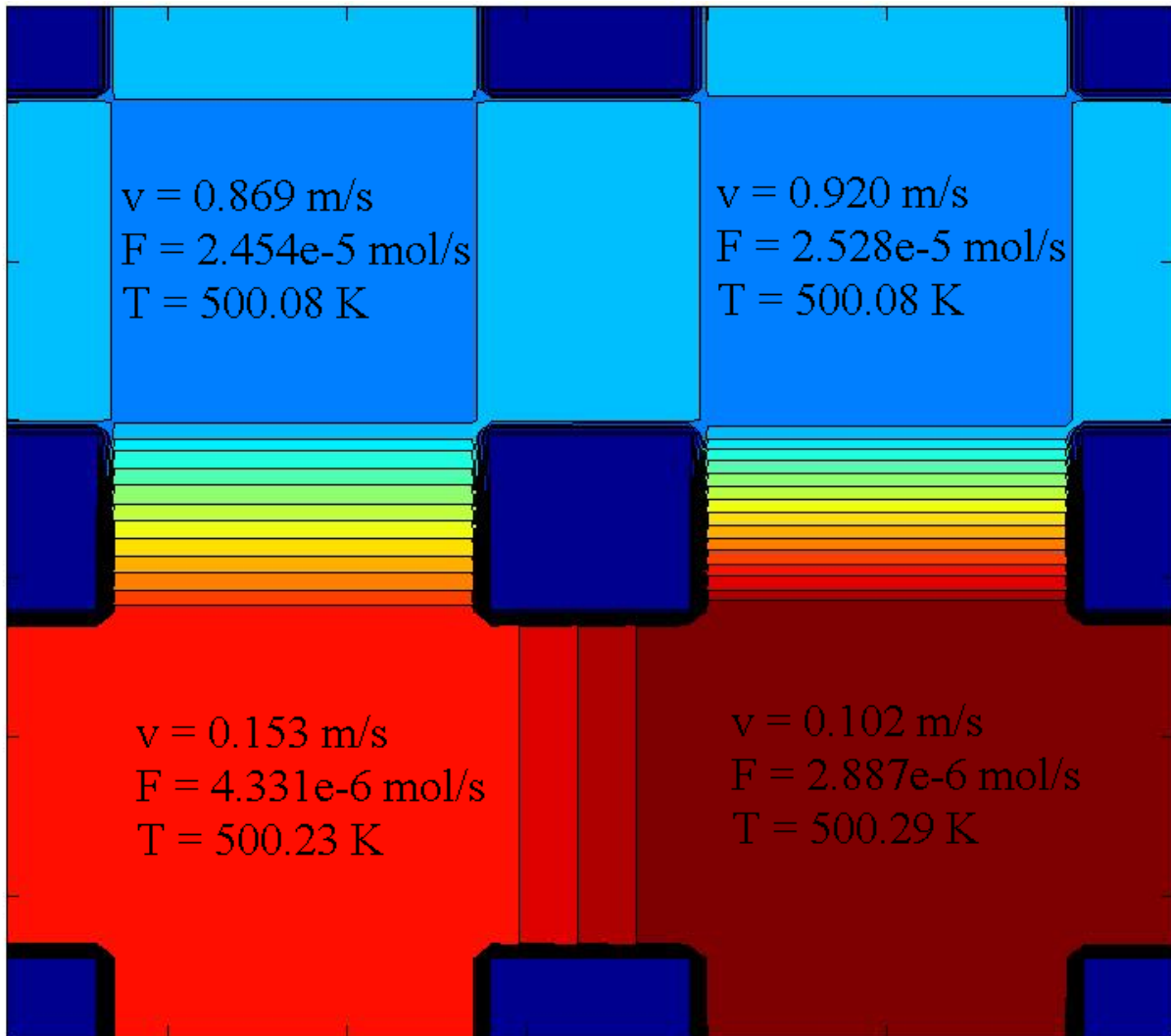


Figure 35. Four channel model with different flows to each channel, high flow in the top channels and low flow in the bottom channels. Bottom left is channel 1, bottom right is channel 2, top left is channel 3 and top right is channel 4. Note that the cross section is in segment 10.

Once again the segment investigated is segment 10. The flow is higher in the top two channels and a lot lower in the bottom two. This result is a much relative higher temperature in the bottom channels. Each individual channels conversion and the system conversion of the included components can be seen in Table 11.

Table 11. Comparison between conversion in individual channels and the entire system in a 4 channel configuration where the flow is much higher in two of the channels. The inlet temperature is 500K.

| Channel | Flow (mole/s) | CO | HC | NO | O ₂ |
|---------|---------------|-------|-------|-------|----------------|
| 1 | 4.331e-6 | 98.23 | 48.88 | 41.77 | 0.66 |

| | | | | | |
|--------|----------|-------|-------|-------|------|
| 2 | 2.887e-6 | 99.69 | 67.79 | 60.32 | 0.84 |
| 3 | 2.454e-5 | 53.41 | 8.90 | 7.11 | 0.19 |
| 4 | 2.528e-5 | 51.41 | 8.40 | 6.71 | 0.18 |
| System | | 58.18 | 14.62 | 12.19 | 0.26 |

Individual channels where the flow is low experience almost 100 % conversion of carbon monoxide. However the channels where the flow instead is bigger decrease the total system conversion of carbon monoxide. Comparing Table 10 and Table 11 shows that it is better from a system point of view to have a more evenly distributed flow to the DOC.

In Figure 36 the temperature is increasing much more than in channel 1 compared to the upper channel, channel 3. This is related to the higher velocity making the higher convective flow cooling of the channel.

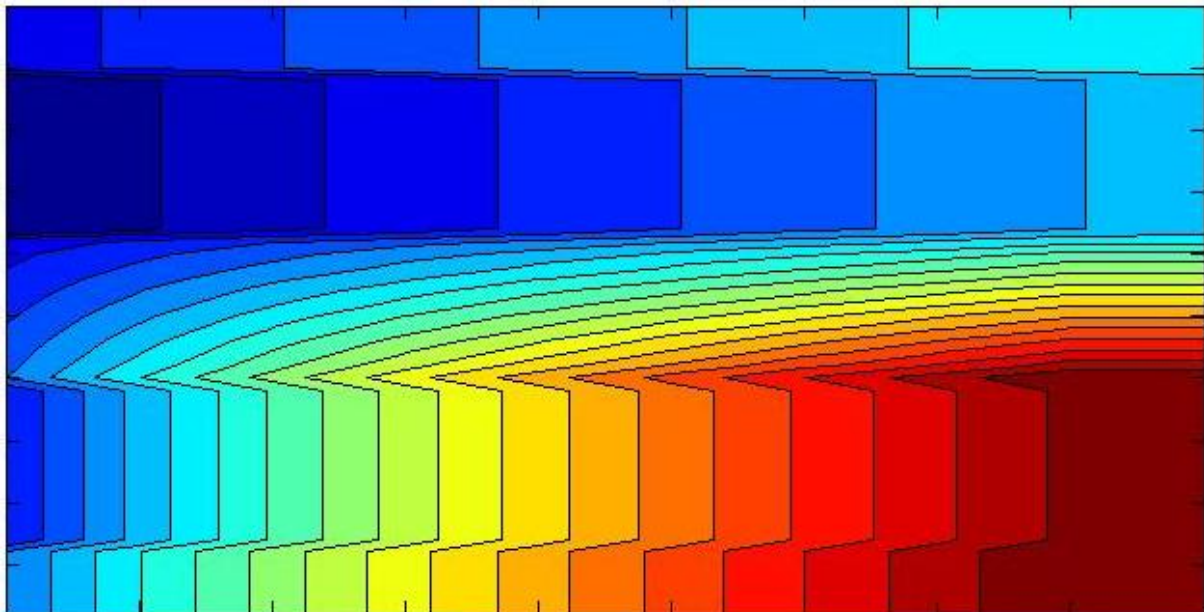


Figure 36. Temperature distribution between channels 1 and 3 along the channels, bottom part is channel 1 and top part is channel 3. The flow is higher in the top channel compared to the bottom channel. Note the difference in the top channel to the bottom one, a higher flow in the top channel results in lower temperature increase.

4.4.2 Nine (9) channel configuration

The results in this section will not be as thorough as in the 4 channel configuration section. This is because the trends are the same and the reader is instead referred to the code testing specific system settings.

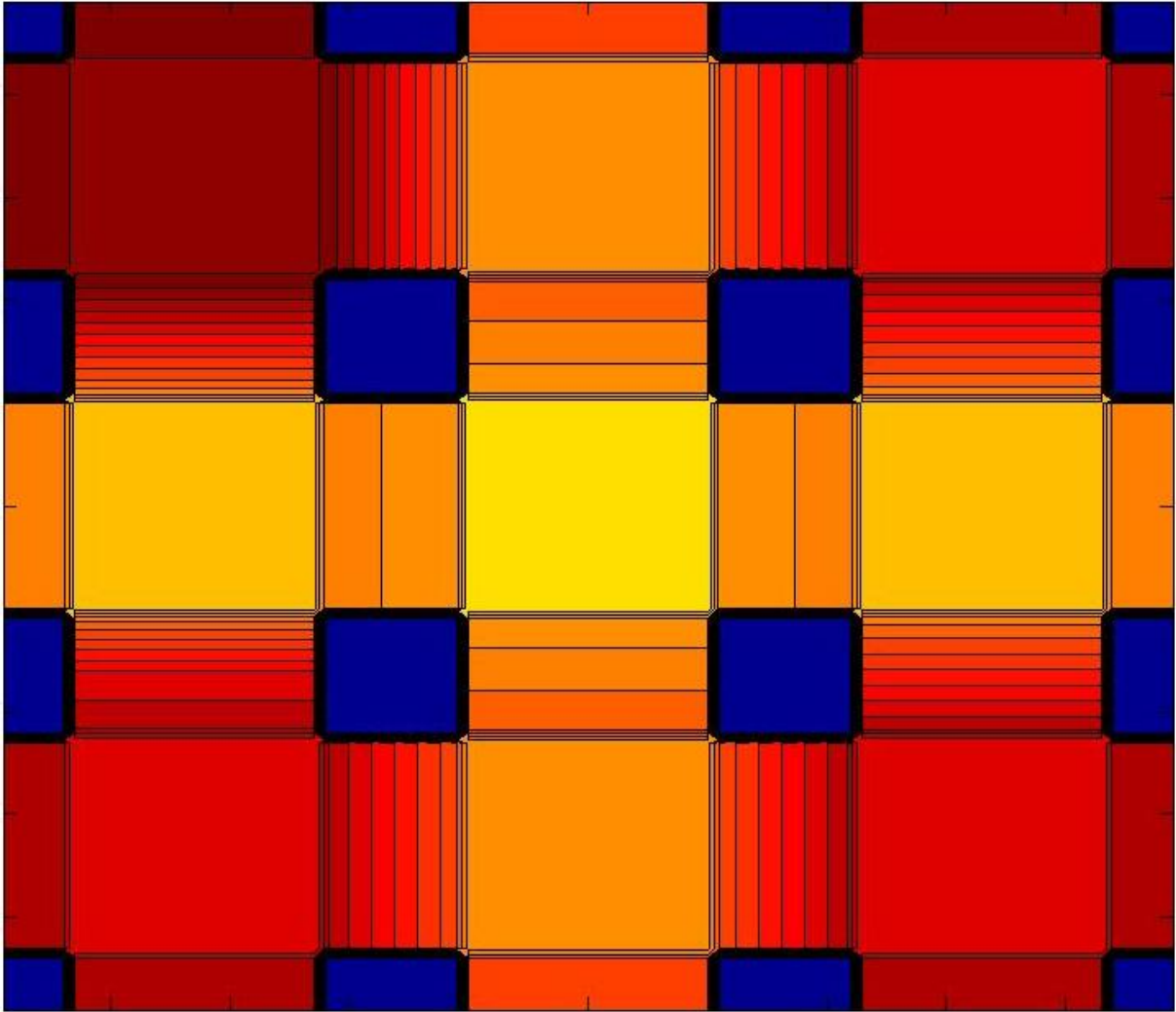


Figure 37. *Nine channel configuration with a flow that is as close as possible to resemble a fully distributed pipe flow with only nine channels. The flow is highest in the middle and is reduced further from the center of the system.*

In Figure 37 a nine channel system is simulated, where the flow is set to resemble a fully distributed pipe flow, where the corners experience the lowest flow, the edges experience a middle level of flow and the center channel experience the highest flow. Note that the flow is lowest in the top left channel, number 7.

Figure 38 shows channel 1, 4 and 7 along the center of these channels. It can be seen that the temperature is a bit higher in channel 7 where the flow is the lowest. The highest flow is in channel 4.

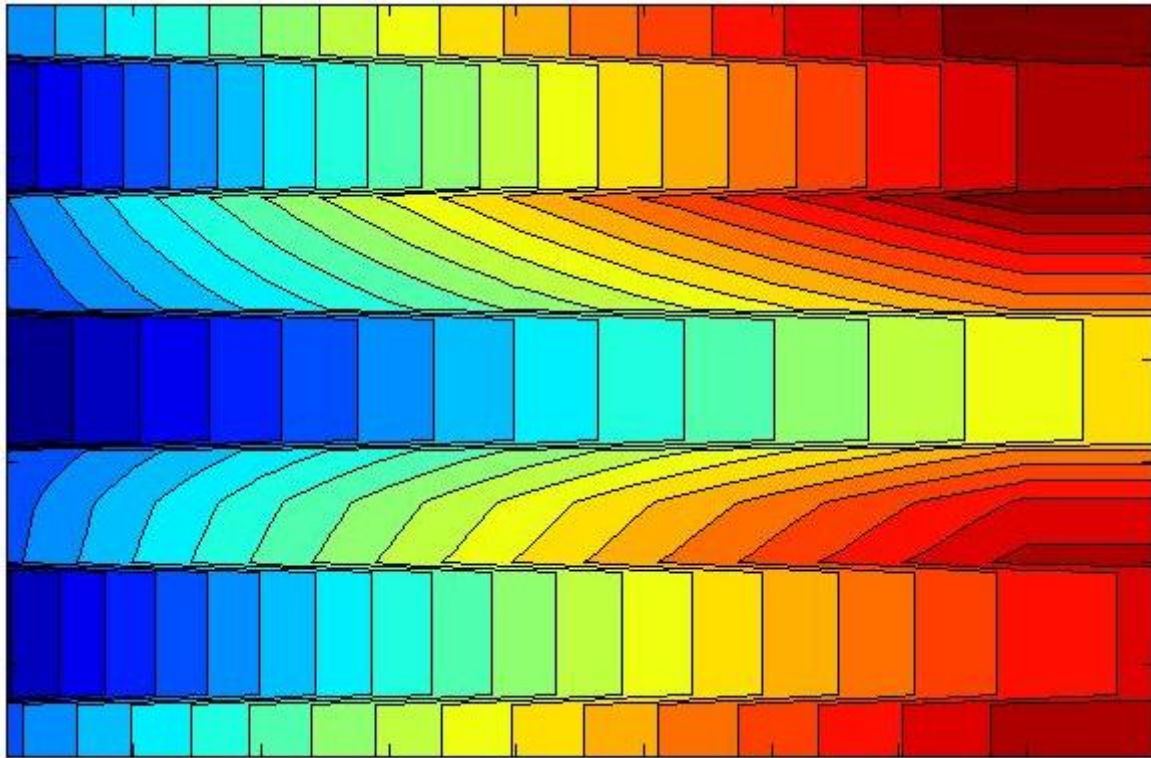


Figure 38. *Temperature distribution between channels 1,4 and 7 along the channels, bottom part is channel 1, middle part is channel4 and top part is channel 7. The highest flow is in the center channel hence the temperature increase is somewhat lower.*

4.4.3 Circular configuration

This section is named circular configuration. This is only a modified truth, in fact the system is built as circular as possible with the highest number of allowed channels in the simulation. Note that increasing the system to say above 30 channels will result in a very long simulation time. However this is not the limitation, but instead since the number of ordinary differential equations increases with 470 equations for every added channel, the computer RAM memory limits the program. All these equations are solved simultaneously, and the computer can only handle a limited number of equations.

In Figure 39 the results from the 24 channel simulation can be seen. Note that only a quarter of the full result is showed in this figure. This is because the figure otherwise would be too big to include and the walls neighboring the surrounding would only seem completely black. Note also that the flow profile in the simulation is symmetrical over the four segments included.

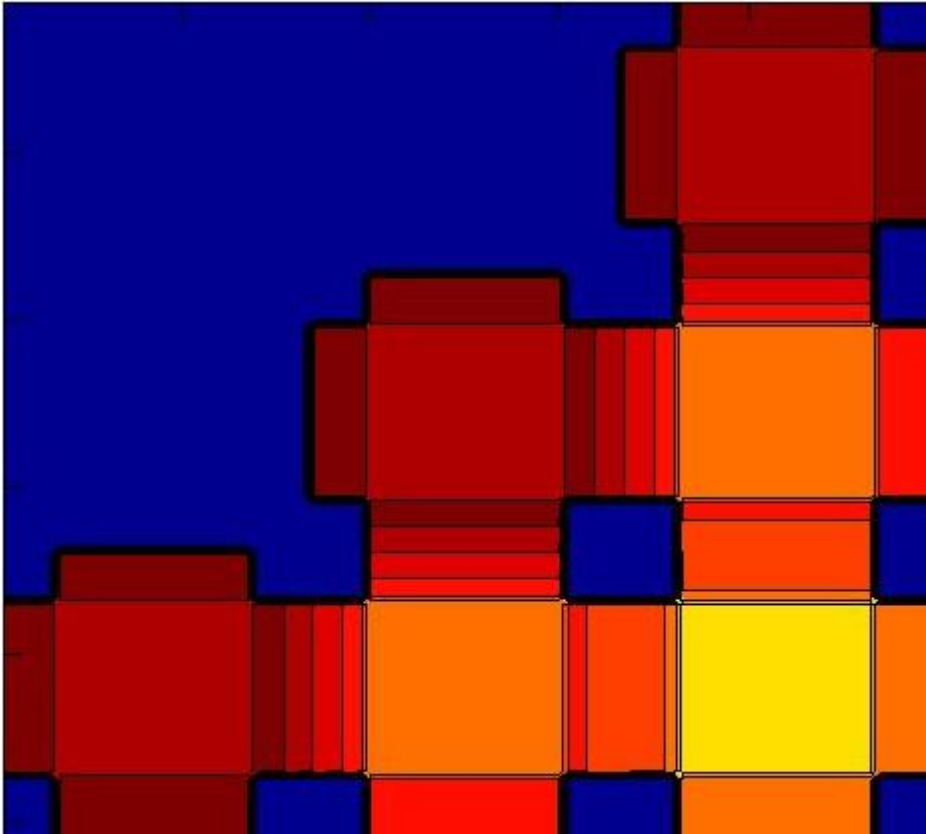


Figure 39. A quarter of the 24 channel simulation. The 3 bottom channels are channel 13, 14 and 15. The middle 2 channels are 19 and 20. The top channel is channel 23. A higher flow closest to the center of the system.

The flow profile is once again supposed to resemble a parabolic flow distribution to the DOC. Again the flow is highest close to the middle and lowest close to the walls. Base settings are used in the simulation. No deeper analysis is performed on this setup, the results that can be obtained for this system are the same as described under section 4.3.1.

5. Discussion

5.1 Discretised code discussion

As mentioned under section 4.1 the discretised code was too slow to continue with. Therefore this approach was abandoned. It is possible that this code could have been improved to get the procedure faster. This could have been done by lowering the tolerances in the system, the downside with this would have been that the calculated values would have been further from the real values. One reason for the relatively slow code was that the time step had a maximum size which was very small. This was because of the low velocity of the system. For the solution not to diverge the number of cells had to be large. Even though the code was one dimensional the simulation time was too long. Note also that this did not include layers in the washcoat or any type of heat balances. The idea was to include these after the component mass balances was in order, but already with the mass balances the calculation time was too long.

Another time prolonging aspects of the discretized code is the fact that every unknown variable is recalculated for each iteration, at least this is the procedure used in the code. The communication between function files in Matlab is not rapid enough for this procedure to work. It is possible that a similar programming language would have worked faster, such as e.g. Fortran. However this is outside the scope of this project since Matlab is the desirable software because in the future this program might be integrated with simulink.

The theory regarding the CFD-like code can be found under section 2.5. It turned out that manually discretize equations are extremely time consuming.

5.2 Tanks in series discussion

5.2.1 Program discussion

There is always possible that specific subprograms contain errors. It should be noted that the user of the code should go through and understand the code in order to locate specific system settings that might vary from the basic case.

The kinetic data used in the system is as earlier mentioned adopted from (Wang, 2008). These are the data that needs to be estimated in order to describe a specific system. However the results from the simulations using the adopted data all seem reasonable. It corresponds to the overall notion of a DOC behavior. It corresponds to the fact that carbon monoxide is subjected to the highest conversion.

If the number of segments in the DOC together with the layers in the washcoat were to be increased it is possible that the programs would be more correct in describing the process. However increasing the number of tanks in the system also prolongs the calculation time. This is because the number of equations that needs to be solved is simultaneously increased.

5.2.2 Program limitations

The code in its current version has a number of limitations, aside from the already mentioned fact that the no particulate matter is included in the model. Most of the limitations are outside of a “normal” use of a DOC, which has been worked much with. Another limitation is that only carbon monoxide, hydro carbons in the form of propylene, nitric oxide, nitrous oxide and oxygen is included in the model. These components are however assumed to be a sufficient in the model.

When it comes to the flow in the DOC it is not possible to simulate a lower flow than 0.08 mol/s to the system or more specifically 2.31×10^{-6} mol/s to an individual channel if the temperature in the system is 500 K or above. This makes it impossible to simulate in a multiple system that any channel or cluster of channels is blocked and have no flow. This should be remembered when the program is used. It is instead recommended that specific sections are subjected to the lowest possible flow if this is the desire. There is however no maximum flow limitation to a channel. However while the flow goes towards infinity the conversion goes towards zero.

It is also important to be aware of the temperature limitations in the system. Since the conversions is decreasing when the temperature is decreased in the system there is a low

interest in simulations below 273.15 K, however this is possible. Note that from 210 K and below using base settings, none of the included components will have reacted at all.

There is also a top temperature limitation in the system. This stems from the fact that initially fully transient simulations are performed on both mass fractions and temperatures. These simulations are only run for a few second (currently varying depending on the starting temperature) and the fractions obtained in these fractions are used as a starting guess when the full simulation is started. In the full simulation the mass fractions are simulated as steady state based on the temperature that each node has at the end of the shorter simulation. Since the temperature increase in the system in general is backlogging compared to the mass fractions, the steady state value that is calculated from the shorter simulation is lower than the actual steady state conversion in the longer simulation. This means that when the temperature in the system is increased enough the initial conditions from the short simulation is to far from the “real” values. When this happens the simulation will stop and the user will be subjected to an error message saying that the starting guess is to poor to continue the simulation. Using the basic values this happens when the starting temperature is higher than 680 K.

In the communication between nodes there are a number of limitations. Mass transfer in the flow direction in the solid phase is not simulated. However the relationship between width and height of the solid layers are that the channels is more than 500 time wide than thick, hence the diffusion between neighboring cells are neglected.

In a channel the mass and heat balances are solved over different amounts of nodes. In the mass balances one segment is seen as one node at every depth of the washcoat. This means that one depth layer is seen as one tank all around the channel. The volume, the heat and mass transfer area to that node is calculated from the entire inside of a channel. This means that 10 segments with 4 depth layers result in 40 nodes in the solid part of a channel for the mass balances. Instead looking at the heat balances the reaction taking place in the solid phase, the different layers is summed together and represents a fourth of what is connected to a neighboring channel. To simplify; since a channel is connected to 4 other (assuming the system is at least 9 channels and the interested one is the one in the middle) heat transfers to or from neighboring channels depending upon the individual channels. The surrounding washcoat of the center channel “feels” four other channels, meaning that the net result to the center channel temperature is a fourth of every surrounding channel.

5.2.3 One channel results

Since no experimental data has been obtained in this project, the basic data used is somewhat of a potpourri of data used throughout similar experimental setups found in the literature. It is not only the experimental data that is lacking, but also all physical data regarding one or more specific DOC:s. Instead of comparing experimental data with simulation data the produced model was subjected to a parameter study. A number of different parameters that could vary in the simulation are varied and their specific influence on the system is visualized.

The first parameter that is investigated is the temperature of the system. This is of interest because the temperature distribution of the system is what is asked for by the constituent. It should be noted that the model is built in a way that assumes a uniform starting temperature in the system and this temperature is consistent with the surrounding temperature. It is also of interest that the surrounding temperature is always the same as the starting temperature. This

gives the result that outside the wall of the DOC the temperature is always the same as the system initial temperature. This can of course be questioned, meaning that if an object is heated the surrounding fluid (or solid) is also heated to some extent. This could have been simulated adding some kind of air film layer outside the DOC. Since the code is written so that the number of channels can be varied by the user, adding a film layer would be rather complicated. The way that the code now is used it is assumed that there is a convective flow outside the DOC that keep the surrounding air to a specific temperature, the same temperature as the starting temperature.

Moving on to the actual simulations where the temperature is varied shows that the conversion is increasing when the temperature is increased in the system. This might not come as a surprise for the reader or the user of this code. It can be found under section 4.2 that all of the included reaction rates increases when temperature is increased. From Figure 25 it can be seen that the steady state conversion of carbon monoxide reaches some kind of local maximum with the specific system settings used. Also that if the temperature is then increased more the conversion slightly decreases.

What is really interesting in the model is the actual temperature increase from in the system when the starting temperature is altered. Using the base case temperature the actual temperature increase is rather modest seen in absolute values. However looking at Figure 32 the impact of system starting temperature on the system absolute temperature increase can be seen and it is necessary to use a starting temperature above 600 K to reach a temperature increase higher than 2 K. At the base case the increase is only between 0.1 and 0.2 K. The temperature comes from the exothermic nature of the reactions. All reactions except for the reduction of NO_2 to NO are exothermic and contribute to the temperature increase via the heat bound in the molecules.

The heat subjected to the DOC is one of the things that affect the performance of the DOC together with e.g. mechanical wear and tear from the particulate matter flowing through it. It should be noted that this is not simulated in the model. Instead it could in some way be assumed that what is affected by wear and tear in the DOC is the amount of catalyst material. If the user of the code is interested in simulating an older DOC where the efficiency has been reduced, it is one recommendation to try and lower the amount of catalyst material in the system. However this should of course be done with caution. It can also be other things in an actual DOC that is affected by wear and tear, such as structural differences, cracks and breakings. The deactivation of a DOC in reality is very large.

Pressure does not affect the steady state conversion as much as temperature. In Figure 26 it can be seen that more or less only carbon monoxide changes its steady state conversion worth mentioning. And as a consequence of carbon monoxide also the oxygen changes its steady state conversion. The base pressure used in the system is 1500 kPa corresponding to around 1.5 times atmospheric pressure. It should be noted that it is necessary to have a pressure in the system that is bigger than the surrounding system in order for the flow to exist. In reality it requires a pressure drop over the system for the gas to flow. Therefore the pressure needs to be higher than the surrounding pressure. But when it comes to actual conversion the impacts to steady state conversion are rather small.

Not surprising does the flow have a large impact on the conversion of the components included in the system. The steady state conversion is lowered when the flow is increased. This could be explained by the fact that a shorter residence time for each molecule result in a lower probability of reaction. Even if the total reaction rate is kept the same the flow is higher and the total amount converted per unit of volume is decreased. This is illustrated in Figure 27. The steady state conversion for NO and HC are rapidly increasing if the flow is as low as 0.5 mol/s and lowered more. This leads to the fact that according to this model with higher flows and current setting it is not possible to obtain a conversion higher than 20 % of these two components when the flow is increased.

It is possible to create DOC with different dimensions. As mentioned under section 4.3.5 an explicit investigation of varying the DOC diameter has not been included. Doing this would with a constant flow to the system only reduce the flow to each individual channel. If for instance the DOC front area is doubled and the flow kept constant the flow to each individual channel would only be half compared to before. This can be investigated in section 4.3.4 where the flow is varied.

Changing the length of the DOC will very much influence the steady state conversion of the system. This is because the total amount of catalyst material in the system is increased. Simply the possibility of letting each individual molecule react is increased hence the higher conversion. In Figure 28 it can once again be seen that the conversion of CO is limited by mass transfer while HC and NO seem to be limited by reaction rate.

Varying the amount of oxygen to the system is a rather important factor. In Figure 29 it is visualized with the steady state conversion if the fraction of oxygen is increased. Looking at the curve describing CO it is noted that it is leveling out, still increasing but with a lower derivative after a certain fraction of oxygen. This leads to the belief that something else is limiting the conversion of carbon monoxide. It is possible that the mass transfer is the limiting factor in this case. It could be that the transfer between the gas phase and the solid phase is delayed compared to the velocity of the gas through the system. The components HC and NO seem to be increasing linearly with the amount of oxygen to the system. In absolute values the steady state conversion is doubled for HC and NO if the fraction of oxygen is doubled. This might mean that the reaction rate is what is limiting the conversion of these components.

If the amount of HC is altered in the system it can be seen in Figure 30 that initially the outlet gas temperature is increasing, reaches a maximum and then decreases again. It can also be seen that the steady state conversions of all the included components, except for oxygen, decreases with increasing fraction of HC in the inlet gas. This is related to the Langmuir expression used in the reaction rates. Looking again at equation (2.2.1.17), the Langmuir expression:

$$G(X_{s,j}, T_s) = T_s \left(1 + K_1 X_{s,CO} + K_2 X_{s,C_2H_6} \right)^2 \left(1 + K_3 X_{s,CO}^2 X_{s,C_2H_6}^2 \right) \left(1 + K_4 X_{s,NO}^{0.7} \right)$$

The adsorption equilibrium constant K_3 is multiplied with the fraction of hydro carbons. The Langmuir term is then in the reaction rate expression divided with the product of the fraction of the current component and oxygen. This term seems then to reduce the reaction rate of all the included components. A bit surprisingly is that this is the fact also for hydrocarbons. Is

could be expected that an increased fraction of hydro carbons would increase the reaction rates having 1:st or 2:nd order reactions in mind. It seems like there is a level where the level of hydrocarbons makes the Langmuir expression counteract the numerator in the reaction rate term so that the temperature increase becomes limited.

Changing the catalyst load gives results that can be expected. This can be seen in Figure 31. However once again it seems like other things than the actual reaction rate is limiting the conversion of carbon monoxide. A more or less linear increase of the conversion of HC and NO with the increase of catalyst load makes it believable that the reaction rate is the limiting factor for these two components.

5.2.4 Multiple channel results

The results from the multiple channel simulations are found under section 4.4. There is a large variation of different simulation setups possible when it comes to multiple channels. The flow configuration can be set by the user, however this requires that the user enters the file setup.m and changes the values manually. This is in itself not a problem, however it is important to be familiar with how the flow is calculated. Based on the flow specified to the system an average flow to one channel is calculated. This flow is then altered after demand of the user. The average flow to one channel is then multiplied with a factor that describes the desired flow. It is important that these factors before the specific channels summed together equals the amount of channels simulated. Figure 40 below explains the situation.

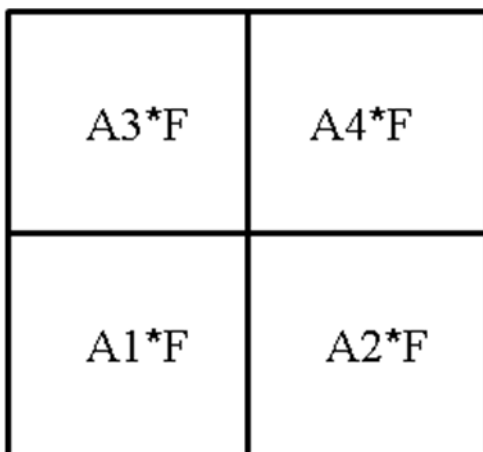


Figure 40. A four channel system with a flow configuration where the channels are subjected to different flow. The parameters A1 to A4 is required to sum up to the number of channels in the system, in this case four.

The factors in front of the F (flow) are completely individual but it is required that they fulfill the expression; $A1+A2+A3+A4=4$ since the system consist of four channels in total. If the system were to consist out of 9 channels instead the expression; $A1+A2+\dots+A8+A9=9$ needs to be fulfilled. This is because otherwise the total flow to the system would differ from what the user have specified.

In Figure 33 to Figure 36 a four channel system is investigated. The conversions in each individual channel is calculated and compared to the other channels. It can be seen that decreasing the flow will increase the conversion of a specific channel, but will instead result in a higher flow in the neighboring channels. These channels will then not reach the same high conversion. When the total conversion of a four channel system is then investigated it

turns out that the conversion is lower than if the flow to the channels would have been more homogenous. For optimal use of the DOC system it is recommended that the flow is kept more or less the same to all the channels. If this would have been the case this project would have been redundant and it would have been necessary to simulate only one channel.

From the nine channels setup in Figure 37 it can be seen that the steady state temperature is higher near the edges of the DOC and the lowest temperature is in the middle. It should be noted that this happens when the flow is highest in the middle and lower along the sides. The simulation is supposed to resemble a parabolic flow distribution.

In Figure 39 we can see the system supposed to resemble a circular system. The system is maybe not as circular as desired. But including more channels into the system would increase the calculation time much. Also the memory requirements to the hardware used increases. The hardware used in this project limits the number of channels to a maximum number of 25.

5.2.5 Future work

In future work with this project it is necessary to calibrate the kinetic data to experimental data. So far the model can only be used to give guidelines and hints to what will happen in a DOC.

Further there are a lot of ways to improve the code and the calculation setups. If for instance the flow profile to the DOC is known and displays some kind of symmetry this could be used to improve the simulations. If for instance the system can be divided into smaller parts the number of channels can be kept constant but the result would still be valid for a larger system.

There are a number of ways to make the code describe the reality closer, such as simulating the wash coats individually on each side of the DOC channel. When it comes to fractions this is not that important but looking at the temperature in the walls on each side of a channel might be different. In an extension of reaching a high temperature increase it is possible that different temperatures at different walls will push the conversion higher in different walls even inside one specific channel. This will lead to the need of simulating the different wash coat sides in a channel individually for a full description of the system.

The possibility of including different fractions during one cycle is interesting and not at all unrealistic. This is possible to do now in small scale, but it requires some changes to the code. It requires fully transient simulations because a steady state never really occurs. According to how the code now is written the fully transient simulation is only taking place in the beginning of the simulation. A more extended code simulating varying fractions would be very interesting for future work.

6. Conclusions

Conclusions regarding this project will be listed in points. The conclusions will treat both the code and the system behavior.

- It is more efficient using a tank in series approach compared to discretised code method when solving this kind of problem in Matlab.

- It is necessary to calibrate and validate the model towards experimental data before the code can be used to describe a specific system behavior.
- It is possible to describe a DOC channel or a cluster of channels simulating mass balances as steady state. This is because the timescales of mass balances and heat balances differs.
- Steady state conversion of all components is affected by system initial temperature, system pressure to some extent, flow, DOC dimensions, catalyst load and initial fractions of the included components.

References

- Andersson, B. Andersson, R. Håkansson, L. Mortensen, M. Sudiyo, R. van Wachem, B. 2010.** *Computational fluid dynamics for chemical engineers*. sixth edition. Gothenburg : s.n., 2010.
- DieselNet. 2010.** Emission standards: Cars and light trucks. [Online] DieselNet, 03 2010. [Cited: 01 19, 2011.] <http://www.dieseln.net.com/standards/eu/ld.php>.
- EPA. 2003.** Questions and answers on using a diesel oxidation catalyst in heavy-duty trucks and buses. *US Environmental Protection Agency*. [Online] 06 2003. [Cited: 01 12, 2011.] <http://epa.gov/cleandiesel/documents/420f03016.pdf>.
- Fogler, S. H. 2006.** *Elements of chemical reaction engineering*. 5th edition. Westford : Pearson Education Inc, 2006. 0-13-127839-8.
- Hauff, K. Tuttlies, U. Eigenberger, G. Nieken, U. 2010.** A global description of DOC kinetics for catalysts with different platinum loadings and aging status. *Applied Catalysis B: Environmental*. 08 06, 2010, Vol. 100, 1-2, pp. 10-18.
- Hesterberg, T.W, Long, C.M, Lapin, C.A, Hamade, A.K, Valberg, P.A. 2010.** Diesel exhaust particulate (DEP) and nanoparticle exposures: What do DEP human clinical studies tell us about potential human health hazards of nanoparticles. *Inhalation toxicology*. 07 2010, Vol. 22, 8, pp. 679-694.
- Pandaya, A. Mmbaga, J. Hayes, R. E. Hauptmann, W. Votsmeier, M. 2009.** Global kinetic model and parameter optimization for a diesel oxidation catalyst. *Topics in catalysis*. 2009, Vol. 52, 13-20, pp. 1929-1933.
- Patel, H. Eo, S. Kwon, S. 2011.** Effects of diesel particulate matters on inflammatory responses in static and dynamic culture of human alveolar epithelial cells. *Toxicology letters*. 01 2011, Vol. 200, 1-2, pp. 124-131.
- Schejbal, M. Stepánek, M. Marek, M. Koci, P. Kubicek, M., 2010.** Modelling of soot oxidation by NO₂ in various types of diesel particulate filters. *Fuel*. September 2010, Vol. 89, 9, pp. 2365-2375.
- Siuru, B. 2007.** *The Difference Between Diesel and Gasoline Engines*. s.l. : Greencar.com, 01 10, 2007. <http://www.greencar.com/articles/difference-between-diesel-gasoline-engines.php>.
- Tronconi, E. Forzatti, P. 1992.** Adequacy of lumped parameter models for SCR reactors with monolith structure. *AIChE Journal*. February 1992, Vol. 38, 2, pp. 201-210.

Wang, T. J, Baek, S. W, Lee, J. H. 2008. Kinetic parameter estimation of a Diesel Oxidation catalyst under actual vehicle operating conditions. *Industrial engineering chemistry*. 03 13, 2008, Vol. 47, 8, pp. 2528-2537.

Vasanth Kumar, K. Porkodi, K. Rocha, F. 2008. Langmuir-Hinshelwood kinetics - A theoretical study. *Catalysis communication*. 01 2008, Vol. 9, 1, pp. 82-84.

Welty, R. W, Wicks, E. C, Robert, E. W, Gregory, R. 2001. *Fundamentals of momentum, heat and mass transfer*. s.l. : John Wiley & Sons, 2001. Vol. 4. 0-471-38149-7.

Wilcox, D. C. 2006. *Turbulence modelling for CFD*. 3. San Diego : DCW Industries, 2006. 978-1-928729-08-2.

WSUEEP. 2003. Washington state university extension energy program. [Online] 2003. [Cited: 01 12, 2011.] <http://www.energy.wsu.edu/ftp-ep/pubs/renewables/DieselOxidation.pdf>.

Zheng, M. Banerjee, S. 2009. Diesel oxidation catalyst and particulate filter modeling in active - Flow configurations. *Applied Thermal Engineering*. 04 2009, Vol. 29, 14-15, pp. 3021-3035.

Appendix 1 – Program user manual

This text is written to help the user of the program, for simple use of the code and for understanding the code. This text is also written for a person that is looking to develop or change the code in any way desirable. Initially every program included in this project will be explained further.

Tank_serie.m

This is the first program that the user should turn to. Tank_serie.m contains information regarding simulation procedure. It contains information on how the simulation can be started, it is mentioned that the simulation should only consist 1, 4, 9, 16, 25 or 24 channels. All of these systems except for 24 channels are square systems. The 24 channels system is built up according to Figure A1.1.

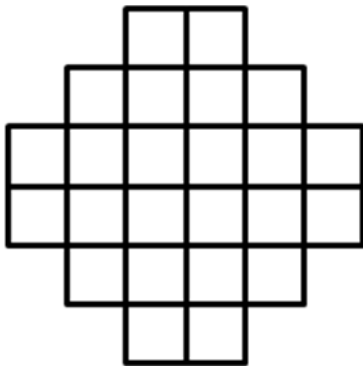


Figure A1.1. *The configurational setup for 24 channels. Is supposed to resemble a circular setup.*

The figure is supposed to resemble a near circular configuration using as few as 24 channels in the system. If the 24 channel system is simulated the files that are called for by the program differs some compared to the square case.

Initially the file setup.m is called to receive a number of physical properties and physical data for the system, this will be explained further under the section setup.m. The next step in Tank_serie.m is to compress the mass matrix used in the initial part of the simulation. Then the step size is determined for the initial simulation. The step size depends on the system temperature. Increasing temperature leads to a shorter step size. When the step size is decreased the initial simulation will take somewhat longer. Note that there is a possibility of changing the step size to a desired value, this can be done if it is found that the simulation gets stuck to specific time steps.

The initial simulation is looping through every channel individually for 2.5 seconds to receive steady state fractions. All the diagonal elements in the mass matrix are initially set to 1, meaning that all equation is simulated as transient. The result of the component mass fractions from the initial simulation are extracted and used as starting guess values in the full time simulation. Here all the mass balances are simulated as steady state by setting the diagonal elements in the mass matrix handling the mass balances to 0. Note that the values from the initial simulation regarding the temperature in the system is unused in the full simulation, instead the initial temperature is reset in the system and the heat balances are now the only balances simulated as transient.

In the end of Tank_serie.m the results from all channels are used to calculate the total fractions of all included components together with the conversion and the reduction of the components. This is then displayed in the form of a table in the command window in order for the user to see what behavior the system indicates. The program also calls for the program contourfigure2.m in order to display a number of plots, but this will be explained further later.

setup.m

This file is the file that the average user of the code turns to the most. Here it is possible to specify all the physical properties of the system investigated. The reader is referred to the code in order to get an understanding of what can be specified. Based on what is specified by the user the program calculates all necessary data required for simulations, especially all dimensions of the DOC.

All thermal and physical properties such as heat transfer coefficient, heat capacity, lumped mass transfer coefficients, density and reaction heats for all the reaction are calculated by calling different files. This will be described in individual sections.

The next part in setup.m is to specify the flow profile to the system, this is closely described under section 5.2.4 in the report and will not be handled further. It should be remembered that the all channels are awarded flow by multiplication of an individual channel factor with average flow. These factors are required to sum up to the number of channels simulated otherwise the flow will not be what is initially specified.

In the final part of setum.m the starting vector for the ode solvers are created by looping up the initial fraction together with the initial temperatures in the system. It should be noted that these vectors are the vectors that are replaced with steady state fractions in Tank_serie.m

heat_trf_coef.m

This file uses the Dittus-Boelter correlation to calculate the heat transfer coefficient in based on the system temperature, pressure and dimensions. This is described further under section 2.4.6. It should be noted that thermal conductivity is required to calculate the heat transfer coefficient and is called for in the file therm_cond.m.

therm_cond.m

This file requires temperature and pressure to calculate the thermal conductivity of the gas phase in the system. Since the gas phase is simulated as air this is done by interpolation over both temperature and pressure. Then returns the result to the file heat_trf_coef.m.

Cp_gas.m

Similar to therm_cond.m the heat capacity of the gas phase is interpolated over temperature and pressure and returned to the setup.m for use in the simulation. Note that the solid heat capacity is set constant assuming no or small changes with temperature and pressure.

gam_g.m and gam_s.m

These two files calculate the lumped mass transfer coefficients in the system. The file gam_g.m calculates the lumped mass transfer coefficient between the gas phase and the solid

phase and the file `gam_s.m` for two solid layers. They both require system temperature, pressure and dimensions for calculation. These methods are further explained under section 2.6.2. `gam_g.m` calls to the programs `mass_trf_coef.m` and `D_eff.m` for further information. The file `gam_s.m` calls for `D_eff.m` for effective diffusivity.

mass_trf_coef.m

This file calculates the mass transfer coefficient between the solid phase and the gas phase using temperature, pressure and system dimensions. This is described further under section 2.4.3.

D_eff.m

The effective diffusivity is calculated based on temperature and pressure of the system. It also requires binary diffusion coefficients for each component in the gas mixture and that is obtained by calling the file `diffusivity.m`. How the effective diffusivity is calculated is explained further under section 2.6.4.

diffusivity.m

Calculates the binary diffusivity for each component in the gas mixture, note that the gas mixture is assumed to be air. This is further explained under section 2.4.4. `diffusivity.m` requires temperature and pressure of the system to calculate the binary diffusivity.

rho_bulk.m

This file uses again temperature and pressure to calculate the bulk density. The bulk is also here represented by air. `Rho_bulk.m` is thoroughly described under section 2.4.1.

deltaH.m

In this file the heat of reaction is obtained based on the system temperature. Reaction heat has been investigated for all the reactions and a basic fitting has been performed to the data. In this way the specific temperature will affect the heat of reaction. More information regarding heat of reaction can be found under section 2.3.

ode_calc_serie.m

This is the file called by `Tank_serie.m` initially and is used for the initial simulations where steady state mass fractions are obtained. In the first part some values are calculated based on the user specifications in the file `setup.m`

The next thing taking place in `ode_calc_serie.m` is that each channel is solved separately assuming that the surrounding temperature is constant. Fortunately this assumption is rather valid as long as the initial temperature is below 680 K. After this the temperature increase in the system will push the reactions further and a steady state simulation of mass fractions is no longer valid. The actual looping over the channels takes place in the file `Tank_serie.m` and that file calls for `ode_calc_serie.m` one channel at the time.

Looping for one channel takes place initially looping the components, then the segments, then the gas phase and solid phase layers. After the solid and gas phase layers the wall layers are looped and finally the directions in one channel. The different nodes are connected as described under section 2.6. As previously mentioned the results from these simulations are

used for the steady state mass fraction in the following full time simulation, where the heat balances are solved for all the nodes in all the channels simultaneously. Note also that the file `contourfigure2.m` plots the transient simulation for the all components except oxygen in the final channel simulated. This means that if the system contains 4 channels, the results from channel 4 will be plotted. This is to make sure that the mass balances have reached a steady state behavior.

Inside `ode_calc_serie.m` the reaction rates of all the included components are updated at every time step. Note that it is only the reaction rates that are updated because it is a function of temperature and fractions of individual components. The reaction rates are calculated by calling the program `reactionrate.m`.

The thermo dynamical properties of the solid phases such as wall and washcoat are set in the different `ode_calc`-files respectively and not in the setup file.

ode_calc_3D.m

This file is the file calculating the full time simulation. The time stepping in this file is initially very short but is increasing after certain amount of time. The steps are large after a few minutes in the system because the system strides towards a steady state behavior. The looping is the same as in `ode_calc_serie.m` except the initial looping is over the number of channels simulated in the system.

The result that is received in the full time simulation is obtained in a matrix where every node is represented by a column and the rows of the matrix is the result at a specific time step. The time steps can be found under the variable t and the results under variable x in the workspace of Matlab. It is important to know how the data is extracted from the matrix in order to get information about the system, because of this an explanation is included below.

| | |
|------------------------|--|
| Component fractions: | $x(t,470(c-1)+50(i-1)+5(k-1)+(n-1)+1)$ |
| Gas temperature: | $x(t,470(c-1)+250+k)$ |
| Wash coat temperature: | $x(t,470(c-1)+260+k)$ |
| Wall temperature: | $x(t,470(c-1)+270 +50(d-1)+5(k-1)+l)$ |

It is important to remember what the different letters stand for in this formulation. The letter c represents the channel you are interested in. If only one channel is simulated this figure should be set to 1. If you are interested in channel 7 this number is 7 and so on. The number of channels is the only thing that varies between different simulations. The letter t represents a specific time step.

The letter i is the component number and the components are numbered from 1 to 5 according to:

| | |
|-------|-------------------------------------|
| $i=1$ | Carbon monoxide (CO) |
| $i=2$ | Hydro carbons (HC) |
| $i=3$ | Nitric oxide (NO) |
| $i=4$ | Nitrogen dioxide (NO ₂) |
| $i=5$ | Oxygen (O ₂) |

The letter k represents the segment in the DOC and varies between 1 and 10, since one channel is divided into 10 segments.

The n represents the layer in the specific segment of the DOC. There are 5 layers in the DOC where if $n=1$ the gas phase value is obtained. If $n>1$ the layers are in the washcoat of the DOC, 2 is closest to the gas phase, 3 is the second closest and so on up to 5.

Looking at the expression for obtaining result from of the wall temperature two more indexes are used, the first one being d . This represents the direction of the DOC. Since every channel is simulated as a square channel there are 4 directions. This means that the d varies between 1 and 4. It is important to keep track of what number is what direction so the reader is referred to Figure A1.2.

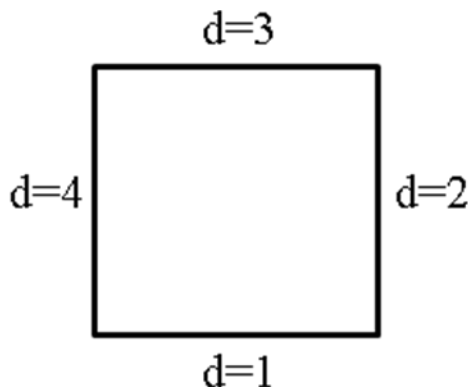


Figure A1.2. The directions represented by index d in the system. The channel has four walls all represented by number between 1 and 4 in the code.

To really clarify; $d=1$ means down, $d=2$ right, $d=3$ up and $d=4$ left. Note also that the directions only describe the wall temperature in a specific direction. The washcoat temperature is simulated as the same all around the channel.

The other index used in simulation of the wall temperature is l and represents the wall layers in a specific direction. It varies between 1 and 5 since it is assumed that the wall is 5 layers thick connected to every channel. Note then that to reach a neighboring channel gas phase there are 10 layers of wall that needs to be passed through.

In order for the reader to really understand the concept of the indexes a few examples is presented below to find what values are used in order to find a specific entity at a specific location.

Example 1. Assuming a simulation of 3600 second has been made on 9 channels and you are interested in knowing the steady state fraction of NO_2 in the gas phase in the 6:th segment of the 5:th channel. What element should be extracted from the matrix x ?

| | |
|--|-------|
| Since you are interested in channel five: | $c=5$ |
| The interesting component is NO_2 : | $i=4$ |
| Interesting segment is number 6: | $k=6$ |

Relevant phase is the gas phase:
Steady state value:

$n=1$
 $t=end$

Note that it is important that the system has reached steady state. Otherwise the values might not really be steady state values, and this is controlled by the simulation time. As long as the time is bigger than a few seconds the fractions will have reached steady state, but the temperature needs at least a minute to reach steady state, preferably more. To sum up this example the desired fraction at the desired location and time will be obtained by calling:

$x(end,470(5-1)+50(4-1)+5(6-1)+(1-1)+1)=x(end,2056)$

Example 2. Once again we have performed a simulation of 3600 second but this time on 4 channels and we are interested in two values, the steady state wall temperatures on both sides of the intersection wall layers between channel 1 and channel 3. The location in the DOC is directly after the inlet. The interesting points can be seen on each side of the red line in Figure A1.3. What two elements should be extracted from the matrix x?

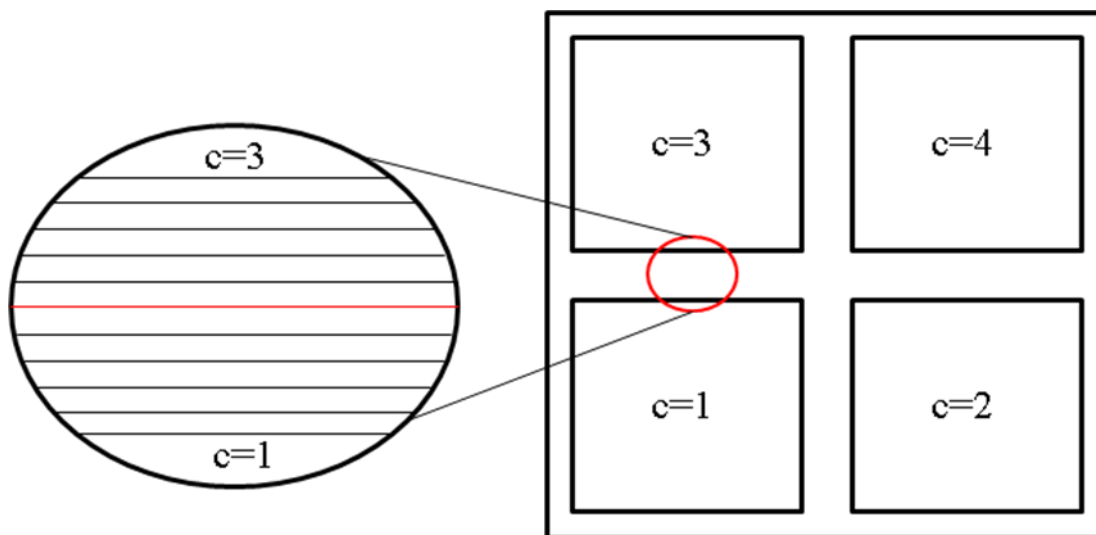


Figure A1.3. Describing the interesting points in example 2. Values from each side of the red line are asked for.

Value from channel one:

The channel number is 1: $c=1$
The direction for reaching channel 3 is 3: $d=3$
Segment closest to the inlet is the first one: $k=1$
The layer is layer 5, the one closest to next channel: $l=5$
Steady state value: $t=end$

Value from channel three:

The channel number is 3: $c=3$
The direction for reaching channel 1 is 1: $d=1$
Segment closest to the inlet is the first one: $k=1$
The layer is layer 5, the one closest to next channel: $l=5$
Steady state value: $t=end$

The solution from this example gives that we searching from the following values:

Channel one: $x(\text{end}, 470(1-1)+270+50(3-1)+5(1-1)+5)=x(\text{end}, 375)$

Channel three: $x(\text{end}, 470(3-1)+270+50(1-1)+5(1-1)+5)=x(\text{end}, 1215)$

ode_calc_24.m

This file is a special case of `ode_calc_3D.m` and is automatically called for instead of `ode_calc_3D.m` if the user specifies that 24 channels is the number to simulate. The difference to `ode_calc_3D.m` is that the system setup is not quadratic but instead as circular as possible with only 24 channels. This requires that the looping over the wall temperatures differs since the structure is different. The basic idea is the same as in `ode_calc_3D.m`, but the wall looping differs. Note that if data is extracted from a system of 24 channels it is important to have in mind the numbering of the channels.

reactionrate.m

As mentioned earlier the reaction rate is updated on a time step basis. This since the reaction rates are dependant on the fractions of each component. How the reaction rates are calculated can be found under section 2.2 and kinetic data together with adsorption equilibrium data can be found in Table 4 and in Table 5.

contourfigure2.m

This file extracts a number of data from the x-matrix and plots it in graphs for an easier visual display of the results. It also makes contour plots that are made into a movie-sequence. The user is asked to specify a number, either 1 or 2. Choosing 1 gives the temperature development in a cross section of the DOC. Choosing 2 instead gives the temperature development along the DOC. Since this contour plot is 2 dimensional the result can only be seen in a limited number of channels. For instance if there are 4 channels simulated the user will see a cross section of 2 channels from the side.

The idea is that from learning how to extract data from the x-matrix the user should be able to fulfill what ever results necessary.

Figure_24c.m

`Figure_24c.m` is called from `contourfigure2.m` if the specified number of channels is exactly 24. Performs the same thing as `contourfigure2.m` where the contour plots are produced. Once again the user is given the choice between a temperature development in a cross section of the entire DOC or along the DOC.

Appendix 2 – Calculation of system properties

This appendix explains the calculation of some entities used in this project that is not explained in the report. The reason for bringing them up here is that they might help the user understand the code and to know how to proceed when the code needs to be subjected to changes.

Calculation of concentration

Concentration is calculated using the universal gas law:

C – Concentration [mol/m³]
n – Number of moles [-]
V – Volume [m³]
P – Pressure [Pa]
R – Universal gas constant [J/mole/K]
T – Temperature [K]

$$C = \frac{n}{V} = \frac{P}{RT} \quad (A2.1)$$

Calculation of dimensions

Dimensions are calculated using geometric relationships:

L – DOC length [m]
D – DOC diameter [inch]
W_t – Wall thickness [m]
WC_t – Wash coat thickness [m]
CD – Cell density [cpsi]
CS – Channel width and height [m]
C_{nr} – Number of channels next to each other in 1 inch
x – Segment width [m]
z – Washcoat layer thickness [m]
l – Wall layer thickness [m]
A_k – Area between solid and gas phase in segment [m²]
A_s – Area between two neighboring solid segments in the washcoat [m²]
A_l – Area between two wall layers [m²]

$$C_{nr} = \sqrt{CD} \quad (A2.2)$$

$$CS = \frac{1 [\text{inch}]}{C_{nr}} 0.0254 \left[\frac{\text{m}}{\text{inch}} \right] - 2WC_t - W_t \quad (A2.3)$$

$$A_k = 4 * CS * \Delta x \quad (A2.4)$$

$$A_s = WC_t * CS * 4 \quad (A2.5)$$

$$V_{cell,g} = CS^2 * \Delta x \quad (A2.6)$$

$$V_{\text{cell,g}} = \frac{WC_t * CS * \Delta x}{4} \quad (\text{A2.7})$$

$$A_l = \frac{A_k}{4} \quad (\text{A2.8})$$

$$\Delta x = \frac{L}{10} \quad (\text{A2.9})$$

$$\Delta z = \frac{WC_t}{4} \quad (\text{A2.10})$$

$$\Delta l = \frac{W_t}{10} \quad (\text{A2.11})$$

Calculating channel velocity

The velocity in each channel is calculated according to:

v – Channel velocity [m/s]

F_c – Flow in a channel [mol/s]

C_{tot} – Total bulk concentration [mol/m³]

A_c – Channel opening [m²]

$$v = \frac{F_c}{C_{\text{tot}} * A_c} \quad (\text{A2.12})$$

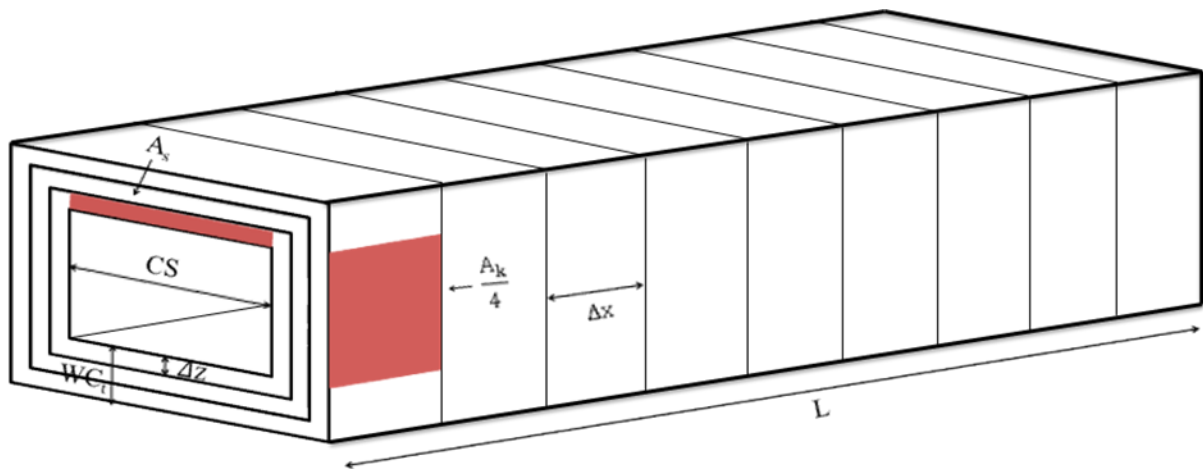


Figure A2.1. Description of some of dimensions in the channel. Note that the walls are not included in this figure, only the channel with wash coat.

Appendix 3 – One channel DOC the CFD-way

Mass balances

The two phases of the DOC is described with two different but coupled mass balances, one mass balance describing the gas phase and one describing the solid phase. The mass balances used have been adopted by Wang et al. (Wang, 2008) For the solid phase the balance is written as:

$$\underbrace{\varepsilon \frac{\partial X_{s,i}}{\partial t}}_{\text{Accumulation}} = \underbrace{k_m a_{sf} (X_{g,i} - X_{s,i})}_{\text{Mass transfer between phases due to concentration gradient}} - \underbrace{\frac{a_c R_i}{C_{tot}}}_{\text{Reaction term}} \quad (\text{A3.1})$$

The solid phase mass balance does not contain any convective term; the only derivative in the equation is the accumulation term. Mass balance nomenclature is described in Table. The gas phase mass balance is written as:

$$\underbrace{(1 - \varepsilon) \frac{\partial X_{g,i}}{\partial t}}_{\text{Accumulation}} = - \underbrace{u_D \frac{\partial X_{g,i}}{\partial x}}_{\text{Convection}} - \underbrace{k_m a_{sf} (X_{g,i} - X_{s,i})}_{\text{Mass transfer between phases due to concentration gradient}} \quad (\text{A3.2})$$

The gas phase mass balance contain a term both for accumulation and for convective flow, there is no reaction term in the gas phase mass balance, only a term describing the transfer between the gas and the solid phase. The exclusion of a diffusion term in the gas phase mass balance is made during the assumption that convection is larger then axial diffusion hence the diffusion is negligible. In Table the nomenclature of the mass balances is explained.

Table A3.1. Nomenclature of terms included in the mass balances.

| | |
|---------------|---|
| ε | Porosity [-] |
| $X_{s,i}$ | Mole fraction of component i in solid phase [-] |
| $X_{g,i}$ | Mole fraction of component i in gas phase [-] |
| k_m | Mass-transfer coefficient between gas and solid phase [m/s] |
| a_{sf} | Gas/solid interfacial area per unit reactor volume [m^2/m^3] |
| a_c | Catalyst surface area per unit reactor volume [$\text{m}^2\text{cat}/\text{m}^3$] |
| C_{tot} | Total molar concentration of exhaust gas [mol/m^3] |
| R_i | Reaction rate of specie i [$\text{mol}/\text{m}^2 \text{ s}$] |
| u_D | Superficial velocity [m/s] |

Heat balances

Similar to the mass balance, the heat balances are expressed as two balances, one for the solid phase and one for the gas phase. The contribution of the heat balances to the algorithm is smaller than the mass balances because it is not necessary to express one heat balance for each component in each phase. Instead only two are used in total. The heat balance has been adopted by Hauff et al. describing a standard model for DOC. The gas phase heat balance includes convection, heat transfer to the solid and axial heat conduction and is written as: (Hauff, 2010)

$$\underbrace{(1 - \varepsilon)C_{P,g}\rho_g \frac{\partial T_g}{\partial t}}_{\text{Accumulation}} = - \underbrace{(1 - \varepsilon)C_{P,g}\rho_g u_D \frac{\partial T_g}{\partial x}}_{\text{Convection}} + \underbrace{a_{geo}\alpha(T_s - T_g)}_{\text{Heat transfer between phases due to temperature gradient}} + \underbrace{(1 - \varepsilon)\lambda_g \frac{\partial^2 T_g}{\partial x^2}}_{\text{Diffusion}} \quad (\text{A3.3})$$

Nomenclature of the heat balance is explained in Table A3. The solid phase heat balance includes axial heat conduction, heat transfer to the gas phase and heat released by the reaction and is described as:

$$\underbrace{\varepsilon C_{P,g}\rho_g \frac{\partial T_s}{\partial t}}_{\text{Accumulation}} = \underbrace{\varepsilon \lambda_s \frac{\partial^2 T_s}{\partial x^2}}_{\text{Diffusion}} - \dots \dots \underbrace{a_{geo}\alpha(T_s - T_g)}_{\text{Heat transfer between phases due to temperature gradient}} + \underbrace{a_{geo} \sum_{j=1}^3 (-\Delta H_{Rj}) R_j}_{\text{Change in temperature due to reactions}} \quad (\text{A3.4})$$

Table A3.2 Nomenclature of terms included in the heat balances.

| | |
|---------------|--|
| ε | Porosity [-] |
| T_s | Temperature in the solid phase [K] |
| T_g | Temperature in the gas phase [K] |
| $C_{P,s}$ | Specific heat capacity of the solid phase [J/kg K] |
| $C_{P,g}$ | Specific heat capacity of the gas phase [J/kg K] |
| ρ_s | Density of the solid phase [kg/m ³] |
| ρ_g | Density of the gas phase [kg/m ³] |
| u_D | Superficial velocity [m/s] |
| a_{geo} | Specific geometric surface [m ² /m ³] |
| α | Heat transfer coefficient [W/m ² K] |
| λ_s | Thermal conductivity of the solid phase [W/m K] |

| | |
|------------------|--|
| λ_g | Thermal conductivity of the gas phase [W/m K] |
| $\Delta H_{R,i}$ | Reaction enthalpy of reaction i [J/mol] |
| R_i | Reaction rate of specie i [mol/m ² s] |

Navier-Stokes equation

Since the system is not running at steady state conditions an equation including the change in momentum must be included in the solver. This is taken care of by introducing the Navier-Stokes equation. Note that since the gas phase is the only phase where movement is taking place in axial direction the Navier-Stokes equation is only solved for the gas phase. As a simplification the flow is assumed to be incompressible and the viscosity is constant rendering the Navier-Stokes equation to be solved: (Wilcox, 2006)

$$\rho \left(\frac{\partial \mathbf{u}_D}{\partial t} + \mathbf{u}_D * \nabla \mathbf{u}_D \right) = -\nabla P + \mu \nabla^2 \mathbf{u}_D + \mathbf{f} \quad (\text{A3.5})$$

The term \mathbf{f} represents other body forces to the system such as gravity but it will be neglected in the following treatment of the system. This could be rewritten in one dimensional form generating the expression:

$$\underbrace{\rho \frac{\partial u_D}{\partial t}}_{\text{Unsteady acceleration}} + \underbrace{\rho u_D \frac{\partial u_D}{\partial x}}_{\text{Convective acceleration}} = - \underbrace{\frac{\partial P}{\partial x}}_{\text{Pressure gradient}} + \underbrace{\mu \frac{\partial^2 u_D}{\partial x^2}}_{\text{Viscosity}} \quad (\text{A3.6})$$

Table A3.3. Nomenclature of the terms included in Navier-Stokes equation.

| | |
|--------|---|
| ρ | Density of the gas phase [kg/m ³] |
| u_D | Linear velocity [m/s] |
| P | Pressure [Pa] |
| μ | Viscosity [Pas] |

General discretization

The DOC channel will be solved in one dimension using equidistant spacing between nodes. The control volume will then become a control line over which the included terms will be discretized. Solving the general transport equation over a control volume in time generates the following expression: (Andersson, 2010)

$$\underbrace{\int_{\text{c.v.}} \left(\int_t^{t+\Delta t} \rho \frac{\partial \phi}{\partial t} dt \right) dV}_{\text{Accumulation}} + \underbrace{\int_t^{t+\Delta t} \left(\int_{\text{c.v.}} \frac{\partial (U_j \phi)}{\partial x_j} dV \right) dt}_{\text{Convection}} = \underbrace{\int_t^{t+\Delta t} \left[\int_{\text{c.v.}} \frac{\partial}{\partial x_j} \left(\Gamma \frac{\partial \phi}{\partial x_j} \right) dV \right] dt}_{\text{Diffusion}} + \underbrace{\int_t^{t+\Delta t} \left(\int_{\text{c.v.}} S_\phi dV \right) dt}_{\text{Source term}} \quad (\text{A3.7})$$

Since the problem is in one dimension in space coordinates it can be expressed differently in the space derivative. The space and time grid is illustrated in Figure A3.1.

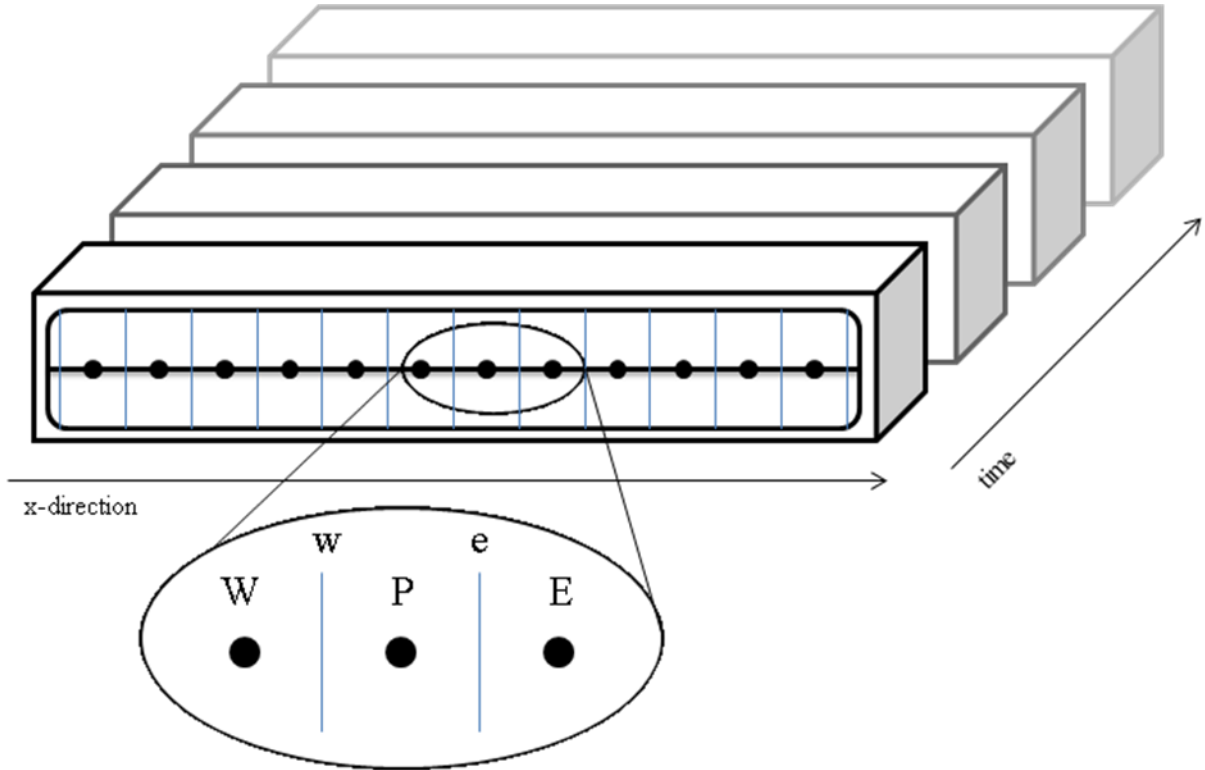


Figure A3.1. The space and time discretization of the DOC, where P denotes the present node, n , capital W (west) is node $n-1$, capital E (east) is node $n+1$, lower case w is the face value before current node and lower case letter e is the face value after the present node.

The general transport equation can now be expressed only using one space dimension, here x -direction: (Andersson, 2010)

$$\int_w^e \left(\int_t^{t+\Delta t} \rho \frac{\partial \phi}{\partial t} dt \right) dx + \int_t^{t+\Delta t} \left(\int_w^e \frac{\partial(U\phi)}{\partial x} dx \right) dt = \int_t^{t+\Delta t} \left[\int_w^e \frac{\partial}{\partial x_j} \left(\Gamma \frac{\partial \phi}{\partial x_j} \right) dx \right] dt + \int_t^{t+\Delta t} \left(\int_w^e S_\phi dx \right) dt \quad (\text{A3.8})$$

The main idea with the discretization in both time and in space is to remove all the integrals and derivatives in order to solve a set of algebraic expressions. The derivatives are expressed as differences between the nodes and the face values in the discretization.

Before explaining how the system balances has been discretised an explanation is given in how it is performed theoretically for all the included terms in the general transport equation in one dimension using central differencing.

Transient term

$$\int_w^e \left(\int_t^{t+\Delta t} \rho \frac{\partial \phi}{\partial t} dt \right) dx = \rho [\phi_P(t + \Delta t) - \phi_P(t)] \Delta x \quad (\text{A3.9})$$

The transient term is integrated over space resulting in a multiplication with delta x here defined as the subtraction of w from e. The difference between the face values are exclusively set to the distance delta x, which is constant in a uniform space discretization. However if the face values of the cells would be set to different distances delta x would vary depending on where in the grid the calculation takes place. (Andersson, 2010)

Diffusion term

$$\int_t^{t+\Delta t} \left[\int_w^e \frac{\partial}{\partial x} \left(\Gamma \frac{\partial \phi}{\partial x} \right) dx \right] dt = \int_t^{t+\Delta t} \left(\Gamma_e \frac{\phi_E - \phi_P}{\Delta x} - \Gamma_w \frac{\phi_P - \phi_W}{\Delta x} \right) dt \quad (\text{A3.10})$$

The derivative of the arbitrary entity phi is expressed as a difference between its values in the eastern and western face. In order to get the values of phi in the cell faces the difference between the values of the present node and the value at the node closest to the face is used, the value at E of the current face is e and the value at W if the currents face is w.

To obtain the value of phi for each time step it is possible to calculate it as the value at t, the value at t+ t or a combination of the two values. In order to express the value of phi a weight factor theta can be included:

$$\int_t^{t+\Delta t} \phi dt = [\theta \phi(t + \Delta t) + (1 - \theta) \phi(t)] \Delta t \quad (\text{A3.11})$$

If theta is set to zero the solution will be fully explicit, only the old value of phi is used for calculations of phi in each time step. Using fully explicit solutions puts some constraints on the time step size versus the space step size. The advantage is that there is no need for sub iterations within each time step hence the solution will converge faster. Instead if theta is set to one this is referred to as a fully implicit solution. This does not in theory put any constraint on the time step but since the number of iterations should be kept low in each time step the time step size should still be set with consideration. The introduction of the weight factor leads to the conclusion that it is possible to write the diffusion term as:

$$\int_t^{t+\Delta t} \left(\Gamma_e \frac{\phi_E - \phi_P}{\Delta x} - \Gamma_w \frac{\phi_P - \phi_W}{\Delta x} \right) dt = \left[\theta \left(\Gamma_e \frac{\phi_E - \phi_P}{\Delta x} - \Gamma_w \frac{\phi_P - \phi_W}{\Delta x} \right) + \dots \right. \\ \left. \dots (1 - \theta) \left(\Gamma_e \frac{\phi_E^0 - \phi_P^0}{\Delta x} - \Gamma_w \frac{\phi_P^0 - \phi_W^0}{\Delta x} \right) \right] \Delta t \quad (\text{A3.12})$$

where the superscript zero denotes value at time t and no superscript on phi means the value at time t+ t. (Andersson, 2010)

Convective term

$$\int_t^{t+\Delta t} \left(\int_w^e \frac{\partial (U_j \phi)}{\partial x} dx \right) dt = \int_t^{t+\Delta t} [(\rho U \phi)_e - (\rho U \phi)_w] dt \quad (\text{A3.13})$$

Again the derivative is described as the difference between the eastern and western face values of the 1 D cell. Using the weight factor defined above and making use of linear

interpolation between neighboring nodes the integration of the convective term over time yields:

$$\int_t^{t+\Delta t} [(\rho U \phi)_e - (\rho U \phi)_w] dt = \int_t^{t+\Delta t} \left[\rho U \left(\frac{\phi_P - \phi_E}{2} \right) - \rho U \left(\frac{\phi_W - \phi_P}{2} \right) \right] dt =$$

$$\left[\theta \left(\rho U \left(\frac{\phi_P - \phi_E}{2} \right) - \rho U \left(\frac{\phi_W - \phi_P}{2} \right) \right) + \dots \right.$$

$$\left. \dots (1 - \theta) \left(\rho U \left(\frac{\phi_P^0 - \phi_E^0}{2} \right) - \rho U \left(\frac{\phi_W^0 - \phi_P^0}{2} \right) \right) \right] \Delta t \quad (\text{A3.14})$$

Source term

In general the source term is described with an S and takes care of generation and dissipation of the entity described in the general transport equation. It can describe things like reaction of a chemical compound or transfer between phases as in the DOC case. To eliminate integrals in the term describing the source term a mean value is used of S inside the cell: (Andersson, 2010)

$$\int_t^{t+\Delta t} \left(\int_w^e S_\phi dx \right) dt = \int_t^{t+\Delta t} (\tilde{S}_\phi \Delta x) dt = \left[\theta \tilde{S}_\phi + (1 - \theta) \tilde{S}_\phi^0 \right] \Delta x \Delta t \quad (\text{A3.15})$$

Now a discretization of all terms described has been made generally and the following sections cover the discretization of the heat and mass balances used in the one channel DOC.

Discretization of mass balances

The solid phase mass balance is a simple ordinary differential equation but the gas phase mass balance is a partial differential equation depending both on time and length. To solve these coupled equations they need to be discretised. Usually this type of problem is assumed to be steady state or quasi steady state generating both the accumulation term in the solid phase and the gas phase mass balance to be equal to zero. This procedure simplifies the situation only having to solve one algebraic equation together with one partial differential equation. (Wang, 2008) (Hauff, 2010) However an interest in the transient solution prohibits this procedure resulting in slightly more difficult equations to solve.

In order to solve the above defined mass balances they will be solved term by term and then presented as full equations in the end.

Transient term

In accordance to what was presented earlier regarding the transient term in a general mass balance the expression for the transient term in the solid phase will be written as:

$$\int_w^e \left(\int_t^{t+\Delta t} (1 - \varepsilon) \frac{\partial X_s}{\partial t} dt \right) dx = (1 - \varepsilon) [X_s(t + \Delta t) - X_s(t)] \Delta x \quad (\text{A3.16})$$

The transient term in the solid phase will be written in the exact same manner except the subscript s here denoting the solid phase is switched to g, denoting the gas phase.

Convective term

It is only in the gas phase that a convective term is included hence the notations in the equation will be from the gas phase mass balance.

$$\int_t^{t+\Delta t} \left(\int_w^e u_D \frac{\partial X_E}{\partial x} dx \right) dt = \int_t^{t+\Delta t} \left(u_D [(X_g)_e - (X_g)_w] \right) dt \quad (\text{A3.17})$$

Linear interpolations from neighboring cells are used to describe the face values according to:

$$(X_g)_e = \frac{(X_E)_P + (X_E)_E}{2} \text{ and } (X_g)_w = \frac{(X_E)_W + (X_E)_P}{2}$$

This procedure leads to the expression:

$$\begin{aligned} \int_t^{t+\Delta t} \left(u_D [(X_g)_e - (X_g)_w] \right) dt &= \int_t^{t+\Delta t} \left(u_D \left[\frac{(X_E)_P + (X_E)_E}{2} - \frac{(X_E)_W + (X_E)_P}{2} \right] \right) dt = \\ \int_t^{t+\Delta t} \left(u_D \frac{[(X_E)_E - (X_E)_W]}{2} \right) dt \end{aligned} \quad (\text{A3.18})$$

Integration in time yields an expression including the weight factor theta.

$$\begin{aligned} \int_t^{t+\Delta t} \left(u_D \frac{[(X_E)_E - (X_E)_W]}{2} \right) dt &= \\ u_D \left(\theta \frac{[(X_E)_E - (X_E)_W]}{2} + (1 - \theta) \frac{[(X_E)_E^0 - (X_E)_W^0]}{2} \right) \Delta t \end{aligned} \quad (\text{A3.19})$$

The superscript of zero denotes the value in the previous time step. The value assigned to theta is set to 1, leaving the previous time step unused in the currents solution making it fully implicit.

Source terms

There are two different source terms in the mass balances, the solid phase mass balance contains a reaction source term and a mass transfer source term describing transfer between phases. The subscript of the solid phase mass balance will be used in both examples. The mass transfer source term is written as:

$$\begin{aligned} \int_t^{t+\Delta t} \left(\int_w^e k_{mj} a_{sf} (X_{gj} - X_{sj}) dx \right) dt &= \\ \int_t^{t+\Delta t} a_{sf} \left(\frac{[k_{mi} (X_{gi} - X_{si})]_W + 2[k_{mi} (X_{gi} - X_{si})]_P + [k_{mi} (X_{gi} - X_{si})]_E}{4} \right) \Delta x dt &= \end{aligned}$$

$$\left(\theta \left[\frac{[k_{m,i}(X_{gi}-X_{si})]_W + 2[k_{m,i}(X_{gi}-X_{si})]_P + [k_{m,i}(X_{gi}-X_{si})]_E}{4} \right] + \dots \right. \\ \left. \dots (1 - \theta) \left[\frac{[k_{m,i}^0(X_{gi}^0 - X_{si}^0)]_W + 2[k_{m,i}^0(X_{gi}^0 - X_{si}^0)]_P + [k_{m,i}^0(X_{gi}^0 - X_{si}^0)]_E}{4} \right] \right) \Delta X \Delta t \quad (A3.20)$$

Once again the weight factor is set to 1 making the solution fully implicit. The other source term in the mass balance is only appearing in the solid phase mass balance and includes reaction.

$$\int_t^{t+\Delta t} \left(\int_W \frac{a_c R_i}{C_{tot}} dX \right) dt = \int_t^{t+\Delta t} \left(\frac{a_c}{C_{tot}} \left[\frac{(R_i)_W + 2(R_i)_P + (R_i)_E}{4} \right] \Delta X \right) dt = \\ \frac{a_c}{C_{tot}} \left(\theta \left[\frac{(R_i)_W + 2(R_i)_P + (R_i)_E}{4} \right] - (1 - \theta) \left[\frac{(R_i)_W^0 + 2(R_i)_P^0 + (R_i)_E^0}{4} \right] \right) \Delta X \Delta t \quad (A3.21)$$

Complete balances

Now, all the terms in the mass balances has been described and discretized making it possible to write them in their full appearances. The solid phase mass balance is written as:

$$(1 - \varepsilon) [X_{sj}(t + \Delta t) - X_{sj}(t)] \Delta X = \\ \left(\theta \left[\frac{[k_{m,i}(X_{gi}-X_{si})]_W + 2[k_{m,i}(X_{gi}-X_{si})]_P + [k_{m,i}(X_{gi}-X_{si})]_E}{4} \right] + \dots \right. \\ \left. \dots (1 - \theta) \left[\frac{[k_{m,i}^0(X_{gi}^0 - X_{si}^0)]_W + 2[k_{m,i}^0(X_{gi}^0 - X_{si}^0)]_P + [k_{m,i}^0(X_{gi}^0 - X_{si}^0)]_E}{4} \right] \right) \Delta X \Delta t - \dots \\ \dots \frac{a_c}{C_{tot}} \left(\theta \left[\frac{(R_i)_W + 2(R_i)_P + (R_i)_E}{4} \right] - (1 - \theta) \left[\frac{(R_i)_W^0 + 2(R_i)_P^0 + (R_i)_E^0}{4} \right] \right) \Delta X \Delta t \quad (A3.22)$$

The gas phase mass balance is written as:

$$\varepsilon [X_{gj}(t + \Delta t) - X_{gj}(t)] \Delta X = \\ -u_D \left(\theta \left[\frac{(X_{gi})_E - (X_{gi})_W}{2} \right] + (1 - \theta) \left[\frac{(X_{gi})_E^0 - (X_{gi})_W^0}{2} \right] \right) \Delta t - \dots \\ \dots \left(\theta \left[\frac{[k_{m,i}(X_{gi}-X_{si})]_W + 2[k_{m,i}(X_{gi}-X_{si})]_P + [k_{m,i}(X_{gi}-X_{si})]_E}{4} \right] + \dots \right. \\ \left. \dots (1 - \theta) \left[\frac{[k_{m,i}^0(X_{gi}^0 - X_{si}^0)]_W + 2[k_{m,i}^0(X_{gi}^0 - X_{si}^0)]_P + [k_{m,i}^0(X_{gi}^0 - X_{si}^0)]_E}{4} \right] \right) \Delta X \Delta t \quad (A3.23)$$

The expressions for the mass balances seem very unmanageable, but simplifying the expressions, extracting the variable calculated in every iteration and putting the weight factor to one yields for the solid phase:

$$\begin{aligned}
[X_{sj}]_P &= \frac{a_{sf}}{(1-\varepsilon)} \left[\frac{[k_{m,i}(X_{gi}-X_{si})]_W + 2[k_{m,i}(X_{gi}-X_{si})]_P + [k_{m,i}(X_{gi}-X_{si})]_E}{4} \right] \Delta t \dots \\
&\dots + \frac{a_c}{(1-\varepsilon)C_{tot}} \left[\frac{(R_i)_W + 2(R_i)_P + (R_i)_E}{4} \right] \Delta t + [X_s]_P^0
\end{aligned} \tag{A3.24}$$

And for the gas phase:

$$\begin{aligned}
[X_{gj}]_P &= -\frac{u_D}{\varepsilon} \left[\frac{(X_{gi})_E - (X_{gi})_W}{2} \right] \frac{\Delta t}{\Delta x} - \dots \\
&\dots \frac{a_{sf}}{\varepsilon} \left[\frac{[k_{m,i}(X_{gi}-X_{si})]_W + 2[k_{m,i}(X_{gi}-X_{si})]_P + [k_{m,i}(X_{gi}-X_{si})]_E}{4} \right] \Delta t + [X_{gj}]_P^0
\end{aligned} \tag{A3.25}$$

Discretization of heat balances

The heat balances has been discretized in an equal manner to the mass balances only with different entities in the equations. For that reason this will not be explained again for the parts of the heat balance including the transient term and the convective term. The source term in the mass balances that includes reaction will however be explained together with the diffusion term that is not included in the mass balances at all.

Source term

The reaction source term is once again only included in the solid phase balance, because only in the solid phase reaction is taking place. The subscript i in this case denotes the three reactions; oxidation of carbon monoxide, hydrogen carbons (propylene) and nitric oxide.

$$\begin{aligned}
\int_t^{t+\Delta t} \left(\int_e^w a_{geo} \sum_{j=1}^3 (-\Delta H_{Rj}) R_j dx \right) dt &= \int_t^{t+\Delta t} a_{geo} \sum_{j=1}^3 \frac{[(-\Delta H_{Rj})R_j]_W + [(-\Delta H_{Rj})R_j]_E}{2} dt = \\
\int_t^{t+\Delta t} a_{geo} \sum_{j=1}^3 \frac{[(-\Delta H_{Rj})R_j]_W + 2[(-\Delta H_{Rj})R_j]_P + [(-\Delta H_{Rj})R_j]_E}{4} dt &= \\
a_{geo} \left(\theta \sum_{j=1}^3 \frac{[(-\Delta H_{Rj})R_j]_W + 2[(-\Delta H_{Rj})R_j]_P + [(-\Delta H_{Rj})R_j]_E}{4} - \dots \right. \\
&\dots \left. (1 - \theta) \sum_{j=1}^3 \frac{[(-\Delta H_{Rj})R_j]_W^0 + 2[(-\Delta H_{Rj})R_j]_P^0 + [(-\Delta H_{Rj})R_j]_E^0}{4} \right) \Delta t
\end{aligned} \tag{A3.26}$$

Note that since there are three reactions taking place the contribution to the source term will be bigger but they are here expressed as a sum in order to keep the size of the equation to a minimum.

Diffusion term

The diffusion term is present in both the balance for the solid phase and for the gas phase, but the notations in this example is valid for the solid phase.

$$\begin{aligned}
& \int_t^{t+\Delta t} \left(\int_e^w (1 - \varepsilon) \lambda_s \frac{\partial^2 T_s}{\partial x^2} dx \right) dt = \int_t^{t+\Delta t} (1 - \varepsilon) \left[\lambda_{se} \frac{T_{sE} - T_{sP}}{\Delta x} - \lambda_{sW} \frac{T_{sP} - T_{sW}}{\Delta x} \right] dt = \\
& \int_t^{t+\Delta t} (1 - \varepsilon) \left[\left(\frac{\lambda_{sE} + \lambda_{sP}}{2} \right) \frac{T_{sE} - T_{sP}}{\Delta x} - \left(\frac{\lambda_{sP} + \lambda_{sW}}{2} \right) \frac{T_{sP} - T_{sW}}{\Delta x} \right] dt = \\
& (1 - \varepsilon) \left(\theta \left[\left(\frac{\lambda_{sE} + \lambda_{sP}}{2} \right) \frac{T_{sE} - T_{sP}}{\Delta x} - \left(\frac{\lambda_{sP} + \lambda_{sW}}{2} \right) \frac{T_{sP} - T_{sW}}{\Delta x} \right] - \dots \right. \\
& \left. \dots (1 - \theta) \left[\left(\frac{\lambda_{sE}^0 + \lambda_{sP}^0}{2} \right) \frac{T_{sE}^0 - T_{sP}^0}{\Delta x} - \left(\frac{\lambda_{sP}^0 + \lambda_{sW}^0}{2} \right) \frac{T_{sP}^0 - T_{sW}^0}{\Delta x} \right] \right) \Delta t \tag{A3.27}
\end{aligned}$$

Complete balances

Enough terms have been described in order to express the full heat balances for the solid and the gas phase. First the gas phase heat balance is written and then the solid phase heat balance.

$$\begin{aligned}
& \varepsilon c_{p_g} \rho_g [T_g(t + \Delta t) - T_g(t)] \Delta x = \\
& -\varepsilon c_{p_g} \rho_g u_D \left(\theta \left[\frac{(T_E)_E - (T_E)_W}{2} \right] + (1 - \theta) \left[\frac{(T_E)_E^0 - (T_E)_W^0}{2} \right] \right) \Delta t + \dots \\
& \dots a_{geo} \left(\theta \left[\frac{[\alpha(T_E - T_s)]_W + 2[\alpha(T_E - T_s)]_P + [\alpha(T_E - T_s)]_E}{4} \right] + \dots \right. \\
& \left. \dots (1 - \theta) \left[\frac{[\alpha^0(T_E^0 - T_s^0)]_W + 2[\alpha^0(T_E^0 - T_s^0)]_P + [\alpha^0(T_E^0 - T_s^0)]_E}{4} \right] \right) \Delta x \Delta t + \dots \\
& \dots \varepsilon \left(\theta \left[\left(\frac{\lambda_{Eg} + \lambda_{EP}}{2} \right) \frac{T_{Eg} - T_{EP}}{\Delta x} - \left(\frac{\lambda_{EP} + \lambda_{EW}}{2} \right) \frac{T_{EP} - T_{EW}}{\Delta x} \right] - \dots \right. \\
& \left. \dots (1 - \theta) \left[\left(\frac{\lambda_{Eg}^0 + \lambda_{EP}^0}{2} \right) \frac{T_{Eg}^0 - T_{EP}^0}{\Delta x} - \left(\frac{\lambda_{EP}^0 + \lambda_{EW}^0}{2} \right) \frac{T_{EP}^0 - T_{EW}^0}{\Delta x} \right] \right) \Delta t \tag{A3.28}
\end{aligned}$$

The solid phase heat balance is described as:

$$\begin{aligned}
& (1 - \varepsilon_s) c_{p_s} \rho_s [T_s(t + \Delta t) - T_s(t)] \Delta x = \\
& (1 - \varepsilon) \left(\theta \left[\left(\frac{\lambda_{sE} + \lambda_{sP}}{2} \right) \frac{T_{sE} - T_{sP}}{\Delta x} - \left(\frac{\lambda_{sP} + \lambda_{sW}}{2} \right) \frac{T_{sP} - T_{sW}}{\Delta x} \right] - \dots \right. \\
& \left. \dots (1 - \theta) \left[\left(\frac{\lambda_{sE}^0 + \lambda_{sP}^0}{2} \right) \frac{T_{sE}^0 - T_{sP}^0}{\Delta x} - \left(\frac{\lambda_{sP}^0 + \lambda_{sW}^0}{2} \right) \frac{T_{sP}^0 - T_{sW}^0}{\Delta x} \right] \right) \Delta t - \dots \\
& a_{geo} \left(\theta \left[\frac{[\alpha(T_E - T_s)]_W + 2[\alpha(T_E - T_s)]_P + [\alpha(T_E - T_s)]_E}{4} \right] + \dots \right. \\
& \left. \dots (1 - \theta) \left[\frac{[\alpha^0(T_E^0 - T_s^0)]_W + 2[\alpha^0(T_E^0 - T_s^0)]_P + [\alpha^0(T_E^0 - T_s^0)]_E}{4} \right] \right) \Delta x \Delta t + \dots
\end{aligned}$$

$$\begin{aligned}
& a_{gso} \left(\theta \sum_{j=1}^3 \frac{[(-\Delta H_{R,i})R_i]_{W} + 2[(-\Delta H_{R,i})R_i]_{P} + [(-\Delta H_{R,i})R_i]_{E}}{4} - \dots \right. \\
& \left. \dots (1 - \theta) \sum_{j=1}^3 \frac{[(-\Delta H_{R,i})R_i]_{W}^0 + 2[(-\Delta H_{R,i})R_i]_{P}^0 + [(-\Delta H_{R,i})R_i]_{E}^0}{4} \right) \Delta t \quad (A3.29)
\end{aligned}$$

Once again the equations seem unmanageable, but if the interesting variables are extracted and the weight factor theta is set to one, they will turn out as:

$$\begin{aligned}
[T_g]_P &= -u_D \left(\frac{[(T_E)_E - (T_E)_W]}{2} \right) \frac{\Delta t}{\Delta x} + \dots \\
& \dots \frac{a_{gso}}{\varepsilon c_{P_E} \rho_E} \left(\frac{[\alpha(T_E - T_s)]_W + 2[\alpha(T_E - T_s)]_P + [\alpha(T_E - T_s)]_E}{4} \right) \Delta t + \dots \\
& \dots \frac{1}{c_{P_E} \rho_E} \left(\left[\left(\frac{\lambda_{EE} + \lambda_{EP}}{2} \right) \frac{T_{EE} - T_{EP}}{\Delta x} - \left(\frac{\lambda_{EP} + \lambda_{EW}}{2} \right) \frac{T_{EP} - T_{EW}}{\Delta x} \right] \right) \frac{\Delta t}{\Delta x} + [T_g]_P^0 \quad (A3.30)
\end{aligned}$$

And for the solid phase:

$$\begin{aligned}
[T_s]_P &= \frac{1}{c_{P_s} \rho_s} \left(\left[\left(\frac{\lambda_{sE} + \lambda_{sP}}{2} \right) \frac{T_{sE} - T_{sP}}{\Delta x} - \left(\frac{\lambda_{sP} + \lambda_{sW}}{2} \right) \frac{T_{sP} - T_{sW}}{\Delta x} \right] \right) \frac{\Delta t}{\Delta x} - \dots \\
& \dots \frac{a_{gso}}{(1-\varepsilon)c_{P_s} \rho_s} \left(\frac{[\alpha(T_E - T_s)]_W + 2[\alpha(T_E - T_s)]_P + [\alpha(T_E - T_s)]_E}{4} \right) \Delta t + \dots \\
& \dots \frac{a_{gso}}{(1-\varepsilon)c_{P_s} \rho_s} \left(\sum_{j=1}^3 \frac{[(-\Delta H_{R,i})R_i]_{W} + 2[(-\Delta H_{R,i})R_i]_{P} + [(-\Delta H_{R,i})R_i]_{E}}{4} \right) \frac{\Delta t}{\Delta x} + [T_s]_P^0 \quad (A3.31)
\end{aligned}$$

Discretization of Navier-Stokes equation

Navier-Stokes equation is discretized in order to solve the velocity of the system. The different terms included are similar to the ones in the mass and heat balances and will not be exemplified for the reader again. The general discretization balances explains very well the included terms. It is worth mentioning that the pressure term in the Navier-Stokes equation is treated constant from experimental data. This means that the pressure drop over every cell in the channel is constant and also assumed to be linear. Expressing Navier-Stokes equation in discretized form gives first:

$$\begin{aligned}
& \int_w^e \left(\int_t^{t+\Delta t} \rho \frac{\partial u_D}{\partial t} dt \right) dx = - \int_t^{t+\Delta t} \left(\int_w^e \rho u_D \frac{\partial u_D}{\partial x} dx \right) dt \dots \\
& \dots - \int_t^{t+\Delta t} \left(\int_w^e \frac{\partial P}{\partial x} dx \right) dt + \int_t^{t+\Delta t} \left[\int_w^e \mu \frac{\partial^2 u_D}{\partial x^2} dx \right] dt \quad (A3.32)
\end{aligned}$$

This is then expressed as:

$$\begin{aligned}
\rho[u_D(t + \Delta t) - u_D(t)]\Delta x &= - \left[\theta \left(\frac{[\rho u_D u_D]_E + [\rho u_D u_D]_F}{2} \right) - \left(\frac{[\rho u_D u_D]_W + [\rho u_D u_D]_P}{2} \right) \right] + \dots \\
\dots (1 - \theta) &\left(\left(\frac{[\rho u_D u_D]_E^0 + [\rho u_D u_D]_F^0}{2} \right) - \left(\frac{[\rho u_D u_D]_W^0 + [\rho u_D u_D]_P^0}{2} \right) \right) \Delta t - \dots \\
\dots \left[\theta \left(\frac{P_E - P_W}{2} \right) - (1 - \theta) \left(\frac{P_E^0 - P_W^0}{2} \right) \right] \Delta t + \dots \\
\dots \left[\theta \left(\frac{\mu_F + \mu_E}{2} \left(\frac{u_{D_E} - u_{D_F}}{\Delta x} \right) - \frac{\mu_W + \mu_P}{2} \left(\frac{u_{D_P} - u_{D_W}}{\Delta x} \right) \right) + (1 - \theta) \left(\frac{\mu_F^0 + \mu_E^0}{2} \left(\frac{u_{D_E}^0 - u_{D_F}^0}{\Delta x} \right) - \right. \right. \\
&\left. \left. \frac{\mu_W^0 + \mu_P^0}{2} \left(\frac{u_{D_P}^0 - u_{D_W}^0}{\Delta x} \right) \right) \right] \Delta t
\end{aligned} \tag{A3.33}$$

The above equation is intended to be solved with the weight factor set to one giving the following equation:

$$\begin{aligned}
[u_D]_P &= - \left[\left(\frac{[u_D u_D]_E + [u_D u_D]_F}{2} \right) - \left(\frac{[u_D u_D]_W + [u_D u_D]_P}{2} \right) \right] \frac{\Delta t}{\Delta x} - \frac{1}{\rho} \left(\frac{P_E - P_W}{2} \right) \frac{\Delta t}{\Delta x} - \dots \\
\dots \frac{1}{\rho} &\left[\frac{\mu_F + \mu_E}{2} \left(\frac{u_{D_E} - u_{D_F}}{\Delta x} \right) - \frac{\mu_W + \mu_P}{2} \left(\frac{u_{D_P} - u_{D_W}}{\Delta x} \right) \right] \frac{\Delta t}{\Delta x} + [u_D]_P^0
\end{aligned} \tag{A3.34}$$